Comparative Transcriptome Profiling

of Expression Patterns and Regulation Mechanisms in

the Plant Pathogen *Burkholderia plantarii* PG1

Dissertation

for obtaining the degree

Doctor rerum naturalium (Dr. rer. nat.)

at the Department of Biology

Subdivision of the Faculty of Mathematics, Informatics and Natural Sciences

of the University of Hamburg

by

Eva Katharina Oellingrath

from Hamburg

Hamburg 2023

The following evaluators recommend the admission of the dissertation:

Prof. Dr. Wolfgang R. Streit

Prof. Dipl.-Ing. Dr. Agnes Weiß

Date of Defence (Disputation): 23.06.2023

Eidesstattliche Erklärung

Hiermit erkläre ich an Eides statt, dass ich die vorliegende Dissertationsschrift selbst verfasst und keine anderen als die angegebenen Quellen und Hilfsmittel benutzt habe.

Declaration on oath

I hereby declare, on oath, that I have written the present dissertation by my own and have not used any other than the acknowledged resources and aids.

Hamburg, 29.01.2023

Abstract

Burkholderia plantarii PG1 (formerly *glumae*) is a model organism known as causal agent of bacterial panicle blight in rice plants and has become one of the most common seed-borne bacterial rice diseases in the world. Nevertheless, this organism has biological interest. First, *B. plantarii* PG1 is the producer of the extracellular lipase LipA to produce enantiopure pharmaceuticals. In addition, *B. plantarii* PG1 is a native rhamnolipid producer which is used in pharmaceutical, chemical, food and cosmetic industries. Furthermore, it is distinguished by a unique Quorum sensing system in Burkholderia and possesses more scientific interesting properties which were investigated in this work. The genome of *B. plantarii* PG1 contains a hydroxyethylthiazole kinase ThiM, which is part of a salvage pathway in the thiamine metabolism conceivably involved in the regulation of the endogenous CRISPR/CAS I-F system due to its unique genomic position upstream of the endonuclease Cas1. For further insights, a comparative transcriptome analysis was performed to elucidate possible effects of a ThiM deletion mutant. Different growth phases and media were investigated, resulting in significant transcriptional changes. In the first analysis of the transcription levels, the absence of the kinase ThiM increased the transcription of *csy1-3* in LB medium and caused a decrease of *csy1-3* in M9 minimal medium without thiamine. However, a comparative analysis demonstrated that the medium effect caused the transcriptional changes. Although this medium effect was present, an influence of the kinase ThiM on the regulation of the CRISPR/CAS I-F system could not be completely excluded. For further advances, a comparative transcriptome profiling should provide insights by identifying expression patterns and analysing metabolic networks under different conditions. The kinase ThiM is part of the salvage pathway in thiamine metabolism to produce thiamine pyrophosphate (TPP), the active form of thiamine. TPP is an essential cofactor in several metabolic pathways. The influence of different media of LB and M9 medium without thiamine and M9 medium with supplemented thiamine were investigated at the late exponential and the late stationary growth phase in *B. plantarii* PG1 and a ThiM deletion mutant. In this analysis, the interplay of metabolic processes related to the thiamine metabolism was revealed. The reduced presence of TPP resulted in a diminished activity of the metabolic pathways of glycolysis, the citrate cycle, oxidative phosphorylation, leucine degradation, arginine biosynthesis, histidine metabolism, thiamine metabolism, nitrogen metabolism and fatty acid metabolism. Finally, it is the most comprehensive transcriptome dataset of *B. plantarii* PG1 providing further insights for investigations.

The regulation of the CRISPR/CAS system was further investigated. Here three putative promoter sites were identified, and their activity experimentally evaluated by constructed

reporter strains. Thus, the activity of the promoter sites was proven. The regulation of the CRISPR/CAS system in *B. plantarii* PG1 is still unknown. Therefore, other possible regulators were investigated and two were identified here. Experimental analysis of the putative regulators investigated in the promoter reporter strains revealed a repression of the activity of the promoter sites of the CRISPR/CAS system. The possible repressors are two cyclic AMP receptor proteins named CRP1 and CRP3 in this study which are dependent on the glucose metabolism. Comparative transcriptome analyses were applied to confirm the observed experimental results. Further experiments are required to verify the regulatory processes and the role of the possible regulators here. As in literature described the CRISPR/CAS system is regulated by the Quorum sensing system in some species and first insights of an influence on the CRISPR/CAS system in *B. plantarii* PG1 were shown in the study of Rong Gao in 2015. Therefore, Rong Gao constructed and investigated three QS deletion mutants (*B. plantarii* PG2-PG4, formerly *glumae*) in *B. plantarii* PG1. Here in this study, the CRISPR/CAS promoter fusions were investigated in the three QS deletion mutants of *B. plantarii* PG2-4 and were exposed to environmental stress conditions via different salt and glucose concentrations. Thereby, effects in the different QS deletion mutant strains as well as in changing salt concentrations were observed. Altered salt concentrations increased the activity of the promoter sites of the CRISPR/CAS system in the wildtype *B. plantarii* PG1 and in the QS deletion mutants of PG3 and PG4, demonstrating the effect of the QS system and additionally of environmental changes on the CRISPR/CAS system.

Zusammenfassung

Burkholderia plantarii PG1 (ehemals *glumae*) ist ein Modelorganismus in der Grundlagenforschung und als Erreger der Rispenfäule bei Reispflanzen bekannt, der große Schäden in der Landwirtschaft weltweit hervorruft. Darüber hinaus zeichnet sich dieser Organismus als ein wichtiger Lipase Produzent in der Biotechnologie aus, welcher zur Herstellung von enantioreinen Pharmazeutika genutzt wird. Neben seinem biotechnologischen Nutzen besitzt *B. plantarii* PG1 noch weitere interessante Eigenschaften, die in dieser Arbeit näher untersucht wurden. So verfügt er über ein einzigartiges Quorum sensing System mit drei AHL-produzierenden Synthasen, über welche regulatorische Mechanismen im Organismus gesteuert werden. Zur Abwehr von Viren und Fremd-DNA dient ein CRISPR/CAS I-F System, welches erstmals im Pesterreger *Yersinia pestis* beschrieben wurde. Das Genom von *B. plantarii* PG1 weist hierbei eine Besonderheit auf. Dem CRISPR/CAS System ist eine, dem Thiamin Stoffwechsel zugehörige, Hydroxyethylthiazolkinase ThiM vorgesetzt. Dabei ist es nicht unüblich, dass die Gene des Thiamin Stoffwechsels einzeln verstreut auf dem Genom vorliegen. Die Position dieser Kinase ist jedoch einzigartig. Erste Transkriptomdatenanalysen einer ThiM Deletionsmutante haben Tendenzen gezeigt, dass diese Einfluss auf das CRISPR/CAS System ausübt, speziell auf die Gene *csy1-3* des *csy surveillance* Komplex. In weiteren Untersuchungen, in verschiedenen Medien, zu unterschiedlichen Wachstumsphasen hat sich gezeigt, dass dieser Effekt auf einen Medium Effekt zurückzuführen ist. Dennoch konnte ein Einfluss auf oder eine Ko- Regulation des Thiamin Stoffwechsels und des CRISPR/CAS Systems nicht ausgeschlossen werden. Daher wurde eine vergleichende Stoffwechsel-Netzwerkanalyse auf Transkriptomebene durchgeführt, in der Expressionsmuster identifiziert und metabolische Zusammenhänge unter verschiedenen Bedingungen rekonstruiert wurden. Der Thiamin Stoffwechsel in *B. plantarii* PG1 besteht aus einem Haupt- und einem Salvage-Stoffwechselweg. Die Kinase ThiM ist ein wichtiger Bestandteil des Salvage-Stoffwechselweges und wird zur Produktion von Thiaminpyrophosphat (TPP) benötigt. Einer der drei aktiven Formen von Thiamin. TPP stellt einen essentiellen Cofaktor in vielen Stoffwechselwegen dar. In der erfolgten Stoffwechsel-Netzwerkanalyse wurden ein Vollmedium (LB-Medium) und ein Minimal Medium (M9-Medium) ohne Zusatz von Thiamin, sowie ein Minimal Medium mit zugesetztem Thiamin (M9 + Thiamin Medium) miteinander verglichen. Die Daten wurden dabei zum Zeitpunkt der späten exponentiellen und der späten stationären Wachstumsphase erhoben. Bei den zu vergleichenden Stämmen handelte es sich um den Wildtyp *B. plantarii* PG1 und um die ThiM Deletionsmutante. Hierbei konnte im Vergleich festgestellt werden, dass durch die reduzierte Produktion von TPP eine verminderte Aktivität

der Stoffwechselwege der Glykolyse, des Zitrat Zyklus, der oxidativen Phosphorylierung, Leucine Degradierung, Arginin Biosynthese, dem Histidin Stoffwechsel, dem Thiamin Stoffwechsel, Stickstoffstoffwechsel und Fettsäurestoffwechsel beobachtet werden konnte. Mit Ausnahme der in der Vergangenheit erhobenen Transkriptomdaten von Rong Gao im Jahre 2015, stellt dieser Datensatz den umfassendsten Transkriptomdatensatz für den Organismus *B. plantarii* PG1 dar und gibt detaillierte Einblicke in das metabolische Netzwerk des Pflanzenpathogens. Des Weiteren wurde in dieser Arbeit das CRISPR/CAS System näher charakterisiert. Dabei konnte über erhobene Transkriptomdaten festgestellt werden, dass das CRISPR/CAS System zunächst nicht als Operon reguliert ist. Es wurden drei putative Promoter Motive im CRISPR/CAS System identifiziert und dessen Aktivität über erstellte Reporterstämme verifiziert. Die Regulation des CRISPR/CAS Systems in *B. plantarii* PG1 ist bislang noch unbekannt. Daher wurde nach weiteren möglichen Regulatoren geforscht und zwei mögliche Kandidaten identifiziert. Diese haben sich in Experimenten mit den zuvor erstellten Promoter Reporterstämmen als mögliche Repressoren herausgestellt. Bei den beiden möglichen Repressoren handelt es sich um zwei zyklische AMP-Rezeptorproteine, die in dieser Studie als CRP1 und CRP3 benannt wurden und in Abhängigkeit zum Glucosestoffwechsel stehen. Zur weiteren Untersuchung der möglichen Repressoren wurden Transkriptomdaten erhoben, welche die experimentellen Resultate bestätigten. Dennoch sind weitere Experimente notwendig, um die regulatorische Rolle der beiden Repressoren zu evaluieren. In der Literatur werden zahlreiche Regulatoren zur Steuerung des CRISPR/CAS Systems beschrieben, die je nach Organismus in ihrer Funktion variieren. In vielen Organismen wird das QS-System als elementares Element in der Steuerung des CRISPR/CAS System beschrieben. Rong Gao konnte in seiner Studie im Jahr 2015 bereits über Transkriptomdatenanalysen und der Erstellung von QS-Deletionsmutanten zeigen, dass das QS-System Einfluss auf das CRISPR/CAS System nimmt. Um diese Aussage zu bestätigen, wurden experimentelle Studien durchgeführt, in denen die erstellten CRISPR/CAS Promotorfusionen in den drei QS-Deletionsmutanten, unter verschiedenen Salz- und Glucosekonzentration als initialer Stressauslöser, untersucht wurden. Dabei wurden sowohl Effekte in den QS-Deletionsmutanten als auch unter erhöhter Salzkonzentration festgestellt, die einen Anstieg der Promotoraktivität im Wildtyp *B. plantarii* PG1 wie auch den beiden Deletionsmutanten PG3 und PG4 aufzeigten. Somit wurde zum einen der Einfluss des QS-Systems auf das CRISPR/CAS System bestätigt, wie auch der Einfluss von unterschiedlichen Salzkonzentrationen.

Table of Contents

1 Introduction

1.1 Burkholderia glumae PG1/ plantarii PG1

The genus Burkholderia comprises individual representatives of species belonging to ß-Proteobacteria. Based on 16S rRNA analysis the representatives are divided into two clusters. Facultative pathogenic representatives in humans, animals and plants are allocated to the first cluster and contains the *Burkholderia cepacia*-complex (BCC complex), the *Bptm* (*B. pseudomallei*, *B. thailandensis*, *B. mallei*) and *Pseudomallei* group. The second cluster of the plant-associated beneficial and environmental group (PBE) includes all environmental and plant-associated representatives (Suárez-Moreno *et al.*, 2012). The species *Burkholderia glumae* is a Gram-negative, rod-shaped, motile soil bacterium up to a size of 0.5 x 2.5 µm with an optimum growth temperature of 28-30°C and a temperature tolerance range of 11-40°C according to the studies of Kurita and Tabei in 1964. *Burkholderia glumae* was first described as rice pathogen in 1956 in Japan (Goto, K., Ohata, 1956) and as *Pseudomonas glumae* in 1967 by Kurita and Tabei (Kurita and Tabei, 1967). Due to morphological and physiological similarities it has been reclassified in 1992 to the genus Burkholderia (Yabuuchi *et al*., 1992) and separated in 1994 in *Burkholderia glumae* (NCBI:txid337) and *Burkholderia plantarii* species (NCBI:txid41899) (Urakami *et al.*, 1994, Azegami *et al*., 1987). *Burkholderia glumae* belongs to the second cluster of Burkholderia and is described as rice pathogen causing great damage in agriculture of Japan, Vietnam, China, Philippines, India, Africa and USA (Cien *et al*., 1996, Cottyn *et al.*, 1996, Jeong *et al*., 2003, Luo *et al.,* 2007, Nandakumar *et al.,* 2007, Trung *et al.*, Ziegler *et al.,* 1989, Zhou, 2013). It is responsible for the panicle blight of rice leading to seedling blighting and sheath rot (Cui Zhou-qi *et al*., 2016). Additionally, it has a wide host spectrum including tomato plants, cereals, pepper, eggplant, potatoes, sunflowers and sesame (Jeong *et al.*, 2003). In the fight against diseases caused by Burkholderia species, new rice lines are being bred and basic research is being supported to elucidate the pathogenicity mechanism (Mizobuchi *et al.*, 2020, Ortega and Rojas, 2021). Although *B. glumae* is so far only known as a plant pathogen, in 2007 a paper was published in which a human pathogenic case was first described. In this case, an eight-month-old boy developed a necrotic lung mass from which *B. glumae* and other representatives were isolated and were responsible for the further development of chronic granulomatous disease (CGD) in this patient (Weinberg *et al*., 2007). While other Burkholderia representatives are known to be human pathogens, this human pathogenic behaviour of *B. glumae* was only been observed in this case. However, like its pathogenic relatives, *B. glumae* forms a tough biofilm and can be cultivated well under laboratory conditions, which makes it an interesting

model organism. Depending on the species, different plant toxins are produced, and various Quorum sensing (QS) systems are present to control metabolic processes (Leo Eberl, 2006, Kim *et al.*, 2014). *B. glumae* PG1 is a production strain for lipases in biotechnology and due to its high degree of relationship to human pathogen representatives, an interesting model organism for basic research (Boekema *et al.*, 2007, Knapp *et al.*, 2016). In 2018 it was renamed as *B. plantarii* PG1 due to Average Nucleotide Identity results to *Burkholderia plantarii* and will be referred to as such in the following (NCBI:txid41899). Genomic analysis of *B. plantarii* PG1 has revealed interesting features. It possesses a special QS system and synthesises three different AHL molecules responsible for the regulation of biofilm formation, motility, extracellular lipolytic activity, plant maceration and plant pathogenicity (Gao *et al.*, 2015). *B. plantarii* PG1 also possesses several secretion systems like the type I, type II, type III and type VI secretion system and its phytotoxicity is based on the production of tropolone instead of toxoflavin as in other representatives of *B. plantarii* (Seo *et al.*, 2015, Vial L *et al.*, 2007). Interestingly, *B. plantarii* PG1 possesses a CRISPR/CAS I-F subtype system which was originally found in *Yersinia pestis* for the defence of foreign DNA and viruses (Voget *et al.*, 2015, Cady *et al.*, 2011). Here, a unique feature was identified, upstream of the endonuclease Cas1 of the CRISPR/CAS system, a hydroxyethylthiazole kinase ThiM is located. This is special and its role depending to the CRISPR/CAS system is still unknown.

1.2   The hydroxyethylthiazole kinase ThiM

The genome of *B. plantarii* PG1 comprises chromosome 1 with 4,163,767 bp (Accession CP002580.1) and chromosome 2 with 3,732,771 bp (Accession CP002581.1). As mentioned before, *B. plantarii* PG1 possesses some special features compared to other related species. It is differentiated by its unique QS system with three different AHL synthetases which are located on chromosome 1 and 2 (*bgal*1= BGL_2c09850, *bgal*2= DNA coordinates 486.784-487.479, *bgal*3= BGL_1c07910 (Gao *et al.*, 2015)), a highly efficient lipase LipA on chromosome 2 (BGL_2c18660), which is used in biotechnology (Knapp *et al.*, 2016) and a CRISPR/CAS I-F subtype system located on chromosome 1 (BGL_1c18810 - BGL_1c18860). Additionally, the thiamine metabolism represented interesting features. The genes of the thiamine metabolism are contributed over the whole genome and comprises the genes *thiC* (BGL_1c10790), *thiD* (BGL_1c07140, BGL_1c24820, BGL_2c23420), *iscS* (BGL_1c26260, BGL_2c20770), *thiS* (BGL_1c03110), *thiO* (BGL_1c03100), *dxs* (BGL_1c10930, BGL_2c21450), *thiG* (BGL_1c03120), *thiE* (BGL_1c03130, BGL_2c21760), *thiL* (BGL_1c05130), *adk*

(BGL_1c30540), *rsgA* (BGL_1c09450), thiaminase I (BGL_2c23410) and *thiM* (BGL_1c18800), on chromosome 1 and 2 (Figure 1).
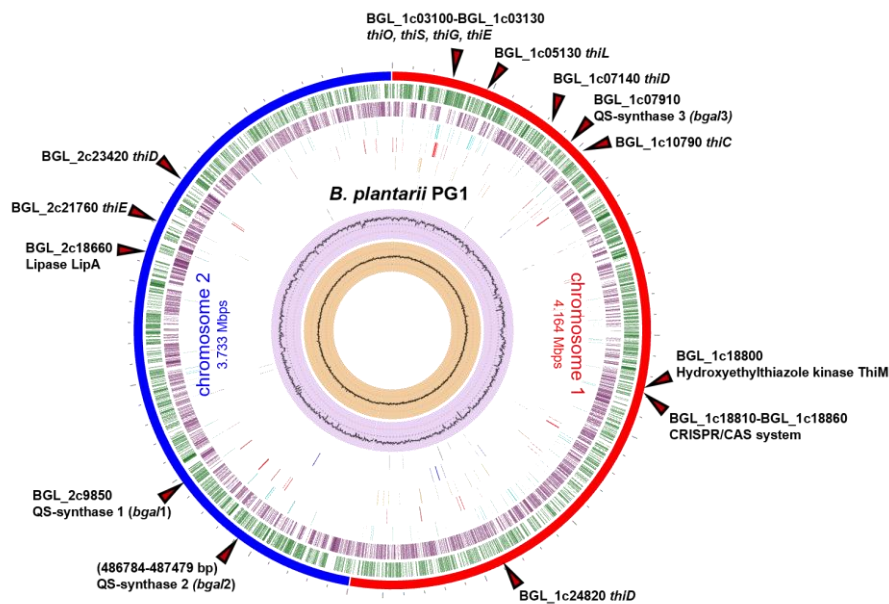

Figure 1: Genomic distribution of selected genes at chromosome 1 and 2 of *B. plantarii* PG1. Chromosome 1 (red) contains genes of the thiamine metabolism (*thiO*, *thiS*, *thiG*, *thiE*, *thiL*, *thiD*, *thiM*), the third QS-synthase *bgal*3 and the CRISPR/CAS system. Chromosome 2 (blue) includes the first and second QS-synthases of *bgal*1 and *bgal*2, the gene coding for the lipase *LipA* and the genes of the thiamine metabolism of *thiE* and *thiD*.

Thiamine plays an important role in the regulation of metabolic processes due to its part as essential co-factor. In the CRISPR/CAS system a unique feature was observed: there is a hydroxyethylthiazole kinase ThiM upstream of the endonuclease Cas1 that is only found in *B. plantarii* PG1. The CRISPR/CAS system is an adaptive bacterial immune system against viruses and foreign DNA. In *B. plantarii* PG1 it consists of six genes with two CRISPR Arrays up- and downstream of the CRISPR/CAS system and a third one further. The endonuclease Cas1 is responsible for the spacer insertion and builds a complex with the endonuclease Cas3 which induces a DSB in the DNA for target cleavage. The csy surveillance complex containing of Csy1-3 are required for the target binding and the Csy4 is responsible for the pre-crRNA processing. The entire gene complex comprises a size of 8.9 kb and is located at DNA coordinates 2142105-2151066 on chromosome 1 (Figure 1 and 2).
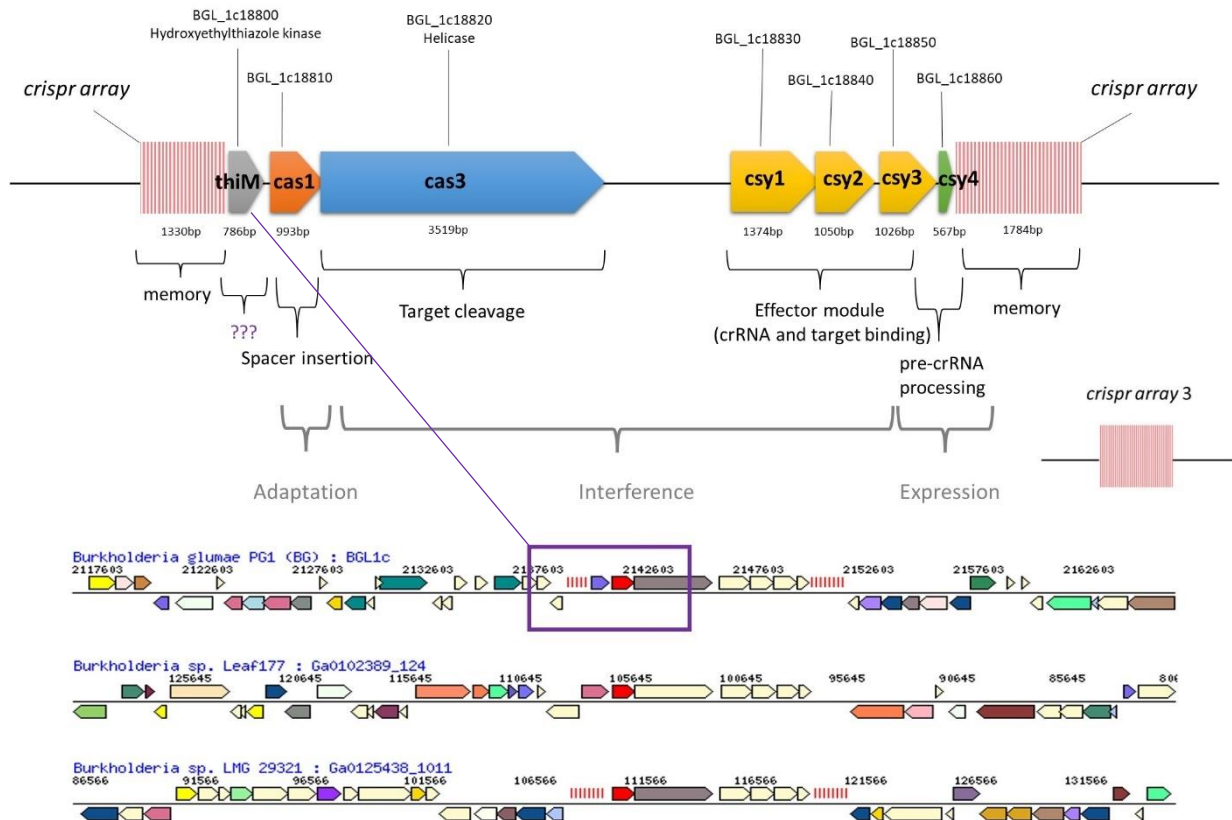
Figure 2: Gene card of the CRISPR/CAS I-F system and unique genomic localisation of the hydroxyethylthiazole kinase ThiM in *B. plantarii* PG1. IMG 2022. The CRISPR/CAS system contains of six genes of *cas1*, *cas3*, *csy1-4* and three CRISPR arrays. In comparison the unique position of *thiM* (violet box) could be verified by a gene neighbourhood region search.

In a gene neighbourhood region search with the same top COG hit (via top homolog) by IMG in other relatives no similarities regarding to a possible gene constellation of ThiM were found (Figure 2). Although it is not unusual for the genes of thiamine metabolism to be distributed throughout the genome and not found in one operon, the position of this hydroxyethylthiazole kinase is special. Its function at this site has not yet been clarified and should investigate more in detail in the following. ThiM is part of the thiamine metabolism. Thiamine acts as a signal molecule of several metabolic pathways. In *B. plantarii* PG1 it is required for the pentose phosphate pathway, propanoate metabolism, the glycolysis, pyruvate metabolism, citrate cycle as well as for the thiamine metabolism (KEGG pathway database – functional search of thiamine in *B. plantarii* PG1, 2022, Settembre *et al*., 2003). There are four active forms of thiamine occurring naturally in cells that are mainly used in metabolic pathways: thiamine monophosphate (TMP), thiamine diphosphate/thiamine pyrophosphate (TPP), thiamine triphosphate (TTP) and adenosine thiamine triphosphate (AThTP) (Jurgenson *et al*., 2009, Beglay *et al*., 1999, Gigliobianco *et al*., 2010).

Figure 3: Thiamine pathway in *B. plantarii* PG1, KEGG bgp00730, modified 2021. The thiamine metabolism comprises the synthesis of two moieties of HMP-PP and HET-P. The genes of *thiC*, *thiD* and *thiE* are involved in the synthesis of HMP-PP and the genes of the salvage pathway, *thiM* and *thiE* are required for the synthesis of HET-P. For the catalysation of thiamine phosphate, the kinases of ThiL and adk are responsible for the conversation of TMP to TDP and TTP.

The thiamine metabolism is based on two independent synthesised moieties of the pyrimidine moiety 4-amino-5-hydroxymethyl-2-methylpyrimidine diphosphate (HMP-PP) and the thiazole moiety hydroxyethylthiazole phosphate (HET-P) which leads to the synthesis of thiamine monophosphate and the other active forms of thiamine. To achieve the pyrimidine moiety in *B. plantarii* PG1, we are starting from the purine metabolism: 1-(5'-phospho-ribosyl)-5-aminoimidazole is converted by the pyrimidine synthase ThiC to 4-amino-5-hydroxymethyl-2-methylpyrimidine phosphate and phosphorylated by the pyrimidine kinase ThiD to HMP-PP for the thiamine biosynthesis. The next enzymatic step from HMP-PP to thiamine phosphate is catalysed by the thiamine-phosphate diphosphorylase ThiE. Thiamine phosphate is converted

to thiamine diphosphate by the kinase ThiL and the conversion to thiamine triphosphate is catalysed by the adenylate kinase adk. The thiazole moiety HET-P is synthesised by the salvage pathway of the metabolism. Here the thiaminase I converts thiamine to precursors as 5-(2-Hydroxyethyl)-4 methylthiazole by degradation. This leads to the phosphorylation to HET-P (5-(2-Hydroxyethyl)-4 methylthiazole phosphate) by the hydroxyethylthiazole kinase ThiM and ends back in the converting cycle from HET-P to thiamine phosphate by ThiE and the following synthesis to thiamine diphosphate and thiamine triphosphate (Figure 3) (Rodionov *et al.*, 2002, Karunakaran *et al.*, 2006, Bettendorf and Wins, 2009, Sannino *et al.*, 2018).
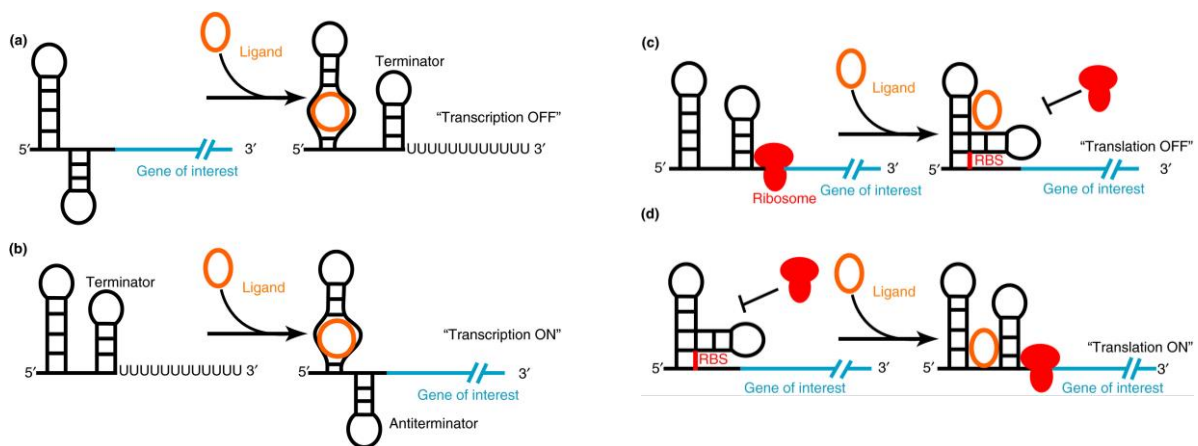

Figure 4: Scheme of riboswitch principle for transcription (a-b) and translation (c-d) control. The different mechanisms of riboswitches lead to a repression (a, c) or to an activation (b, d) of gene expression by binding a ligand to the secondary and tertiary structure of the riboswitch (Nshogozabahizi *et al.*, 2019).

In literature it is described that the thiamine metabolism as well as other metabolisms are regulated by non-coding regulatory RNA structures so called riboswitches. Due to constantly changing environmental conditions, microorganisms are dependent on optimising their gene regulation. Riboswitches are one of these optimisations, which has evolved in microorganisms over time and are considered to emerged during the RNA world (Breaker, 2012, Garst *et al.*, 2011). The functional principle involves a ligand binding to the riboswitch and causing a conformation change of the secondary structure which leads to transcription/translation initiation or termination (Figure 4) (Barrick and Breaker, 2007, Wittmann and Suess, 2012). In thiamine metabolism, a thiamine pyrophosphate (TPP) sensing riboswitch is present, which belongs to the translation regulated riboswitches (Sudarsan *et al.*, 2005).

Figure 5: Prediction structure of the putative riboswitch upstream of ThiM in *B. plantarii* PG1 (Hongli Zhang, 2018).

In *B. plantarii* PG1, a riboswitch-like structure was identified upstream of ThiM in a previous work (master thesis of Hongli Zhang, 2018) at the DNA coordinates 2141012-2141109, but was not further investigated in this work (Figure 5). Nevertheless, its presence is of great importance for understanding a possible influence of ThiM regarding to the CRISPR/CAS system. In the master thesis of Hongli Zhang, a deletion mutant of ThiM (BpPG1Δ*thiM*) was already created for investigations of the kinase, which was used for further analysis in this thesis.

1.3 Thiamine depending metabolic pathways

B. plantarii PG1 has a wide range of metabolic pathways for the adaptation to environmental changes and challenges of its life cycle. The database KEGG (Kyoto Encyclopedia of Genes and Genomes) provides a genomic analysis on high-level of biological systems and enables to understand metabolic processes. The KEGG genomic overview showed that certain metabolic pathways were represented in *B. plantarii* PG1 but only a small number of genes could be mapped. The functional classification revealed that 32.88% of 6576 genes in total, of the protein coding genes are connected to KEGG pathways. Most of the genes were assigned to amino acid metabolism (406 count, 8.61%), carbohydrate metabolism (381 counts, 8.08%), cell motility (111 counts, 2.35%), cellular community (260 counts, 5.51%), energy metabolism (211 counts, 4.48%), lipid metabolism (129 counts, 2.74%), membrane transport (314 counts, 6.66%), metabolism of cofactors and vitamins (253 counts, 5.37%), metabolism of other amino acids (104 counts, 2.21%), signal transduction (223 counts, 4.73%), xenobiotics biodegradation and metabolism (139 counts, 2.95%) and 1252 counts (26.55%) belongs to global and overview maps.
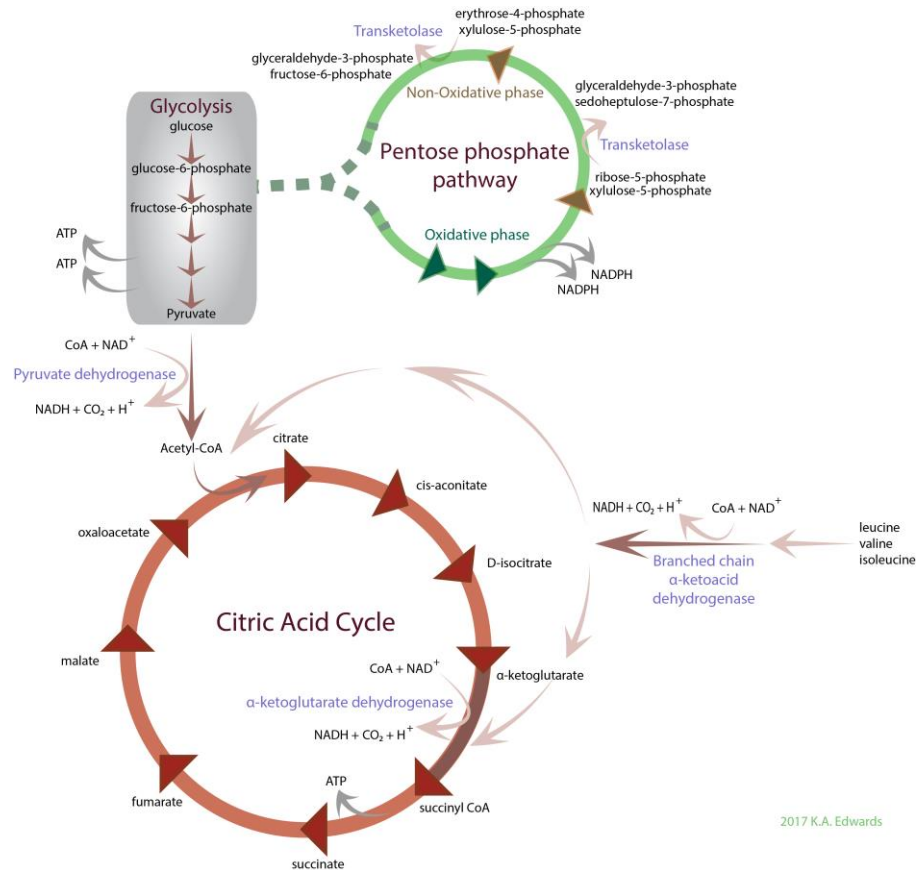
Figure 6: The interplay of glycolysis, pentose phosphate pathway and citric acid cycle in dependence of TPP. Thiamine pyrophosphate displays an important cofactor in several metabolic processes and is essential for maintaining the energy level in the life cycle of the cells. In blue: enzymes using TPP as cofactor (Kraft and Angert, 2017).

Regarding to thiamine as essential cofactor in metabolic pathways in *B. plantarii* PG1 it plays an important role in the synthesis of precursors for other metabolisms. For example, the pentose phosphate pathway is separated in the oxidative and non-oxidative phase. The oxidative phase leads to the production of ribose-5-phosphate, an important precursor of phosphoribosyl pyrophosphate PRPP, the initial point for histidine metabolism. Here TPP is used as cofactor for a transketolase to catalyse the reaction of xylulose-5-phophate and ribose-5-phosphate to sedoheptulose-5-phosphate and glyceraldehyde-3-phosphate. The non-oxidative phase is characterised by the production of glyceraldehyde-3-phosphate and fructose-6-phosphate which passes from there into glycolysis. In the following TPP is used by the pyruvate dehydrogenase in the transition from pyruvate to acetyl-CoA and the branched chain α-ketoglutarate to provide NADH for the citrate cycle (Figure 6) (Škerlová *et al*., 2021). Further investigations of this work will give a more precise insight into thiamine depending metabolic processes in *B. plantarii* PG1.

1.4 CRISPR/CAS

As previously mentioned, ThiM is located at a unique position upstream of the CRISPR/CAS system in *B. plantarii* PG1 but the function here is still unknown. CRISPR/CAS (*clustered regularly interspaced short palindromic repeats and CRISPR-associated proteins*) represents an adaptive bacterial and archaeal immune system against viruses and foreign DNA (Devashish Rath *et al.*, 2015). In 1987, Yoshizumi Ishino discovered short palindromic repeats for the first time in the genome of *E. coli* (Ishino *et al.*, 1987). A bacterial CRISPR/CAS system is composed of a *cas* locus, a leader sequence and one or more CRISPR Arrays. The *cas* locus contains the CRISPR effector molecules, which are responsible for the insertion of new spacer, the crRNA and target binding as well as the pre-crRNA processing and target cleavage. The CRISPR Array represents the adaptive memory of past attacks with foreign DNA. It consists of altering spacer (21-72bp) and repeat sequences (23-47bp). The repeat sequences represent palindromic motifs between the spacer, which forms a stable secondary structure of the corresponding RNA, whereas the spacer represents insertion of foreign DNA of past attacks (Horvath *et al.*, 2010). The leader sequence is located near the CRISPR Array and consists of an AT-rich, non-coding sequence of 100-500bp (Alkhnbashi *et al.*, 2016). According to the different types and numbers of effector molecules, the CRISPR/CAS systems are separated in two classes, six types and 33 subtypes. The first class represents CRISPR/CAS systems with several effector molecules and protein complexes for the adaptive immunity and includes the type I, III and IV system. The class two includes all systems with a single effector protein for the binding and cleavage of foreign DNA and consists of the type II, V and VI system (Figure 7).
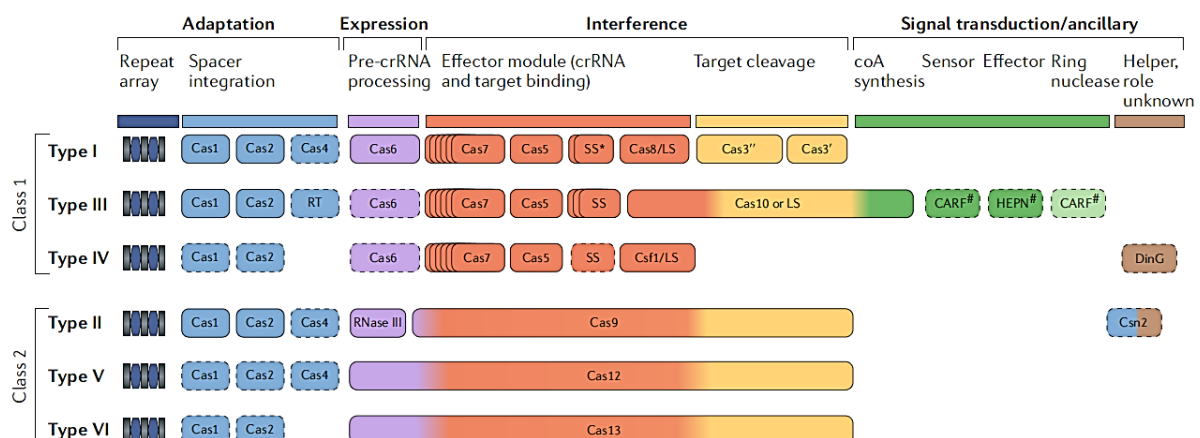

Figure 7: CRISPR/CAS systems divided into different types and functions. The CRISPR/CAS systems are separated in two classes and six types depending on their effector genes and functions, corresponding to the steps of the adaptation, expression, interference and signal transduction/ancillary (Makarova *et al*., 2020).

The endonucleases Cas1 and Cas2 are responsible for the spacer insertion and can be found in every system, whereas the cleavage endonucleases vary from system to system. The systems of class two are used in the biotechnology for genome modification in bacteria, plant, fungi and human cell lines (Makarova *et al*., 2020). Typical representatives of the different systems are for example *E. coli* K12 for subtype I, *Legionella pneumophila* for subtype II, *Staphylococcus epidermis* for subtype III, *Rhodococcus jostii* for subtype IV, *Plantomycetes bacterium* for subtype V and *Fusobacterium perfoetens* for subtype VI. This demonstrates that the occurrence of CRISPR/CAS systems is very diverse and represented in all ecological niches (Makarova *et al*., 2015).

CRISPR/CAS I-F subtype system in *B. plantarii* PG1

B. plantarii PG1 possesses a CRISPR/CAS I-F subtype system like the original Ypest from *Yersinia pestis* (Haft *et al.*, 2005, Cady *et al.*, 2011). The special characteristic of the I-F subtype is the formation of an effector molecule complex to bind foreign DNA. The I-F subtype system in *B. plantarii* PG1 consists of the endonucleases Cas3 for the target cleavage, Cas1 for the spacer insertion and a *csy* surveillance complex comprising of Csy1 (Cas8f), Csy2 (Cas5f), Csy3 (Cas7f and Csy4 (Cas6f). The effector proteins build a complex for the target binding which leads to a conformation change. This change initiates the recruitment of the endonuclease Cas3 for the target binding and elimination of foreign DNA (Figure 8). This complex is currently being studied and interesting aspects regarding possible independent activities of the effector molecules have been revealed (Przybilski *et al.*, 2011, Westra *et al.*, 2012).
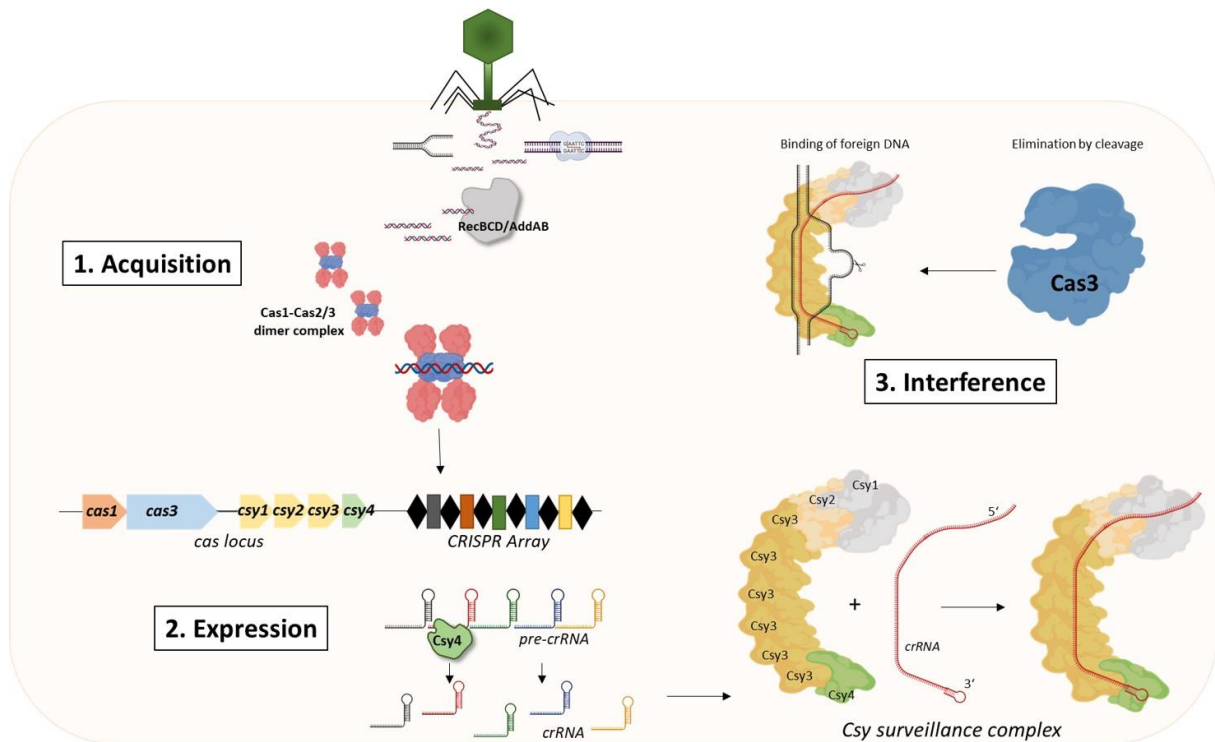
Figure 8: Scheme of CRISPR/CAS I-F subtype system immunity in *B. plantarii* PG1. Three stages of CRISPR/CAS immunity: 1. Acquisition: includes the incorporation of the foreign DNA as a new protospacer into the CRISPR array. 2. Expression: describes the expression of all required enzymes and the transcription of the CRISPR array as well as the further processing to crRNA. 3. Interference is the stage of binding the foreign DNA and recruiting the endonuclease to eliminate the foreign DNA by cleavage (Created with Biorender).

The CRISPR/CAS I-F subtype system belongs to the class 1 CRISPR/CAS systems which are found in ~60% of bacteria and archaea with a CRISPR/CAS system (Hidalgo-Cantabrana *et al.*, 2019). In addition, the system was made accessible for biotechnological applications in the field of genome editing and control of gene expression (Yanli Zheng *et al.*, 2020, Rath *et al.*, 2015, Zheng *et al.*, 2019).

1.5 Quorum sensing

Quorum sensing is the ability of bacteria to sense their own population density and induce a coordinated response (Fuqua *et al.*, 1994). This is possible through the perception and production of diffusible low-molecular, organic signal molecules, so-called autoinducers (AIs) (He *et al.*, 2003). The ability for cell-cell communication is used by bacteria to coordinate processes that are only efficient in association, such as the formation of biofilms, bioluminescence and the secretion of antibiotics or pathogenicity factors (Abisado *et al.*, 2018). Autoinducers are divided into three larger groups of autoinducer-I and -II and autoinducer

peptides (AI-I, AI-II, AIP). Autoinducer-I are acyl homoserine lactones, which are used for the communication between the same species. Autoinducer-II are furanosyl borate diester, which are used for the communication across species boundaries. Whereas autoinducer peptides are only used in Gram-positive bacteria and are transported by special transport systems through the cell and coordinates the expression of virulence factors (Bassler *et al.*, 2006, C. S. Kim *et al.*, 2020, Verbeke *et al.*, 2017).

Quorum sensing in *B. plantarii* PG1

Most representatives of *B. plantarii* possesses one or two AHL-associated QS systems. In 2015, a third QS system was discovered in *B. plantarii* PG1. The first AHL-associated QS system encodes for N-octanoyl-L-homoserine lactones (C8-HSL), whereas the second encodes for N-decanoyl-L-homoserine lactones (C10-HSL) and the third one for C10-HSL or N-dodecanoyl-L-homoserine lactones (C12-HSL). In a previous work, QS deletion mutants were created to investigate the QS system and its influence on the metabolism of the organism (Figure 9). Transcriptome analysis determined that the QS system has an influence on the motility, lipase activity, phytopathogenicity and the CRISPR/CAS system in *B. plantarii* PG1.
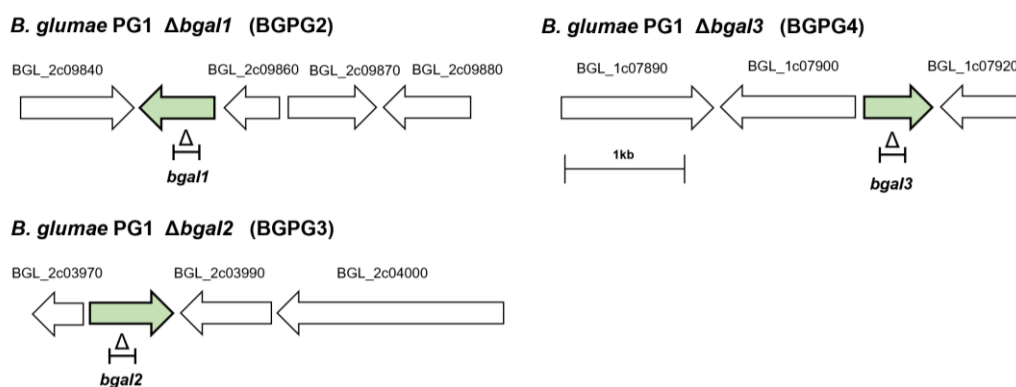

Figure 9: Design of the QS deletion mutants of BpPG2, BpPG3 and BpPG4. The deletion mutants were created by homologous recombination and the insertion of a gentamycin cassette located at the genes of *bgal*1, *bgal*2 and *bgal*3. PG1 (wildtype), PG2 (BGPG1Δ*bgal*1), PG3 (BGPG1Δ*bgal*2), PG4 (BGPG1Δ*bgal*3) (Gao *et al.*, 2015).

The QS deletion mutants were created via homologous recombination by amplifying homologous regions and introducing a gentamycin cassette as a selection marker. They were declared as PG1 (BGPG1 wild type), PG2 (BGPG1Δ*bgal*1), PG3 (BGPG1Δ*bgal*2) and PG4 (BGPG1Δ*bgal*3) and were used in this study for further investigations (Gao *et al.*, 2015). Apart from the influence of QS systems on motility, lipolytic activity and phytopathogenicity, transcriptomic analysis has shown that QS systems also play a role in the regulation of the

CRISPR/CAS system in this organism. The lack of AHL molecules leads to a gradually decreased transcription level of CRISPR/CAS genes in all QS deletion mutants which indicates a kind of network regulation (Figure 10) (Gao *et al.*, 2015).
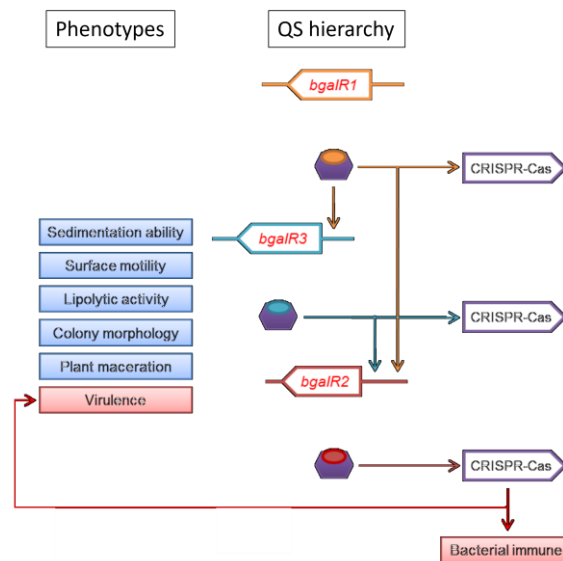

Figure 10: QS hierarchy regarding to the CRISPR/CAS system in *B. plantarii* PG1 according to the study of R. Gao. It displays a QS hierarchy of the different QS synthases and their influence on the phenotype with regard to sedimentation, motility, lipolytic activity, colony morphology, plant maceration, virulence and the CRISPR/CAS system. *bgalR1*= BGPG1Δ*bgal*1, *bgalR2*= BGPG1Δ*bgal*2, *bgalR3*= BGPG1Δ*bgal*3 (modified, R. Gao, 2015).

The impact of the QS system at essential cell functions related to the CRISPR/CAS system has also been described in other studies. For example, the inhibition of the QS system in *Pseudomonas aeruginosa* leads to a reducing resistance against foreign DNA (Høyland-Kroghsbo *et al.*, 2017).

1.6 Intention of this study

In this work, we were interested in the question if the unique position of the hydroxyethylthiazole kinase ThiM is related to the regulation of the CRISPR/CAS I-F system. First insights indicated an influence of the kinase ThiM on the CRISPR/CAS system. Further comparative transcriptome analyses should be performed to verify the role of these kinase. In addition, with the exception of Rong Gao's study in 2015, no transcriptome dataset in this dimension was previously available of this organism. In metabolic network analyses, expression patterns should be analysed, and metabolic pathways reconstructed. Furthermore, the CRISPR/CAS system should be characterised more in detail. Other possible regulators should be investigated here and whether the system is regulated in a QS-associated manner.

2 Material and Methods

2.1 Bacterial strains, vectors, constructs and oligonucleotides

The following table 1 contains all working strains and their characteristics.

Table 1: Bacterial strains, characteristics and references

Bacterial strains	Characteristics	Reference/Source
Burkholderia plantarii PG1	wildtype	Frenken *et al.*, 1992
Burkholderia plantarii PG2	deletion mutant, Δ*bgal*1, GmR	Gao R. *et al.*, 2015
Burkholderia plantarii PG3	deletion mutant, Δ*bgal*2, GmR	Gao R. *et al.*, 2015
Burkholderia plantarii PG4	deletion mutant, Δ*bgal*3, GmR	Gao R. *et al.*, 2015
Burkholderia plantarii PG1Δ*thiM*	deletion mutant, Δ*thiM*	Hongli Zhang, 2018 unpublished

The table 2 displays all plasmids which were used and created constructs. The cloning experiments were first simulated with the Clone Manager software and the specific primers were designed with the SnapGene software.

Table 2: Plasmids, constructs, characteristics and references

Plasmid/Construct	Characteristics	Reference
pBBR1MCS-2 (*E.coli* DH5α)	Broad host range vector, lacZ, *kan*R	Kovach *et al.*, 1995
pBBR1MCS-5 (*E.coli* DH5α)	Broad host range vector, lacZ, *Gen*R	Kovach *et al.*, 1995
pBBR1MCS-2:: mcherry_noprom (*E.coli* DH5α and BpPG1)	Broad host range vector, lacZ, *kan*R mcherry without promoter (negative control)	This study
pBBR1MCS-2:: mcherry_NGR234prom.vv (*E.coli* DH5α and BpPG1)	Broad host range vector, lacZ, *kan*R mcherry with the promoter of NGR234 in reverse direction (negative control)	This study
pBBR1MCS-2:: mcherry_prom_rpoD_BpPG1 (*E.coli* DH5α and BpPG1)	Broad host range vector, lacZ, *kan*R mcherry with the promoter of rpoD of BpPG1 (positive control)	This study
pBBR1MCS-2:: promthiM+Rb::mcherry (*E.coli* DH5α and BpPG1)	Broad host range vector, lacZ, *kan*R mcherry with the promoter of *thiM* with Riboswitch	This study
pBBR1MCS-5:: promcas1::mcherry (*E.coli* DH5α and BpPG1)	Broad host range vector, lacZ, *Gen*R mcherry with the promoter of *cas1*	This study

pBBR1MCS-2:: promcas1::mcherry (*E.coli* DH5α and BpPG1)	Broad host range vector, lacZ, *kan*R mcherry with the promoter of *cas1*	This study
pBBR1MCS-2:: promcsy1::mcherry (*E.coli* DH5α and BpPG1)	Broad host range vector, lacZ, *kan*R mcherry with the promoter of *csy1*	This study
pBBR1MCS-2:: promcsy4::mcherry (*E.coli* DH5α and BpPG1)	Broad host range vector, lacZ, *kan*R mcherry with the promoter of *csy4*	This study
pBBR1MCS-2 ::CRP1 (*E.coli* DH5α and BpPG1)	Broad host range vector, lacZ, *kan*R with the putative regulator CRP1	This study
pBBR1MCS-2 ::CRP3 (*E.coli* DH5α and BpPG1)	Broad host range vector, lacZ, *kan*R with the putative regulator CRP3	This study

The following table 3 includes all used supplements and their standard concentration. Heat insensitive supplements prepared in distilled water and sterile filtrated with a 0.2µm filter (Clearline, Filtre seringue, 30 mm AC, 0.2µm). Ethanol soluble additives were dissolved in 70% ethanol.

Table 3: Antibiotics and supplements

Supplement	Standard concentration (mg/ml]	Solvent
Ampicillin	100	H_2O_{bidest}
Rifampicin	25	MetOH
Kanamycin	25	H_2O_{bidest}
Neomycin	80	H_2O_{bidest}
Spectinomycin	50	H_2O_{bidest}
Streptomycin	50	H_2O_{bidest}
Gentamycin	10	H_2O_{bidest}
Tetracycline	5	EtOH (70%)
Norfloxacin	5	EtOH (70%)
Chloramphenicol	50	EtOH (70%)
Trimethoprim	50	EtOH (70%)
IPTG	1M	H_2O_{bidest}
XGAL	0,04	DMF

The table 4 lists all primer sequences and annealing temperatures which were used.

Table 4: Primer sequences with annealing temperatures

Primer	Sequence 5'-3'	anneali. Tm°C	bp
M13-20_for	TTGTAAAACGACGGCCAGTG	55	229
M13_rev	GGAAACAGCTATGACCATGA		
promcas1_EcoRI_fw	GAATTCCGGCCTGAGGGCGGTG	64	165
promcas1_BamHI_rev	GGATCCTGGCGCCCCGTCATTTTTGT		
promcsy1_SacI_fw	GAGCTCGAGGGCTGCCTGTTCGGCAGAA	61	375
promcsy1_EcoRI_rev	GAATTCTCGGTTTCCTTCGGAATGGGTTTGACG		
promcsy4_SacI_fw	GAGCTCGAGCAAGACGCTTTATCAGGTGCGC	65	303
promcsy4_EcoRI_rev	GAATTCGGCGGTCAGCTCGCGTCG		
mcherry_noprom_fw	AATTCATGGTGAGCAAGG	47	
mcherry_noprom_rev	CACTAGTTCTAGAGCGGC		
CRP1_XbaI_fw	TCTAGAGCCCGCATCATCGCGCAAGC	65	787
CRP1_BamHI_rev	GGATCCCGCTGATCTCAGAGGGATTGAGTTGCATATTCGC		
CRP3_ApaI_fw	GGGCCCCACCTGCTGCATGCCGAGGCTCA	62	825
CRP3_ClaI_rev	ATCGATCGCCGGCTTCTATTCGTCGATGAAGTA		

2.2   Molecular biology methods

Culture media and supplements

All media were autoclaved at 121°C and 2 bar for 20 min. Heat sensitive supplements were added after a cooling to 55°C.

Cultivation and storage of bacteria

All *E. coli* strains were cultivated at 37°C in liquid on shaking at 120rpm and on agar plates in an incubator cabinet. All Burkholderia strains were cultivated at 28°C in liquid at 120rpm and on agar plates in an incubator cabinet. All strains were stored on agar plates at 5°C and in liquid in cryo-cultures, 1:3 added with glycerine at -70°C.

LB medium (Luria-Bertani):

Tryptone	10 g
Yeast Extract	5 g
Sodium Chloride	5 g
(Agar-Agar	14 g)
H_2O_{bidest}	*ad* 1000 ml

M9 medium (Mineral):

375 ml H_2O_{bidest}

(+ 6 g agar) -> autoclave

After autoclaving add:
+ 100 ml   M9 salt solution (5x)
+   1 ml $MgSO_4$ (1M)
+   4 ml   Glucose (50%)
+   0.5 ml $CaCl_2$ (100 mM)
+   10 ml   Casamino acids (10% solution)
+   0.5 ml   Thiamine (vitamin B1, 100 mg/ml)

M9 salt solution (5x) 500 ml:

Na_2HPO_4 x $7H_2O$	120 mM
KH_2PO_4	55 mM
NaCl	20 mM
NH_4Cl	45 mM

2.3   Cloning methods

Isolation of genomic DNA

The isolation of genomic DNA was conducted with the kit NucleoSpin Microbial DNA of Macherey-Nagel GmbH & Co. KG according to the manufacturer's instructions and were eluted in 30µl $_{dd}H_2O$. It is based on the DNA binding mechanism of electronic exchange of positive loaded Silicia molecules to the negative loaded phosphate groups of the DNA.

Purification and Gel extraction of genomic DNA

The purification and gel extraction of DNA were performed with Gel/PCR DNA Fragments Extraction kit NucleoSpin Gel and PCR Clean-up by Macherey-Nagel GmbH & Co KG according to the manufacturer's instructions. The elution volume was reduced to 30µl H_2O_{bidest} and is based on the same mechanism as the genomic DNA Isolation.

Detection of nucleic acids

The gel electrophoresis is a separation method by size and charge to detect macromolecules like DNA. The negative charged DNA passes through an agarose gel to the positive charged anode, which leads to a separating of the DNA fragments by size in an electric field. The samples were supplemented 1:4 with 4x Loading Dye and separated by 0.8 - 2% agarose gels in a 1x TAE buffer solution at 100 V for 60 min.

50x TAE Buffer:

Tris	2 M
EDTA	0.1 M
H_2O_{bidest}	*ad* 1000 ml
HAc	pH 8.0

4x Loading Dye:

30 % Glycerine	60 ml
EDTA	0.05 M
0.25 % Bromophenol blue	0.5 g
H_2O_{bidest}	*ad* 200 ml

Polymerase chain reaction (PCR)

The polymerase chain reaction is a method to generate multiple copies of a specific DNA fragment and is divided into three steps. The first step of denaturation comprises the heat activation of the used DNA polymerase and the DNA melting of the DNA double strand. In the second step, the annealing, the temperature is adjusted according to the melting temperature of the primers for binding to the DNA. In the last step of elongation, the targeted DNA fragment is amplified in multiple copy numbers depending on chosen cycles. The temperatures of the different steps change regarding to the used polymerase, primers and fragment size, shown in the following table.

Table 5: Pipetting scheme of the DCS polymerase PCR

DCS Polymerase	µl/ to 50 µl	Cycler program			
10 x DCS Buffer	5	Initial Denaturation	95°C	5 min	1x
MgCl$_2$ (25 mM)	2.5				
dNTP Mix (10 mM)	2	Denaturation	95°C	30 sec	
Primer fw/rev (10 mM)	1 of each	Annealing	Tm-5°C	30 sec	35x
DMSO	1	Elongation	72°C	min/kb	
DCS Polymerase	0.5				
H$_2$O$_{bidest}$	37	Final Elongation	72°C	5 min	1x

Restriction

For the restriction of DNA fragments, restriction enzymes possess the ability to cut a DNA with blunt or sticky ends at a specific recognition site. The restriction approaches differ by the use of one or two enzymes, the analytic or preparative digest and the possibility of heat inactivation and star activity.

Table 6: Reaction approach for analytic and preparative digest

Analytic digest			Preparative digest		
DNA	0.1-1	µg	DNA	0.1-1	µg
Buffer	1	µl	Buffer	2	µl
Enzyme X	1-2	µl	Enzyme X	1-2	µl
Enzyme X	1-2	µl	Enzyme X	1-2	µl
H$_2$O$_{bidest}$	1-3	µl	H$_2$O$_{bidest}$	12-15	µl

The restriction approaches were incubated at 37°C for 3 - 16h. Enzyme inactivation after incubation was performed by heat inactivation varied between 60°C and 80°C for 20 min or by purification using a silica gel column in case a heat inactivation was not possible.

Ligation

The ligation approach is performed by using the T4 Ligase with different protocols depending on fragment number and type.

Table 7: Reaction approach of the ligation of DNA fragments

Ligation of two DNA fragments		Ligation of DNA fragment and plasmid		Cycler program		
DNA - DNA	1:1	DNA - Plasmid	3:1	10°C	30 sec	
T4 Ligase	1 µl	T4 Ligase	1 µl	30°C	30 sec	x30
10x T4 Ligase Buffer	1 x	10x T4 Ligase Buffer	1 x	75°C	10 min	
		16°C over night or cycling program				

Transformation in *E. coli*

After ligation, the constructs were inserted in chemical or electro-competent cells. For the transformation in chemical competent cells, first the cells were incubated for 10 min on ice. The ligation approach was added in a volume of 5µl to the cells and incubated for 20 min on ice again. By a heat shock of 90 sec at 42°C and following cooling time of 2 min on ice, the construct was inserted into the cells. The transformation approach was combined with 600 µl of LB medium and shaking incubated for 20 min at 37°C for the electro-competent cells until it was platted on selective agar plates in volumes of 50, 100 and 150 µl and incubated for 24h at 37°C.

Electroporation in *E. coli* and *B. plantarii* PG1

For the insertion of a construct in electro-competent cells, the electro-competent cells were incubated for 10 min on ice. In the next step 2 µl of the construct were added to the electro-competent cells and shocked electrically in *E. coli* in 1mm cuvette by 1,8 kV, 25Ω, in BpPG1 by 2,5 kV, 25Ω. The cells were mixed with 800 µl of LB medium and shaking incubated for 2 h at 37°C for *E. coli* and at 28°C overnight for BpPG1. After the incubation the suspension was platted on agar plates in volume of 50, 100 and 150 µl and incubated for 24 h-72 h at the optimal growth temperature.

2.4 RNA isolation of *B. plantarii* PG1

RNA extraction

The RNA extraction from bacterial cultures were performed with Direct-zol RNA MiniPrep Plus kit of Zymo Reserach and were modified as described in the following. In the first step a 20ml bacterial culture was centrifuged for 5 min at 4500 rpm on 4°C for pelleting the cells. The supernatant was discarded until 1ml was left on the pellet. The pellet was resuspended in the left supernatant of the bacterial suspension and transferred into a bashing bead column (ZR BashingBead Lysis Tubes (0.1- & 0.5-mm Beads) of Zymo Research). The suspension was mixed with triple volume of Trizol Reagent of Thermofisher and homogenized with bashing beads on a horizontal shaker with max. speed for 10 min. After incubation on the horizontal shaker the column was centrifuged for 1 min at 13.000 g at 4°C and the supernatant was transferred into a fresh tube. The supernatant was mixed with an equal volume of ethanol (95-100%) and transferred into a Zymo-SpinTM IIC Column in a collection tube and centrifuged for 30 sec at 13.000 g at 4°C. The supernatant was discarded, and the column was washed with the RNA PreWash and RNA wash Buffer as in the instruction manual. The sample was eluted in 50µl of DEPC water.

In the next step, possible RNases must be removed by a purification with RTS DNase Kit of MoBio Laboratories, Inc. with the following modifications.

DNase Digest

10x RTS Buffer	5	µl
DNase	1	µl
RNA (0.1 - 1µg)	44	µL
	->	Incubation at 37°C for 20 min
add	1	µl DNase
	->	Incubation at 37°C for 20 min
	->	Centrifuge for 1 min at 13.000 g
	->	Collect the supernatant in a new collection tube

RNA detection and control

To control the isolated RNA, the RNA was detected by a 0.8% agarose gel and a 16S PCR was performed to avoid residues of DNA. Finally, the RNA was stored at -70°C.

2.5 RNA sequencing

In order to RNA sequencing and transcriptome analysis different BpPG1 strain cultures were collected in biological triplicates at the late exponential (48h) and stationary growth phase (72h) under different medium conditions (4500 g, 5 min, 4°C). RNA transcriptomic analyses were executed at Genomics Laboratory of George-August-University of Göttingen under the supervision of Dr. Anja Poehlein. The transcriptome raw data were uploaded in NCBI at BioProject ID: 925312, Accession: PRJNA925312. The accession numbers of all replicates are displayed in the appendix Table A3.

2.6 Transcriptome analysis of *B. plantarii* PG1 strains under different conditions

By creating growth curves at 28°C in selective media the optimal growth phase was identified to prepare samples for the RNA sequencing. For the RNA isolation, cDNA library preparation and RNA-seq with Illumina, cell pellets of the different samples were prepared and sent to Göttingen Genomics Laboratory of Göttingen University (Göttingen, Germany). The cultures were cultivated in selective media for 48h for the late exponential growth phase and for 72h for the late stationary growth phase at 130 rpm with a start OD_{600} of 0.05 in biological triplicates.

Bioinformatic analysis

The bioinformatical analysis of the differential gene expressions was determined in the Göttingen Genomics Laboratory according to the annotation in NCBI by their bioinformatical service. In further analysis, the annotated genes were classified as greater than log2foldchange of 2 as significant for up-regulated genes and less than -2 as significant for down-regulated genes. The amino sequences of the significant genes were sorted by fa.box and annotated to pathways with BlastKOALA to determine genes distribution in different pathways. For the detailed analysis of metabolic pathways, KEGG mapper was used, and the up- and down-regulated genes were clustered to the different pathways according to their Locus Tags. The following table displays the analysed strains and their growth conditions.

Table 8: Different strains and growing conditions of the RNA-seq.

Bacterial strains	Tm°C	time (h)	medium
BpPG1	28°C	48*	LB + Cm
BpPG1	28°C	48	M9, no thiamine + Cm
BpPG1Δ*thiM*	28°C	48	LB + Cm
BpPG1Δ*thiM*	28°C	48	M9, no thiamine + Cm
BpPG1 pBBR1MCS-2	28°C	48	LB + Cm
BpPG1 pBBR1MCS-2::CRP1	28°C	48	LB + Cm
BpPG1 pBBR1MCS-2::CRP1	28°C	48	LB + Cm

*late exponential growth phase

Bacterial strains	Tm°C	time (h)	medium
BpPG1	28°C	72*	LB + Cm
BpPG1	28°C	72	M9, no thiamine + Cm
BpPG1	28°C	72	M9(-t) + Cm +
			7.5 mM thiamine

*late stationary growth phase

2.7 Promoter and binding motif predictions

The promoter prediction of possible promoter sites in the CRISPR/CAS cluster were performed with softberry analysis. To determine possible regulator binding motifs in the CRISPR/CAS cluster several alignments with organism which possesses a binding motive of the respective regulator and a CRISPR/CAS system, were executed. The data and sequences are displayed in the appendix Table A1.

2.8 Fluorescence detection assays at the plate reader

The different promoter fusion strains were created with the fluorescence protein mcherry. The different strains were cultivated in 42 well plates (Nunclon^{TM} Delta Surface, flat bottom, ThermoFischer) in 1 ml selective medium shaking at 28°C for 24h, 48h and 72h. To examine the fluorescence level of the different strains the plates were measured at the plate reader (Synergy H1 plate reader, BioTek Instruments Inc.) with a monochromator from the bottom of the plates. The non-fluorescence wildtype strain BpPG1 was used as blank control.

2.9 Biofilm assays

To evaluate the static biofilm formation of the different strains the different promoter fusion strains were cultivated in 8 well µ-Slides of ibidi in 300µl per well with a starting OD_{600} of 0.05 for 48h at 28°C in biological triplicates. For the staining, the supernatant was discarded carefully with a pipette and 200µl of the LIVE/DEAD solution was added in each well. The biofilms were incubated for 30-60 min in the dark and detected with a 63x water objective with a Zeiss confocal microscope under the setting conditions displayed in table 6 and 7.

2.10 Confocal microscopy

The fluorescence level of the different promoter fusion strains was analysed with confocal microscopy (LSM 800 by Zeiss). The settings changes depending on the experimental conditions. The following table includes all settings for the fluorescence measurement of liquid cultures.

Table 9: Settings for fluorescence measurement of liquid cultures at the confocal microscope

Settings	mcherry	DAPI
Objective	Plan-Apochromat 63x/1.40 OIL DIC M27	
Reflector	none	none
Contrast method	Fluorescence	Fluorescence
Pinhole	5.20 AU / 266 µm	6.03 AU / 236 µm
Laser wavelength	561 nm; 5.00 %	405 nm; 2.00 %
Extinction wavelength	587	353
Emission wavelength	610	465
Detection wavelength	570-700	400-600
Detector gain	900 V	900 V
Digital detector gain	1.0	1.0

This table includes all settings for the fluorescence measurement of biofilm formation analysis with the used fluorescence levels of mcherry and DAPI.

Table 10: Settings for fluorescence measurement of biofilm formation at the confocal microscope

Settings	mcherry	DAPI
Objective	C-Apochromat 63x/1.20 W Korr UV VIS IR	
Reflector	none	none
Contrast method	Fluorescence	Fluorescence
Pinhole	4.42 AU / 200 µm	4.42 AU / 200 µm
Laser wavelength	405 nm: 10.00 %, 561 nm: 10.00%	405 nm: 10.00 %, 561 nm: 10.00%
Extinction wavelength	587	353
Emission wavelength	610	465
Detection wavelength	590-700	410-500
Detector gain	600 V	600 V
Digital detector gain	1.0	1.0

The settings for the fluorescence measurement of biofilm formation analysis with the fluorescence levels of the LIVE/DEAD staining (LIVE/DEAD™ BacLight™, propidium iodide (red=dead cells) and SYTO9 (green=live cells)) are shown in the following table.

Table 11: Settings for fluorescence measurement of LIVE/DEAD staining at the confocal microscope

Settings	Propidium iodide (PI)	SYTO9 (Syt9)
Objective	C-Apochromat 63x/1.20 W Korr UV VIS IR	
Reflector	none	none
Contrast method	Fluorescence	Fluorescence
Pinhole	1.02 AU / 62 µm	1.05 AU / 51 µm
Laser wavelength	561 nm: 0.2 %	488 nm: 0.2 %
Extinction wavelength	305	483
Emission wavelength	617	500
Detection wavelength	450-700	450-560
Detector gain	700 V	700 V
Digital detector gain	1.0	1.0

3 Results

3.1 A hydroxyethylthiazole kinase as possible regulator of the CRISPR/CAS I-F system

Figure 11: Transcriptome analysis revealed different transcript levels of the CRISPR/CAS system. Here, the gene card of the CRISPR/CAS I-F system in *B. plantarii* PG1 is displayed, containing *cas1*, *cas3* and *csy1-4*. The unique position of *thiM* is shown in grey upstream of *cas1*. An asymmetric transcriptional pattern was observed with increased transcript levels of *thiM*, *csy1*, *csy2* and *csy3*.

The gene neighbourhood region searches with the same top COG hit (via top homolog) by IMG in other relatives confirmed the unique position of the hydroxyethylthiazole kinase ThiM upstream of the endonuclease Cas1 (Figure 2). Despite the genes of the thiamine metabolism are usually distributed over the genome of an organism, the location of the kinase ThiM is still special. First transcriptome analysis of *B. plantarii* PG1 in the early exponential growth phase (28h) in LB-medium performed in Rong Gao's study revealed asymmetric transcriptional patterns with increased transcript levels of the kinase ThiM and the CRISPR/CAS genes *csy1*, *csy2* and *csy3* (Figure 11). This led to the assumption that ThiM could have an influence on the CRISPR/CAS system and could play a role in its regulatory mechanism. The kinase ThiM is part of the salvage pathway of the thiamine metabolism and required for the phosphorylation of precursors to thiamine pyrophosphate (TPP), the active form of thiamine. TPP is an essential cofactor of several metabolic processes in bacteria and TPP as well as the kinase ThiM could also play an active role as a regulator in the control of other processes. For further insights, a comparative transcriptome analysis with new transcriptomic data was performed. Here the wildtype *B. plantarii* PG1 was compared to a previously created deletion mutant of ThiM (BpPG1Δ*thiM*). The samples for the transcriptome analysis were cultivated in different media as in the nutritionally rich LB-medium, in a mineral M9 medium without thiamine and a mineral M9 medium supplemented with 7.5 mM thiamine at the late exponential (48h) and the late stationary growth phase (72h) (Table 8).
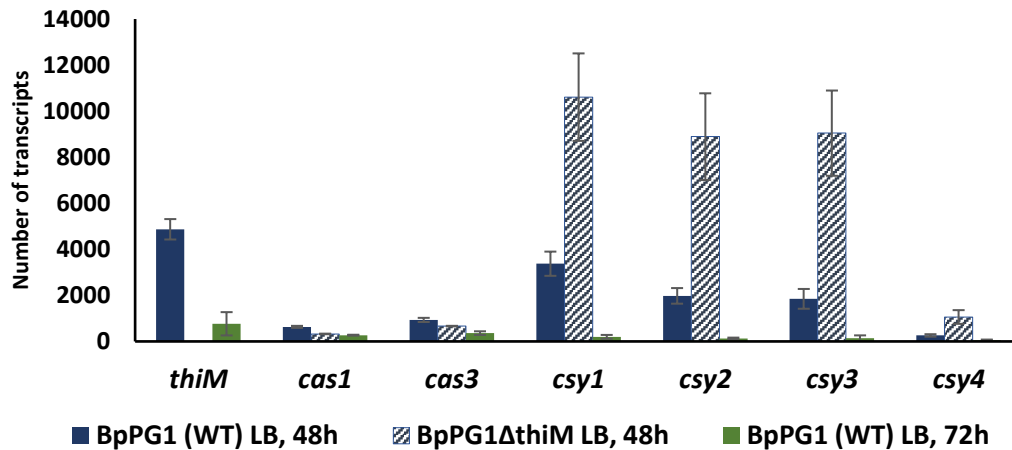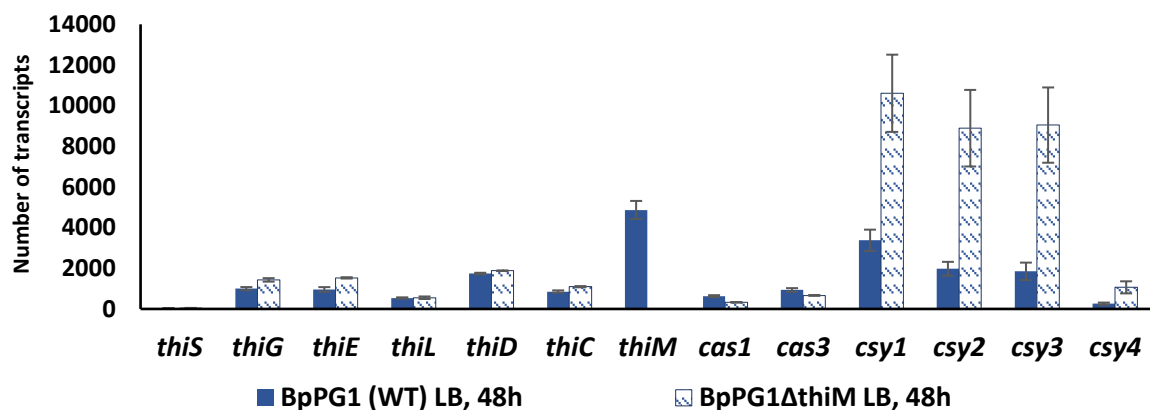
Figure 12: Differential expression analysis of BpPG1(WT) and BpPG1Δ*thiM* in the late exponential growth phase (48h) and BpPG1(WT) in the late stationary growth phase (72h) in LB medium. BpPG1(WT), 48h = blue bars, BpPG1(WT), 72h = dark green bars, BpPG1Δ*thiM*, 48h = pattern filled bars. Display of the number of transcripts of *thiM* and the CRISPR/CAS system. The mean values of three replicates are represented and bars indicate relative standard deviation.

At first the number of transcripts of the genes of the CRISPR/CAS system as well as of the kinase ThiM were determined. The comparison of the number of transcripts of the wildtype *B. plantarii* PG1 (BpPG1) to the deletion mutant BpPG1Δ*thiM* in the late exponential growth phase (48h) and the wildtype BpPG1 in the late stationary growth phase (72) in LB medium revealed an increased transcript level of the genes *csy1-3* in the late exponential growth phase (48h) in the deletion mutant BpPG1Δ*thiM*. Furthermore, the transcript levels of *thiM* and *csy1-3* were increased in the late exponential growth phase (48h) compared to the late stationary growth phase (72h) in the wildtype BpPG1. This was valuable for choosing the optimal growth conditions for further experiments relating to the activity of the CRISPR/CAS system (Figure 12). For further advances the wildtype BpPG1 and the deletion mutant BpPG1Δ*thiM* were compared in LB medium and in M9 medium without thiamine in the late exponential growth phase (48h) (Figure 13 and 14).
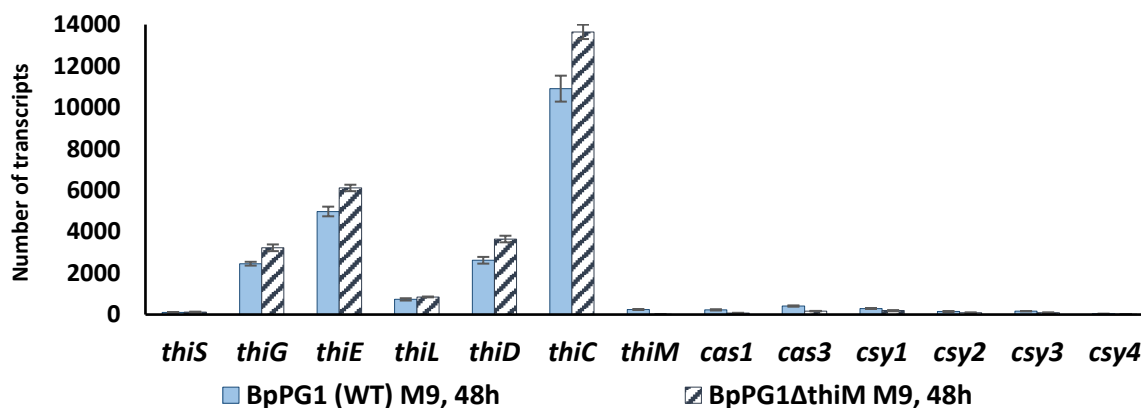
Figure 13: Differential expression analysis of BpPG1(WT) and BpPG1Δ*thiM* in the late exponential growth phase (48h) in LB medium. Display of the number of transcripts of important genes of the thiamine metabolism (*thiS, thiG, thiE, thiL, thiD, thiC, thiM*) and the CRISPR/CAS system *cas1*, *cas3, csy1-4*. BpPG1(WT) = blue bars, BpPG1Δ*thiM* = pattern filled bars. The mean values of three replicates are represented and bars indicate relative standard deviation.

The comparison of the wildtype BpPG1 to the deletion mutant BpPG1Δ*thiM* in LB medium in the late exponential growth phase (48h) showed no major variations in the transcript levels of the genes of the thiamine metabolism. However, the transcript levels of the genes *csy1-3* of the CRISPR/CAS system were highly increased in the deletion mutant BpPG1Δ*thiM* compared to the wildtype (Figure 13).

Figure 14: Differential expression analysis of BpPG1(WT) and BpPG1Δ*thiM* in the late exponential growth phase (48h) in M9 medium without thiamine. Display of the number of transcripts of important genes of the thiamine metabolism (*thiS, thiG, thiE, thiL, thiD, thiC, thiM*) and the CRISPR/CAS system *cas1*, *cas3, csy1-4*. BpPG1(WT) = blue bars, BpPG1Δ*thiM* = pattern filled bars. The mean values of three replicates are represented and bars indicate relative standard deviation.

The analysis of the transcript levels in M9 medium was completely different. Here a higher transcript level of the genes of the thiamine metabolism emerged, and no significant activity of the genes of the CRISPR/CAS system were observed (Figure 14).
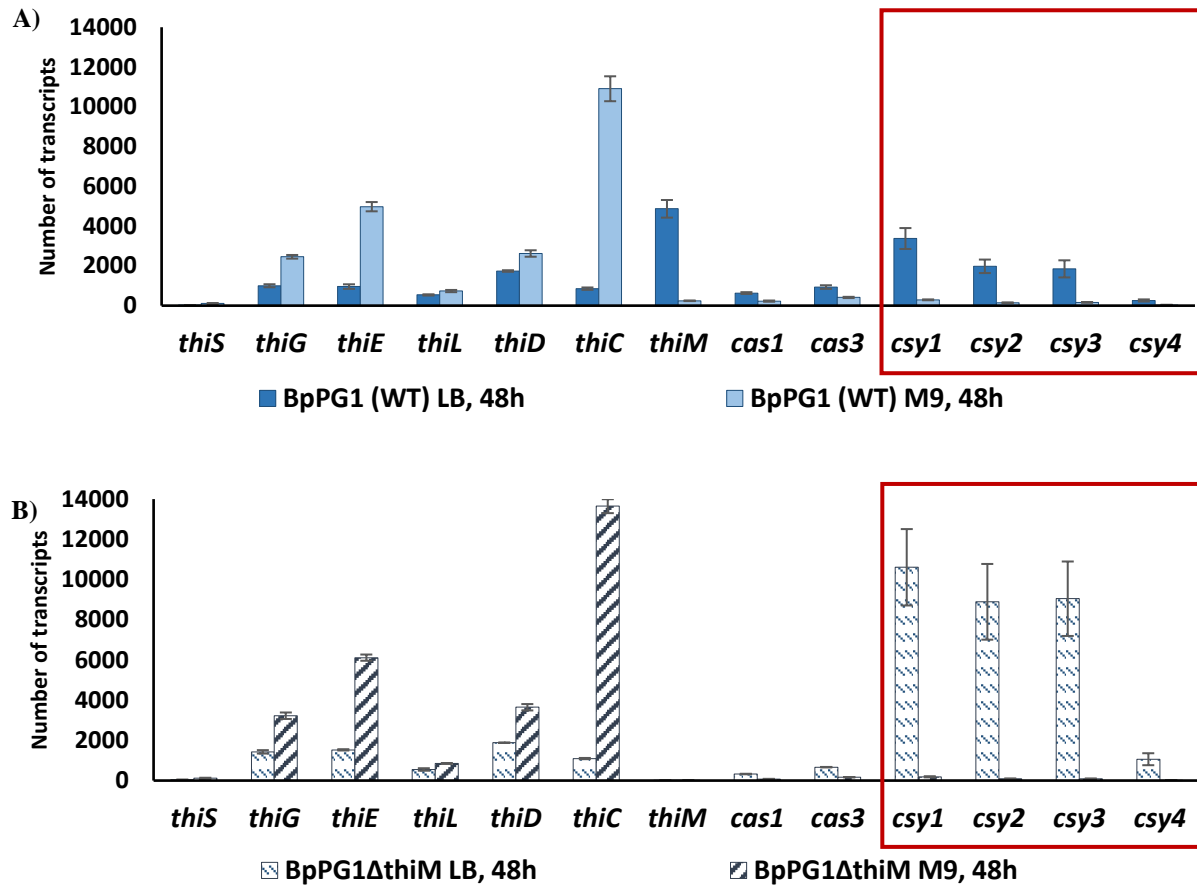
Figure 15: Comparison of the differential expression analysis of BpPG1(WT) and BpPG1Δ*thiM* in the late exponential growth phase (48h) in LB to M9 medium without thiamine. Display of the number of transcripts of important genes of the thiamine metabolism (*thiS, thiG, thiE, thiL, thiD, thiC, thiM*) and the CRISPR/CAS system *cas1*, *cas3, csy1-4*. A) Comparison of BpPG1(WT) in LB (dark blue bars) to M9 medium without thiamine (light blue bars). B) Comparison of BpPG1Δ*thiM* in LB (thin pattern filled bars) to M9 medium without thiamine (big pattern filled bars). Red boxes highlight the differences between the two comparisons of the csy complex. The mean values of three replicates are represented and bars indicate relative standard deviation.

The direct comparison of the wildtype BpPG1 in LB medium to M9 medium without thiamine displayed an increased transcript level of the genes *csy1-3* in LB medium. Whereas several genes of the thiamine metabolism showed a higher activity in M9 medium without thiamine (Figure 15a). In the comparison of the deletion mutant BpPG1Δ*thiM* in LB to M9 medium without thiamine an extremely high increased transcript level of the genes *csy1-3* was determined in LB medium compared to the M9 medium without thiamine. However, the same increasing effect of the M9 medium without thiamine on the transcript level of several genes of the thiamine metabolism was also observed here as in the comparison of the wildtype BpPG1 in LB to M9 medium without thiamine (Figure 15b). These results led to the assumption that the observed effects were based on a medium effect and not displayed any influence of the

kinase ThiM on the CRISPR/CAS system. For further insights, the log2foldchanges of the collected transcriptome data were calculated for searching for potential significant differences. The annotated genes were classified to a log2foldchange ≥2 as significant for up-regulated genes and log2foldchange ≤ -2 as significant for down-regulated genes (Table 12).

Table 12: Comparison of the log2foldchange of the different transcriptome data of BpPG1Δ*thiM* versus BpPG1 WT in the late exponential growth phase (48h).

Locus Tag	Annotation	Δ*thiM*_LB_vs_ WT_LB log2foldchange	Δ*thiM* _M9_vs_ WT_M9 log2foldchange	Δ*thiM*_M9_vs_ Δ*thiM*_LB log2foldchange	WT_M9_vs_ WT_LB log2foldchange
BGL_1c18810	CRISPR-associated protein Cas1	-0.93*	-1.58*	**-2.11**	-1.46*
BGL_1c18820	CRISPR-associated protein Cas3	-0.43*	-1.28*	-1.99*	-1.17*
BGL_1c18830	CRISPR-associated protein Csy1	1.54*	-0.43*	**-5.78**	**-3.48**
BGL_1c18840	CRISPR-associated protein Csy2	**2.04**	-0.45*	**-6.60**	**-3.67**
BGL_1c18850	CRISPR-associated protein Csy3	**2.17**	-0.52*	**-6.56**	**-3.41**
BGL_1c18860	CRISPR-associated protein Csy4	1.73*	-0.61*	**-6.09**	**-2.69**

not significant

The analysis of the log2foldchanges of the wildtype BpPG1 and the deletion mutant BpPG1Δ*thiM* in LB and M9 medium without thiamine confirmed the results of the comparison of the number of transcripts. Here no significantly high differences were observed in the comparison of the strains in the same medium. In contrast, the comparison of the different media demonstrated significant transcriptional changes in both strains.

In conclusion, a direct regulation of the CRISPR/CAS system by the kinase ThiM could not be detected here. Only slight differences in the CRISPR/CAS genes of *csy2* and *csy3* were observed in the deletion mutant of BpPG1Δ*thiM* as well as in LB and M9 medium without supplemented thiamine. As previously mentioned, thiamine plays an important role in metabolic processes in bacteria and a possible coregulation of the thiamine metabolism and the CRISPR/CAS system were not excluded. For this reason, a metabolic network analysis was performed to gain further insights into metabolic processes and to elucidate the role of thiamine in the metabolism of *B. plantarii* PG1 as well as in the deletion mutant of BpPG1Δ*thiM*.

3.2 Comparative transcriptome analysis to identify different expression and regulation patterns

In the following, a metabolic network analysis was performed to identify expression patterns and elucidate metabolic processes. With the exception of Rong Gao's study in 2015, the collected transcriptome data represents the largest current dataset of this organism. In addition, the interplay of metabolic processes related to the thiamine metabolism was revealed regarding to the question if thiamine plays a role in the regulation of the CRISPR/CAS system in this study. *B. plantarii* PG1 is a Gram-negative rod-shaped soil bacterium which causes great diseases in plants and is exposed to constantly changing environmental conditions which forces the organism to metabolic adaptations to the changing environment. To further analyse these metabolic alterations, a comparative transcriptome analysis was performed under different conditions. The aim of this analysis was to understand the organisation of the metabolic pathways in *B. plantarii* PG1 and to investigate changes that occur under altered environmental conditions. The different strains, used media and time points are shown in the following table (Table 13).

Table 13: Bacterial strains and growing conditions of the comparative transcriptome analysis.

Bacterial strains	Tm°C	Time (h)	Medium
BpPG1 WT	28°C	48	LB + Cm
BpPG1 WT	28°C	48	M9, no thiamine + Cm
BpPG1Δ*thiM*	28°C	48	LB + Cm
BpPG1Δ*thiM*	28°C	48	M9, no thiamine + Cm
BpPG1 WT	28°C	72	LB + Cm
BpPG1 WT	28°C	72	M9, no thiamine + Cm
BpPG1 WT	28°C	72	M9(-t) + Cm + 7.5 mM thiamine

The bacterial cultures of the wildtype BpPG1 and the deletion mutant BpPG1Δ*thiM* were cultivated at 28°C to the late exponential (48h) and the late stationary growth phase (72h). As changing environmental conditions, the different media of LB medium and M9 medium without thiamine and M9 medium supplemented with 7.5 mM thiamine were used. All strains were cultivated under chloramphenicol conditions due to the intrinsic antibiotic resistance of *B. plantarii* PG1 (25mM). The following Table 14 contains the comparative conditions which were analysed here.

Table 14: Table of compared transcriptome analyses

Focused strain		Compared partner	Time (h)
BpPG1 WT in M9 medium without thiamine	**vs.**	BpPG1 WT in LB medium	48h
BpPG1Δ*thiM* in M9 medium without thiamine	**vs.**	BpPG1Δ*thiM* in LB medium	48h
BpPG1Δ*thiM* in LB medium	**vs.**	BpPG1 WT in LB medium	48h
BpPG1Δ*thiM* in M9 medium without thiamine	**vs.**	BpPG1 WT in M9 medium without thiamine	48h
BpPG1 WT in M9 medium without thiamine	**vs.**	BpPG1 WT in LB medium	72h
BpPG1 WT in M9-t medium with 7.5mM thiamine	**vs.**	BpPG1 WT in LB medium	72h
BpPG1 WT in M9-t medium with 7.5mM thiamine	**vs.**	BpPG1 WT in M9 medium without thiamine	72h

In the comparison of the significant log2foldchanges of the different strains we have to distinguish between the focusing strain and the compared partner strain. The log2foldchange analyses displayed the changes in the focus strain and is presented at the left column in Table 14. At first the distribution of significant up- and down-regulated genes in the different strains were investigated and visualized in volcano blots. The first-mentioned strains always represent the strains which were focused on.
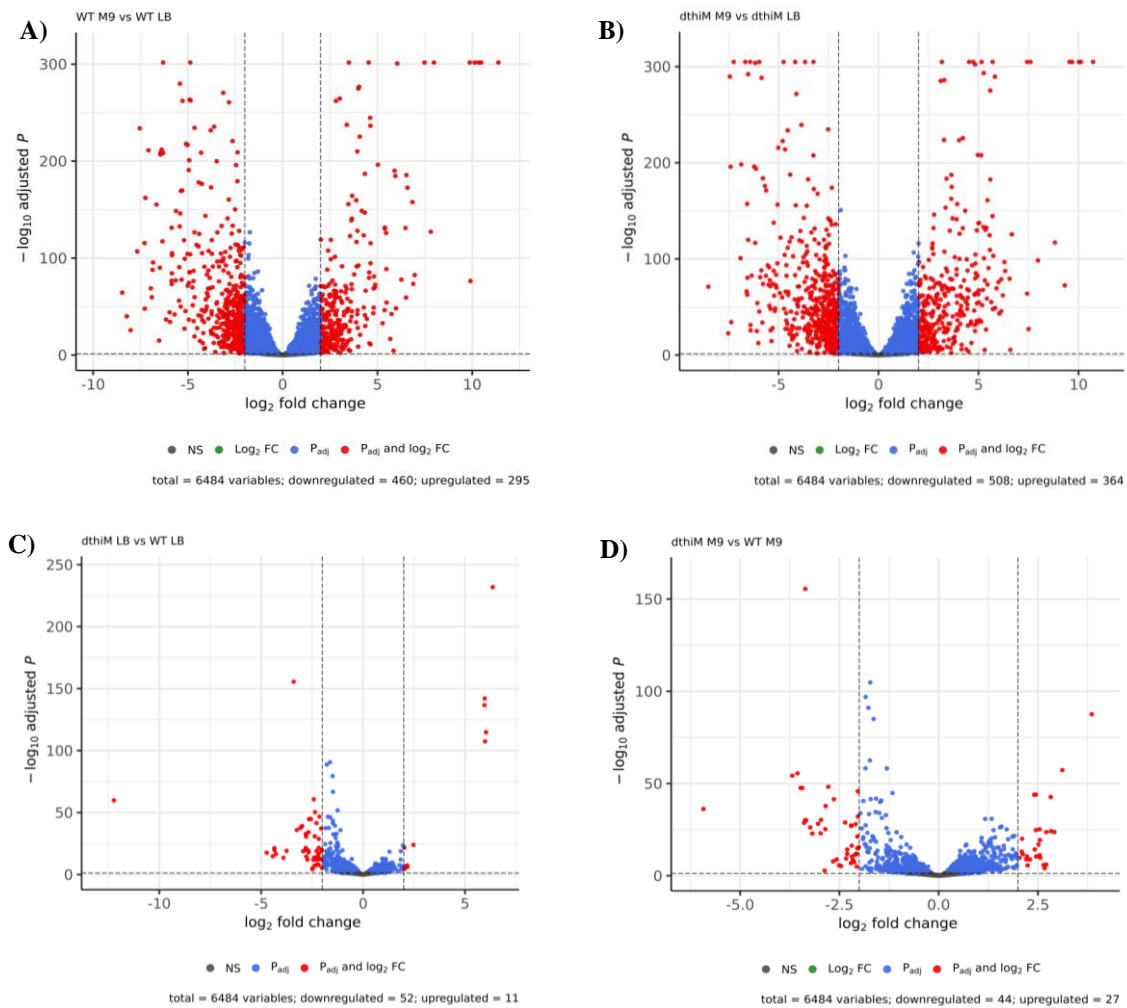
Figure 16: Volcano blots of the gene distribution of significant up- and down-regulated genes of the transcriptome analyses in the late exponential growth phase (48h). The first-mentioned strains always represent the strains which were focused on. A) BpPG1 wildtype in M9 medium without thiamine to LB medium, B) BpPG1ΔthiM in M9 without thiamine to LB medium, C) BpPG1ΔthiM to BpPG1 wildtype in LB medium, D) BpPG1ΔthiM to BpPG1 wildtype in M9 medium without thiamine.

In a first visual analysis of chosen volcano plots in the late exponential growth phase (48h) of up- and down-regulated genes it was striking that in the comparison of the strains in M9 medium without thiamine to LB medium several genes were up- and down-regulated (Figure 16a, b) in contrast to the comparison of the deletion mutant BpPG1ΔthiM to the BpPG1 wildtype in the same medium (Figure 16c, d). This was not surprising due to the previous observed medium effect of M9 medium without thiamine to LB medium. The different transcriptome analyses were compared regarding to essential metabolic pathways and ranked according to the growth phase. For further insights, a PATRIC analysis of the transcriptome analyses were performed and revealed differences regarding to the chosen media conditions and growth phases. This provided a first impression of which genes were prominent in the comparison (Figure 17-18).
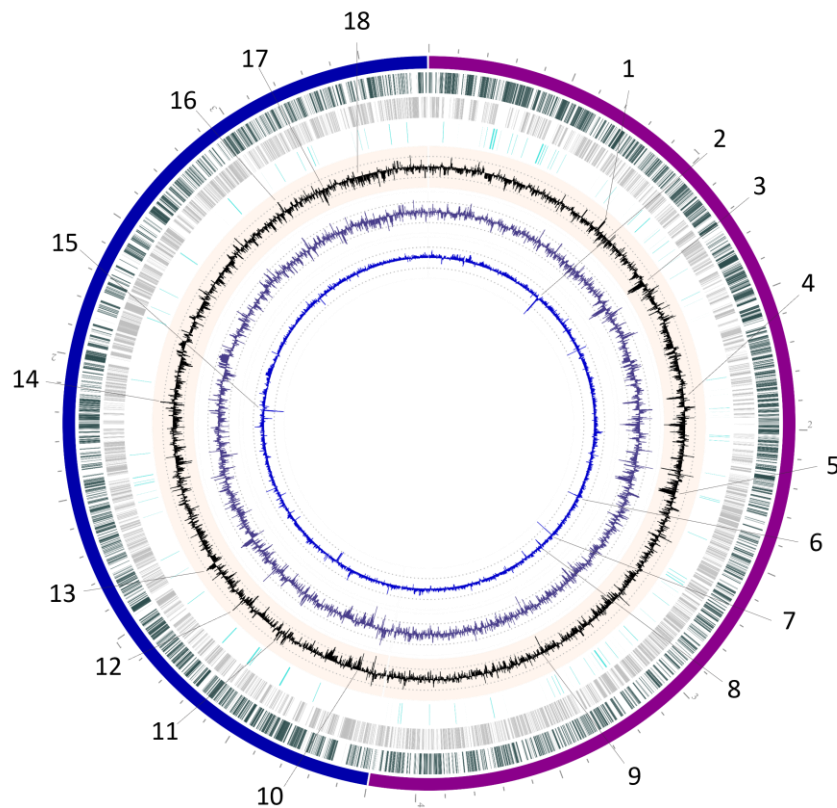
32
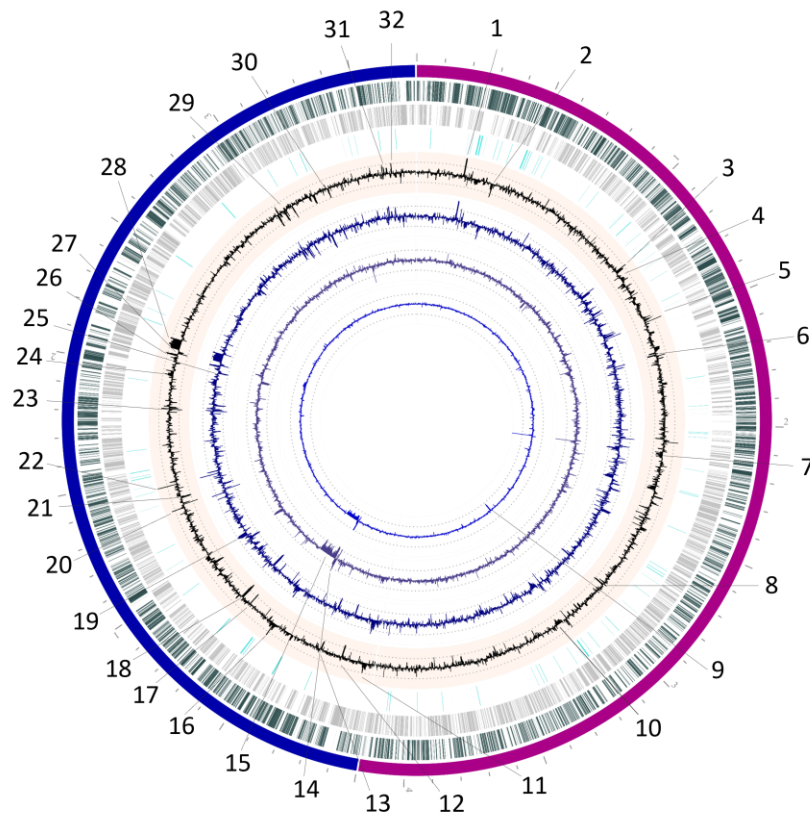
Figure 17: PATRIC Analysis of the transcriptome analyses in the late exponential growth phase (48h). Violet circle = chromosome 1, blue circle = chromosome 2. Comparison of the transcriptomic data from outer to inner circle = BpPG1WT_ M9_vs_WT_LB, BpPG1Δ*thiM*_ M9_vs_Δ*thiM*_LB, BpPG1Δ*thiM*_M9_vs_WT_M9, BpPG1Δ*thiM*_LB_vs_WT_LB. Number 1-32 = highlighted genes, (↑) up-regulated, (↓) down-regulated

1) Hemin ABC transporter (↑)

2) UDP-N-acetylglucosamine 2-epimerase WecB (↓)

3) Arginine N-succinyltransferase (↑)

4) Branched chain amino acid transport

5) Superoxide dismutase SodA, PRC-barrel domain protein, Glycosyltransferase family 9, Mandelate racemase, Major facilitator superfamily MFS-1 transporter (↑)

6) Transcription regulator protein CusR, Catalase (↓)

7) CRISPR/CAS system (↓)

8) Cytochrome c, anaerobe dehydrogenase, cytoplasmic chaperone TorD family protein (↓)

9) Histidine metabolism (↓)

10) Oxidative phosphorylation complex I (↓)

11) Putative thiamine pyrophosphate protein TPP binding domain protein, secretion protein HlyD family, putative MgtC/SapB transporter, phosphatidylserine decarboxylase-like protein (↑)

12) dimethyl sulfoxide reductase DmsA (↓)

13) 2-oxoisovalerate dehydrogenase, leucine degradation (↓)

14) putative XdhC-CoxI family protein, isoquinoline 1-oxidoreductase subunit alpha and beta (↑)

15) 2-aminoethylphosphonate-pyruvate transaminase PhnW (↓)

16) TonB depent siderophore receptor protein (↑)

17) hydoxylamine reductase hybrid-cluster protein, putative methane monooxygenase reductase (↓)

18) tyrosine-specific transport protein TyrP, putative pyridoxal-dependent tyrosine decarboxylase TyrDC, glutamate/gamma-aminobutyrate antiporter (↓)

19) 14-alpha-glucan-branching enzyme (↑)

20) manganese/iron transporter NRAMP family protein (↑)

21) formyl-coenzyme A transferase, oxalyl-CoA decarboxylase Oxc, formyl-CoA:oxalate CoA-transferase Frc (↓)

22) manganese/iron transporter NRAMP family protein (↑)

23) Leucine degradation (↓)

24) thiazolinyl imide reductase, thioesterase type II NRPS/PKS/S-FAS family, transcriptional regulator AraC-family (↑)

25) secretion protein HlyD family (↓)

26) putative ferric uptake regulator Fur family (↑)

27) succinate CoA transferase (↓)

28) Iron metabolism (↑)

29) Nitrogen metabolism (↓)

30) putative transcriptional regulator GntR family (↓)

31) Iron metabolism (↑)

32) cytochrome d ubiquinol oxidase subunit 1 (↑)

33

The results of the first PATRIC analysis of the late exponential growth phase (48h) showed up- and down-regulated genes of various metabolic pathways. Additionally, it was observed that the most transcriptional changes were discovered between the comparisons of the BpPG1 wildtype and the deletion mutant BpPG1Δ*thiM* in M9 medium without thiamine to LB medium. The associated metabolic pathways of glycolysis, citrate cycle, oxidative phosphorylation, leucine degradation, branched chain amino acid metabolism, nitrogen metabolism and others were discovered here. Further differences were identified in the down-regulated histidine metabolism (9), the up-regulated putative XdhC-CoxI family protein and isoquinoline 1-oxidoreductase subunit alpha and subunit beta (14) and the down-regulated 2-aminoethylphosphonate-pyruvate transaminase PhnW (15) which is part of the biosynthesis of secondary metabolites (Figure 17) (KEGG orthology, 2022, Leimkühler *et al.*, 2016, Sato *et al.*, 2013, Kim *et al.*, 2002).

Figure 18: PATRIC Analysis of the transcriptome analyses in the late stationary growth phase (72h). Violet circle = chromosome 1, blue circle = chromosome 2. Comparison of the transcriptomic data from outer to inner circle= BpPG1WT_M9-T_ vs_WT_LB, BpPG1WT_M9+T_vs_WT_LB, BpPG1WT_M9+T_vs_WT_M9. Number 1-18 = highlighted genes, (↑) up-regulated, (↓) down-regulated

1) NADH-FMN oxidoreductase RutF, flavin reductase (DIM6/NTAB) family, Nucleotide-binding universal stress protein UspA family, Major Facilitator Superfamily protein, membrane fusion protein, multidrug efflux system, efflux

transporter, outer membrane factor (OMF) lipoprotein, NodT family (↑)

2) NADH-FMN oxidoreductase RutF, flavin reductase (DIM6/NTAB) family, Nucleotide-binding universal stress protein UspA family, Major Facilitator Superfamily protein, membrane fusion protein, multidrug efflux system, efflux transporter, outer membrane factor (OMF) lipoprotein, NodT family (↓)

3) 1-deoxy-D-xylulose-5-phosphate synthase, pyruvate dehydrogenase E1 component, DNA-binding transcriptional regulator, MarR family, myo-inositol-1(or 4)-monophosphatase, Rieske [2Fe-2S] domain-containing protein, Iron-containing redox enzyme, 4-hydroxy-tetrahydrodipicolinate synthase, hypothetical protein, Aspartate/methionine/tyrosine aminotransferase, Cupin domain-containing protein, Phenylpropionate dioxygenase, large terminal subunit, LuxR family transcriptional regulator, pyruvate dehydrogenase E1 component, glutathione S-transferase, Predicted Peptidoglycan domain-containing protein (↓)

4) KamA family protein, Malate/lactate/ureidoglycolate dehydrogenase LDH2 family, branched-chain amino acid aminotransferase, Taurine dioxygenase, alpha-ketoglutarate-dependent, P-aminobenzoate N-oxygenase AurF, Glyoxylase, beta-lactamase superfamily II, Cupin domain-containing protein (↓)

5) Iron metabolism, ferredoxin--NADP+ reductase, formyltetrahydrofolate deformylase, hypothetical protein, acyl carrier protein, 3-hydroxyacyl-[acyl-carrier-protein] dehydratase, acyl-CoA thioester hydrolase, 3-oxoacyl-[acyl-carrier protein] reductase, acyl-CoA dehydrogenase, P-aminobenzoate N-oxygenase AurF, Pyrroloquinoline quinone (PQQ) biosynthesis protein C, Lysophospholipase, alpha-beta hydrolase superfamily, 3-oxoacyl-[acyl-carrier-protein] synthase II,, Phosphopantetheine attachment site, Major Facilitator Superfamily protein, ferredoxin, Acyl-

coenzyme A:6-aminopenicillanic acid acyl-transferase, Protein N-acetyltransferase RimJ/RimL family, acyl carrier protein, Long-chain acyl-CoA synthetase (AMP-forming), hypothetical protein (↓)

6) 3-oxoacyl-[acyl-carrier protein] reductase (↓)

7) Outer membran protein (↓)

8) molecular chaperone HscB, Iron-binding apoprotein IscA, FeS assembly scaffold apoprotein IscU, cysteine desulfurase IscS, transcriptional regulator, BadM/Rrf2 family (↓)

9) Outer membran protein (↓)

10) peroxiredoxin, Ohr subfamily (↓)

11) catecholate siderophore receptor (↑)

12) CsbD-like, bacterioferritin (↑)

13) 1,4-alpha-glucan branching enzyme, maltose alpha-D-glucosyltransferase/ alpha-amylase, starch synthase (maltosyl-transferring) (↑)

14) iron complex outer membrane recepter protein (↑)

15) iron complex outer membrane recepter protein (↓)

16) Collagen triple helix repeat-containing protein, Isoprenylcysteine carboxyl methyltransferase (ICMT) family protein (↑)

17) DNA-binding transcriptional regulator, MocR family (contains an aminotransferase domain), Glycine/D-amino acid oxidase (deaminating), aldehyde dehydrogenase (NAD+), branched-chain amino acid transport system substrate-binding protein, protein of unknown function (DUF1338), DNA-binding transcriptional regulator, LysR family, Acetyltransferase (GNAT) domain-containing protein (↓)

18) TnsA endonuclease N terminal, Helix-turn-helix domain-containing protein, hypothetical protein, DNA repair exonuclease SbcCD nuclease subunit, DNA repair exonuclease SbcCD ATPase subunit, Methyltransferase domain-containing protein (↓)

The results of the second PATRIC analysis of the late stationary growth phase (72h) showed up- and down-regulated genes of various metabolic pathways, either. Here transcriptional changes were observed in the BpPG1 wildtype in M9 medium with and without thiamine, displayed in the down-regulation of following genes: NADH-FMN oxidoreductase RutF, flavin reductase (DIM6/NTAB) family, Nucleotide-binding universal stress protein UspA family, Major Facilitator Superfamily protein, membrane fusion protein, multidrug efflux system, efflux transporter, outer membrane factor (OMF) lipoprotein, NodT family (2), 3-oxoacyl-[acyl-carrier protein] reductase (6), outer membrane protein (7), molecular chaperone HscB, Iron-binding apoprotein IscA, FeS assembly scaffold apoprotein IscU, cysteine desulfurase IscS, transcriptional regulator, BadM/Rrf2 family (8). The iron complex outer membrane receptor protein (14) which are important for the nitrogen utilization, transport mechanism in

the cell, iron metabolism and others were up-regulated (Figure 18) (KEGG orthology, 2022, Walsh *et al.*, 2013, Paulsen *et al.*, 1997).

To determine the metabolic processes, the transcriptomic data were classified according to the respective metabolic pathways and analysed for particularities. In the following the different transcriptome analyses were separated by their growth phases in two sections and additionally subdivided into the compared analyses shown in Figure 19. In addition, the transcriptional changes of the metabolic pathways were displayed in a heat map according to the reaction steps of the metabolic pathways.

WT_M9^{-t} vs. WT_LB	Δ*thiM*_M9^{-t} vs. Δ*thiM* _LB	Δ*thiM* _LB vs. WT_LB	Δ*thiM* _M9^{-t} vs. WT_M9^{-t}	WT_M9^{-t} vs. WT_LB	WT_M9+T vs. WT_LB	WT_M9+T vs. WT_M9^{-t}

late exponential growth phase (48h)   late stationary growth phase (72h)

Figure 19: Presentation of the different comparative analyses in the late exponential (48h) and the late stationary growth phase (72h). The strains highlighted in bold represents the strains to which the analyses refer. WT= BpPG1 wildtype, Δ*thiM*= BpPG1Δ*thiM*, M9-t= M9 medium without thiamine, M9+T= M9 medium supplemented with 7.5mM Thiamine, LB= LB medium).

The transcriptome analysis of BpPG1 wildtype and the deletion mutant BpPG1Δ*thiM* in M9 medium without thiamine to LB medium revealed similar regulation patterns in the metabolic pathways in the late exponential growth phase (48h). These effects were partly reduced in the late stationary growth phase (72h). Additionally, the metabolic processes, requiring thiamine pyrophosphate (TPP) as cofactor in their reaction, were down-regulated in M9 medium without thiamine in both strains and growth phases. As already mentioned, thiamine plays an important role as a cofactor in the metabolic pathways of glycolysis as well as the citrate cycle and supports its transition. However, it also has effects on other metabolic pathways. The results of the transcriptome analyses were transferred into heat maps showing all genes that can be active in the individual metabolic pathways. The strongest changes were observed in the metabolic pathways of glycolysis, the citrate cycle, oxidative phosphorylation, leucine degradation, arginine biosynthesis, histidine metabolism, oxidative stress regulation, iron metabolism, nitrogen metabolism and fatty acid metabolism. In addition, special attention was paid to thiamine metabolism, as well as to the CRISPR/CAS system.

In the following the metabolic changes were displayed by heat maps of the metabolic network analysis. In the end an overview scheme explains the individual interconnections for obtaining an overall impression (Figure 32).
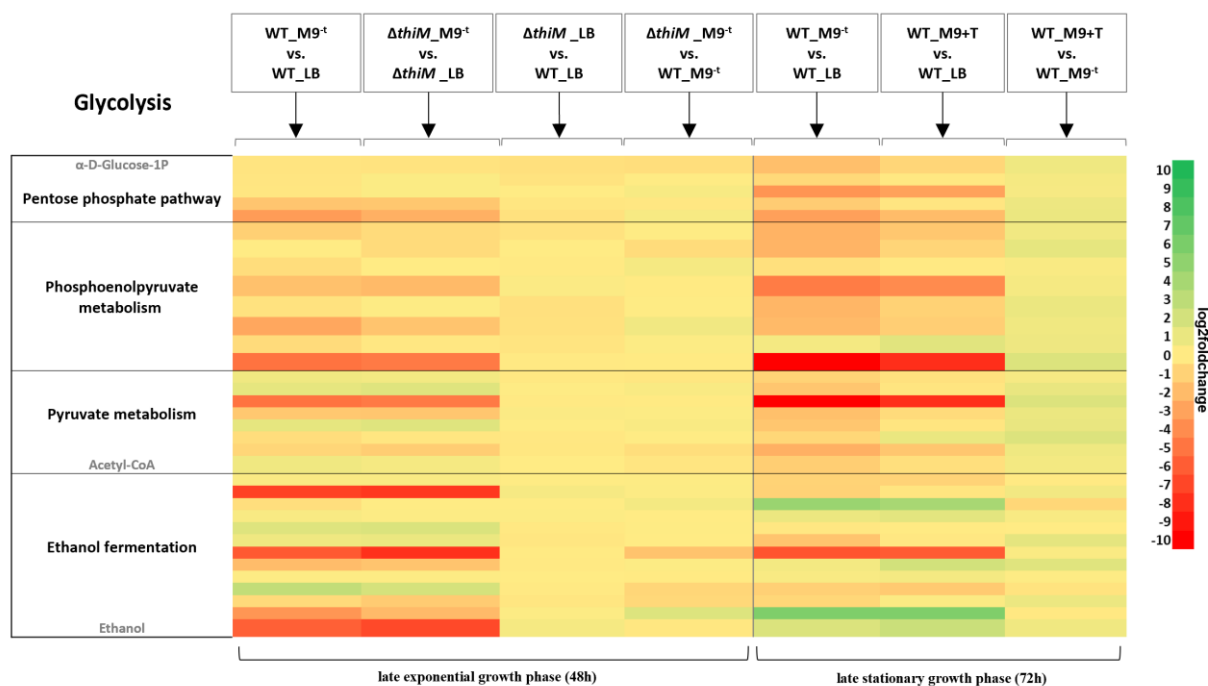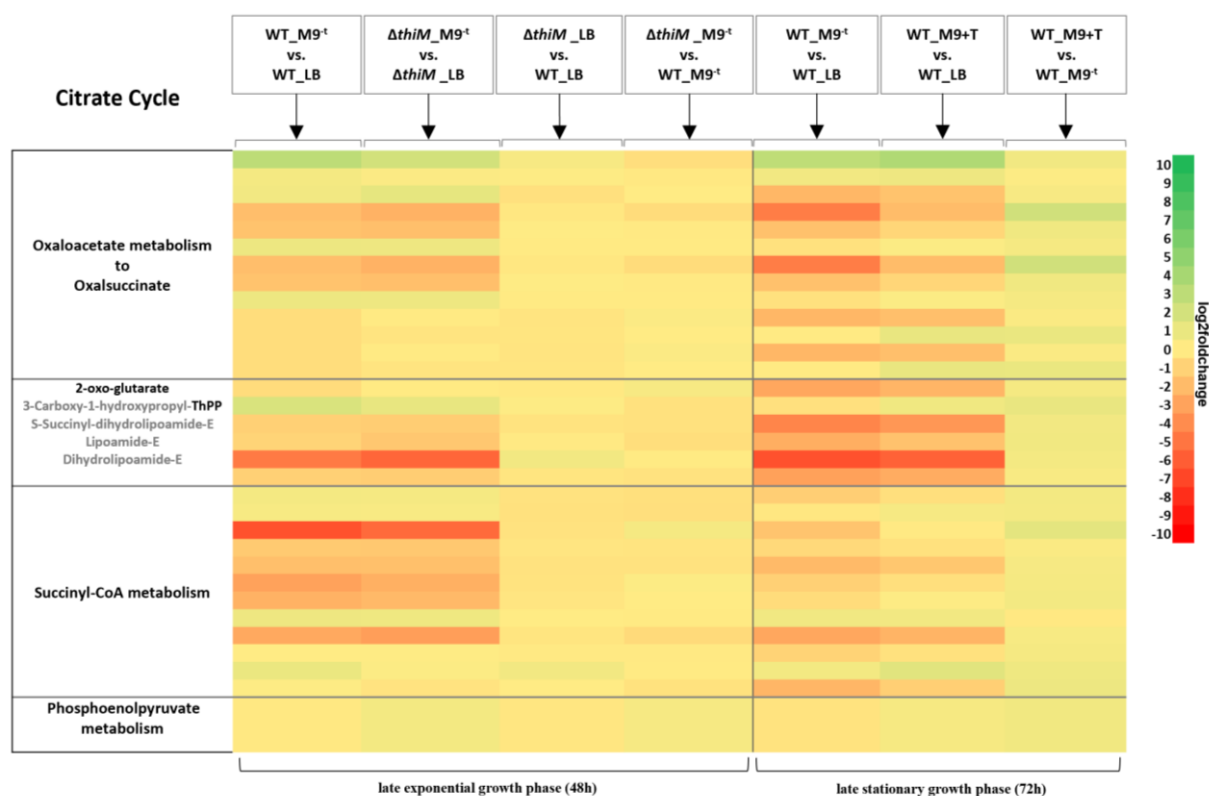

Figure 20: Heat map of expression pattern distribution of the glycolysis in *B. plantarii* PG1 strains. The metabolic processes of the glycolysis were displayed by the metabolic pathways of the pentose phosphate pathway, phosphoenolpyruvate metabolism, pyruvate metabolism and ethanol fermentation. Log2foldchanges are displayed.

Glycolysis is a process in which glucose is converted into pyruvate to provide small amounts of ATP (energy) and NADH (reducing power). In the comparison of the transcriptome analyses in M9 medium with and without supplemented thiamine to LB medium it was observed that the pentose phosphate pathway, the pyruvate metabolism and the conversion of acetyl-CoA to acetate and ethanol were down-regulated in the late exponential (48h) as well as in the late stationary growth phase (72h). In the late exponential growth phase (48h), values in the range of -3.84 to -6.42 log2fold were reached. Whereas, in the late stationary growth phase (72h), values of -8.1 log2fold were achieved during the transition from pyruvate to hydroxyethyl-THPP by the pyruvate dehydrogenase. This was expected, as TPP is required for the conversion in this process. A greater down-regulation were observed in the late stationary growth phase (72h). Nevertheless, it was surprising that in the late stationary growth phase, in the comparison of the BpPG1 wildtype in M9 medium with and without thiamine no differences were observed. Additionally, it was notable that in the late stationary growth phase (72h) the conversion of

acetyl-CoA to acetate by the aldehyde dehydrogenase was up-regulated to a value of 3.91 to 4.56 log2fold, which will be explained in the following by a closer examination of the other metabolic pathways (Figure 20). The comparison of the deletion mutant BpPG1Δ*thiM* to the BpPG1 wildtype in M9 medium without thiamine and in LB medium in the late exponential growth phase (48h) as well as the comparison of BpPG1 wildtype in M9 medium with supplemented thiamine to M9 medium without thiamine in the late stationary growth phase (72h) revealed no significant transcriptional changes.
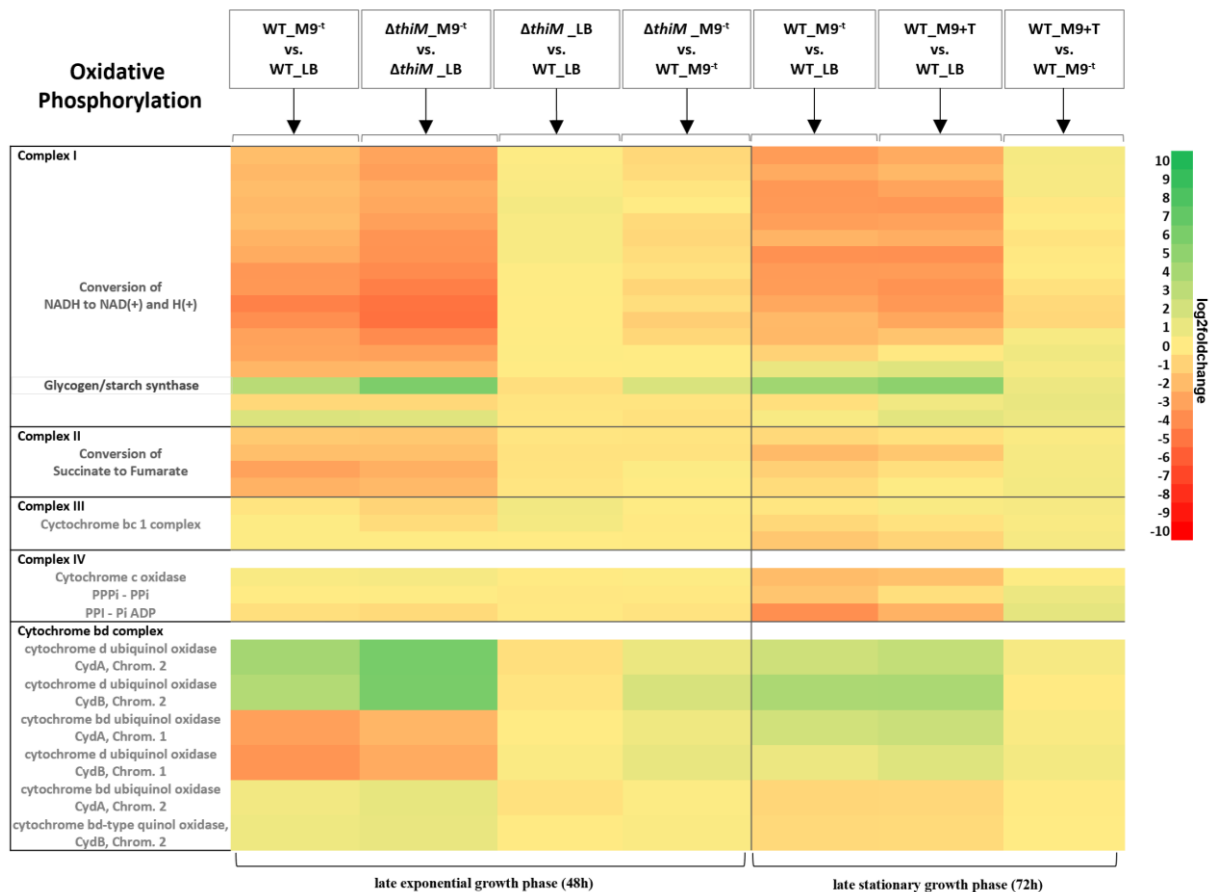

Figure 21: Heat map of expression pattern distribution of the citrate cycle in *B. plantarii* PG1 strains. The metabolic processes of the citrate cycle were represented by the conversion of oxaloacetate to oxalsuccinate, the TPP catalysed reaction of 2-oxo-glutarate, succinyl-CoA and phosphoenolpyruvate metabolism. Log2foldchanges are displayed.

In the next step the glycolysis transit from pyruvate to acetyl-CoA into the citrate cycle. The citrate cycle is an important step in carbohydrate catabolism and represents an important connection between various metabolic pathways for processing of fatty acids, sugars, alcohol and amino acids. In the comparison of the transcriptome analyses in M9 medium with and without supplemented thiamine to LB medium, it was remarkable that a small number of genes were down-regulated in this metabolic pathway in both growth phases. The conversion of 2-oxo-glutarate to dihydrolipoamide-E showed a down-regulation of the involved genes to a value

of -4.54 log2fold in the late exponential growth phase (48h) and a value of -5.27 log2fold in the late stationary growth phase (72h). In the following, the transit reaction of succinyl-CoA to succinate was down-regulated either in the late exponential growth phase (48h) to a value of -5.28 log2fold but only slightly not significant regulated in the late stationary growth phase (72h) (Figure 21). The comparison of the deletion mutant BpPG1Δ*thiM* to the wildtype BpPG1 in LB medium and in M9 medium without thiamine in the late exponential growth phase (48h) as well as the comparison of the wildtype BpPG1 in M9 medium with supplemented thiamine to M9 medium without thiamine in the late stationary growth phase (72h) revealed no significant transcriptional changes as previously observed in the glycolysis.

Figure 22: Heat map of expression pattern distribution of the oxidative phosphorylation in *B. plantarii* PG1 strains. The metabolic processes of the oxidative phosphorylation were represented by the conversion of NADH to NAD$^{(+)}$ and H$^{(+)}$ by complex I, the conversion of succinate to fumarate by complex II, the cytochrome bd 1 complex (complex III), the cytochrome c oxidase (complex IV) and the cytochrome bd complex. Log2foldchanges are displayed.

The respiration is the process of oxidative phosphorylation in which a series of oxidation and reduction reactions catalyse an electron transfer reaction for the conversion of ADP and phosphate to ATP for energy production. In the comparison of the transcriptome analyses in M9 medium with and without supplemented thiamine to LB medium, the first complex (I), dominated mainly by NADH-quinone oxidoreductases in *B. plantarii* PG1, was down-regulated with values of -1.5 to -4.17 log2fold. In this metabolic pathway a glycogen/starch synthase (BGL_1c20790) was displayed, which was highly up-regulated to values of 3.17 – 5.83 log2fold in the late exponential growth phase (48h) and to values of 4.27 – 5.12 log2fold in the late stationary growth phase (72h).

The second complex (II) were down-regulated, catalysing the conversion of succinate to fumarate (Hägerhäll, 1997). The complex III and IV were not significant regulated, whereas in the cytochrome bd complex, the cytochrome d ubiquinol oxidases CydA and CydB located on the second chromosome in the wildtype BpPG1 were up-regulated at the late exponential growth phase (48h) (3.45 - 6.13 log2fold) as well as in the late stationary growth phase (72h) (2.26 - 3.78 log2fold). However, on the first chromosome, the cytochrome bd and d complex was slightly down-regulated in the late exponential growth phase (48h) (-1.76 to -2.93 log2fold) but the cytochrome bd on the second chromosome showed no significant regulation pattern. Additionally, the comparison of the deletion mutant BpPG1Δ*thiM* to the wildtype BpPG1 in LB medium and in M9 medium without thiamine in the late exponential growth phase (48h) as well as the comparison of the wildtype BpPG1 in M9 medium with thiamine to M9 medium without thiamine in the late stationary growth phase (72h) revealed no significant transcriptional changes as previously observed (Figure 22).
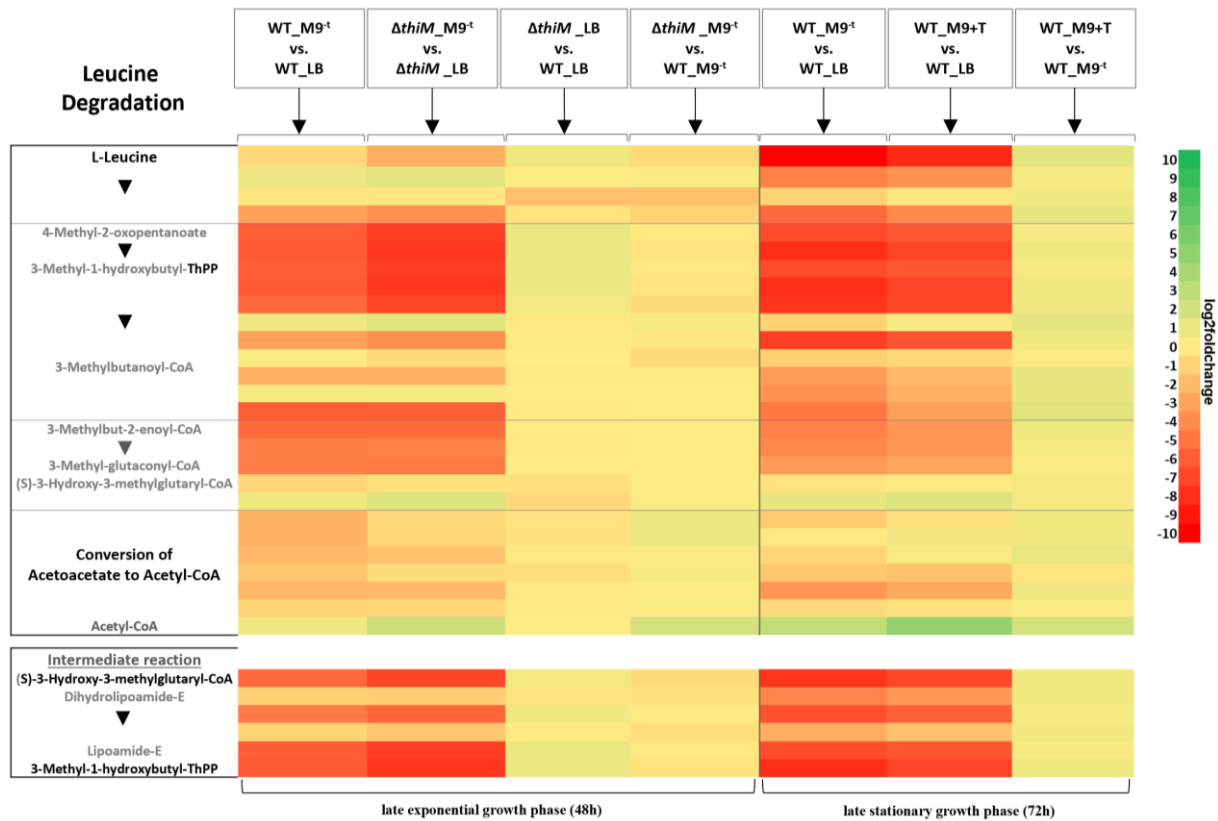
Figure 23: Heat map of expression pattern distribution of the leucine degradation in *B. plantarii* PG1 strains. The metabolic processes of the leucine degradation are TPP dependent and contains the essential step of the conversion of acetoacetate to acetyl-CoA. Log2foldchanges are displayed.

The metabolic network analysis revealed a down-regulation of leucine degradation, which is closely linked to the citrate cycle. In the first step of leucine degradation, 4-methyl-2-oxopentanoate is converted to 3-methyl-hydroxybutyl-ThPP in *B. plantarii* PG1. This step, as well as the following, were down-regulated due to the lack of the required TPP here. This was observed in the late exponential growth phase (48h) as well as in the late stationary growth phase (72h) and either only in the comparative analyses of the wildtype BpPG1 and the deletion mutant BpPG1Δ*thiM* in M9 medium without thiamine to LB medium as well as in the analyses of the wildtype BpPG1 in M9 medium with and without thiamine compared to LB medium. It was striking that the down-regulation of the different processes were nearly equal in intense in the late exponential (48h) as well as in the late stationary growth phase (72h). So far, a reduction of the transcription levels at the transition of the different growth phases were detected. Here however the level remained at the same intensity (Figure 23).
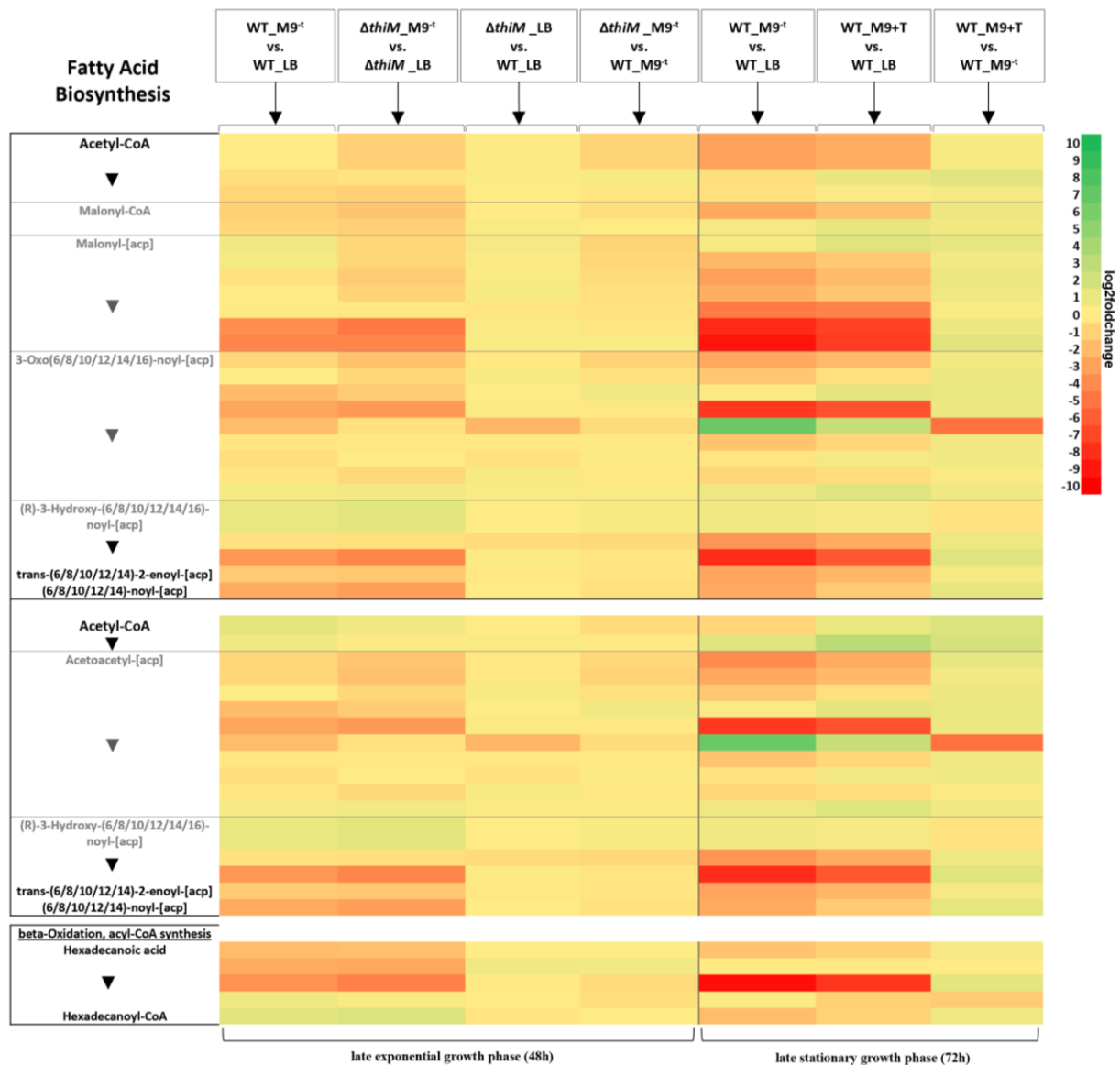
Figure 24: Heat map of expression pattern distribution of the fatty acid metabolism in *B. plantarii* PG1 strains. The metabolic pathway of the fatty acid metabolism is distinguished by the malonyl-CoA and acetyl-CoA pathway as well as the beta-oxidation. Log2foldchanges are displayed.

The fatty acid metabolism is associated to the synthesis of acetyl-CoA. Here, regulatory differences between the late exponential (48h) and late stationary growth phase (72h) were detected. In the late stationary growth phase (72h), a higher down-regulation of the genes in the comparison of the wildtype BpPG1 in M9 medium with and without supplemented thiamine to LB medium were observed. In the late exponential growth phase (48h) in the comparison of the wildtype BpPG1 and the deletion mutant BpPG1Δ*thiM* in M9 medium without thiamine to LB medium, the essential steps in fatty acid metabolism were slightly down-regulated with values of -2 to -4 log2fold. In the comparison of the deletion mutant BpPG1Δ*thiM* to the wildtype

BpPG1 in LB medium and in M9 medium without thiamine in the late exponential growth phase (48h) as well as the comparison of the wildtype BpPG1 in M9 medium with supplemented thiamine to M9 medium without thiamine in the late stationary growth phase (72h) single genes are regulated but the majority revealed no significant transcriptional changes (Figure 24).
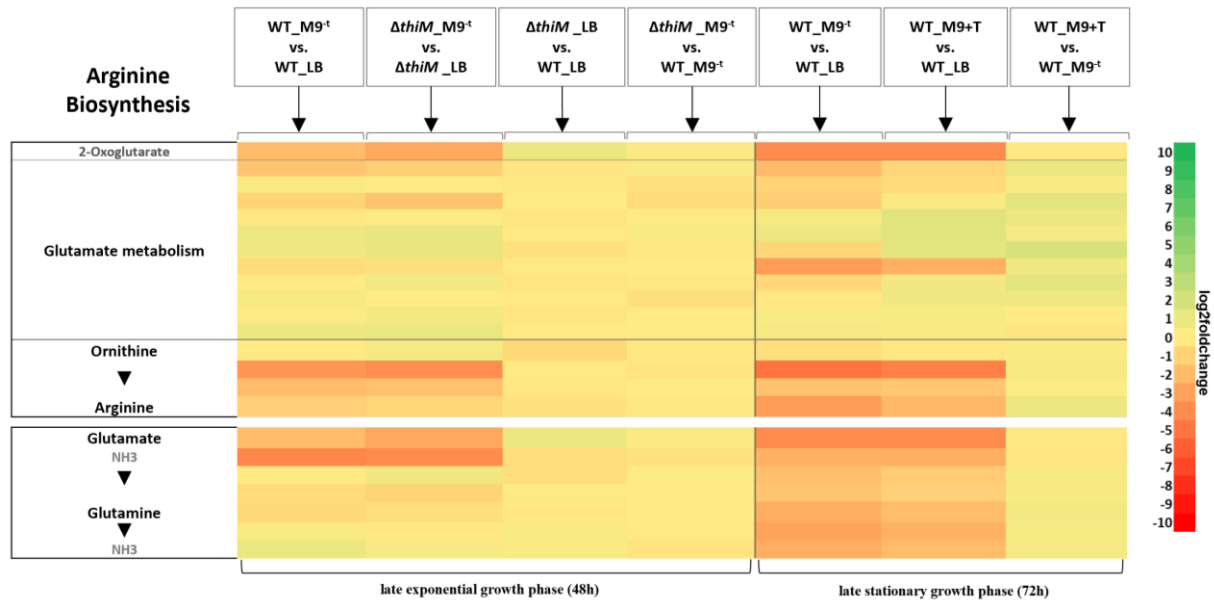

Figure 25: Heat map of expression pattern distribution of arginine biosynthesis in *B. plantarii* PG1 strains. The metabolic processes of the arginine biosynthesis is connected to the glutamate metabolism. Log2foldchanges are displayed.

In the next step, we return to the citrate cycle. The transition to arginine metabolism takes place via 2-oxoglutarate. As mentioned earlier, the citrate cycle was down-regulated which in turn affects other metabolic pathways. In arginine metabolism, down-regulation was also evident, affecting glutamate metabolism and the closely related pyrimidine and purine metabolism. Here the changeover from the citrate cycle to the arginine metabolism via 2-oxoglutarate was slightly down-regulated with -1.58 to -2.27 log2fold in the late exponential growth phase (48h) whereas it was down-regulated to -3.24 to -3.27 log2fold in the late stationary growth phase (72h) in the comparison of the wildtype BpPG1 and deletion mutant BpPG1Δ*thiM* in M9 medium without thiamine to LB medium. This resulted in a reduced synthesis of arginine and a down-regulation in the glutamate metabolism for the conversion to ammonia with values of -1.58 to -3.46 log2fold in both growth phases (Figure 25).
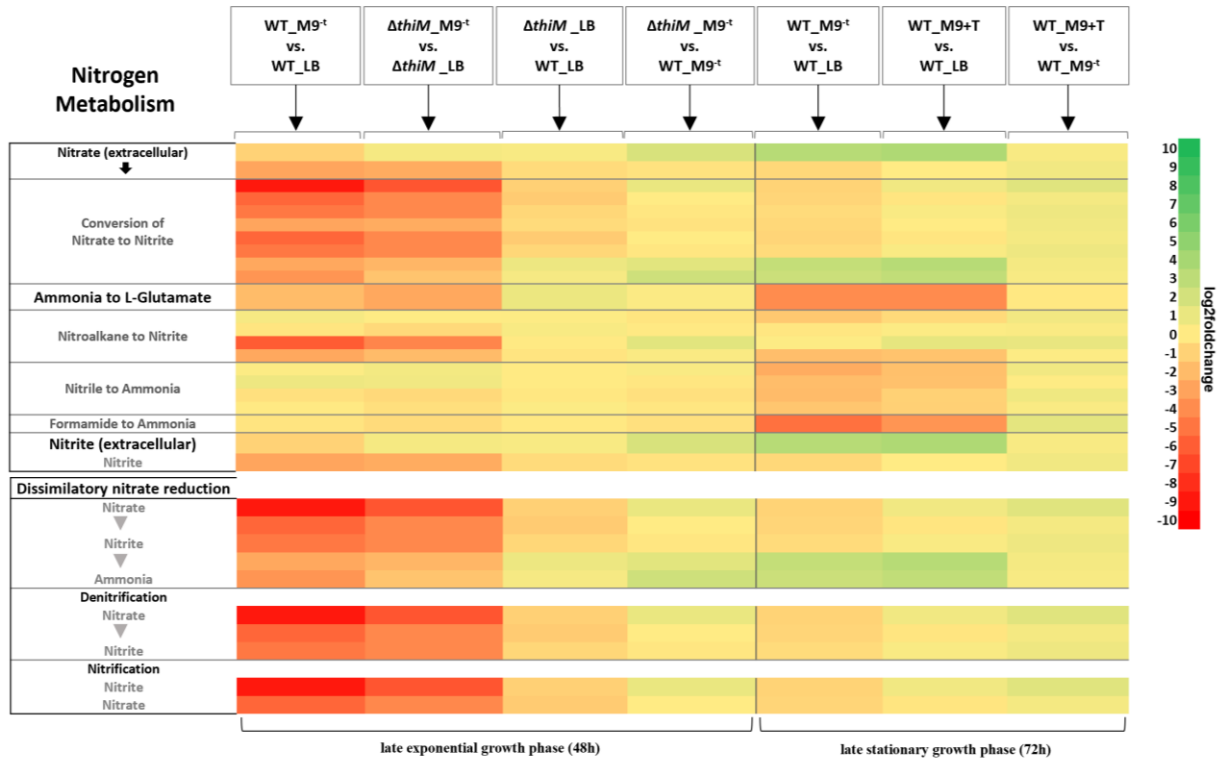
Figure 26: Heat map of expression pattern distribution of the nitrogen metabolism in *B. plantarii* PG1 strains. The nitrogen metabolism describes the processing of extracellular nitrate and includes the processes of the nitrification and denitrification. Log2foldchanges are displayed.

The glutamate metabolism is also associated to the nitrogen metabolism. The nitrogen metabolism is an important part of the general life cycle, as it catalyses several different reactions. The fixation of nitrogen includes the reduction of atmospheric molecular nitrogen to ammonium, which is needed to synthesise amino acids. Here, in the comparison of the wildtype BpPG1 and deletion mutant BpPG1Δ*thiM* in M9 medium without thiamine to LB medium, the down-regulation of the conversion of nitrate to L-glutamate were detected with values of -3.38 to -7.24 log2fold in the late exponential growth phase (48h). This effect was reduced to a value of -0.77 log2fold in the late stationary growth phase (72h). Especially the metabolic pathway of dissimilatory nitrate reduction revealed a higher down-regulation with values of -1.3 to -7.24 log2fold in the late exponential growth phase (48h) whereas the comparative transcriptome analyses in the late stationary growth phase (72h) showed no highly regulation of this pathways (Figure 26).
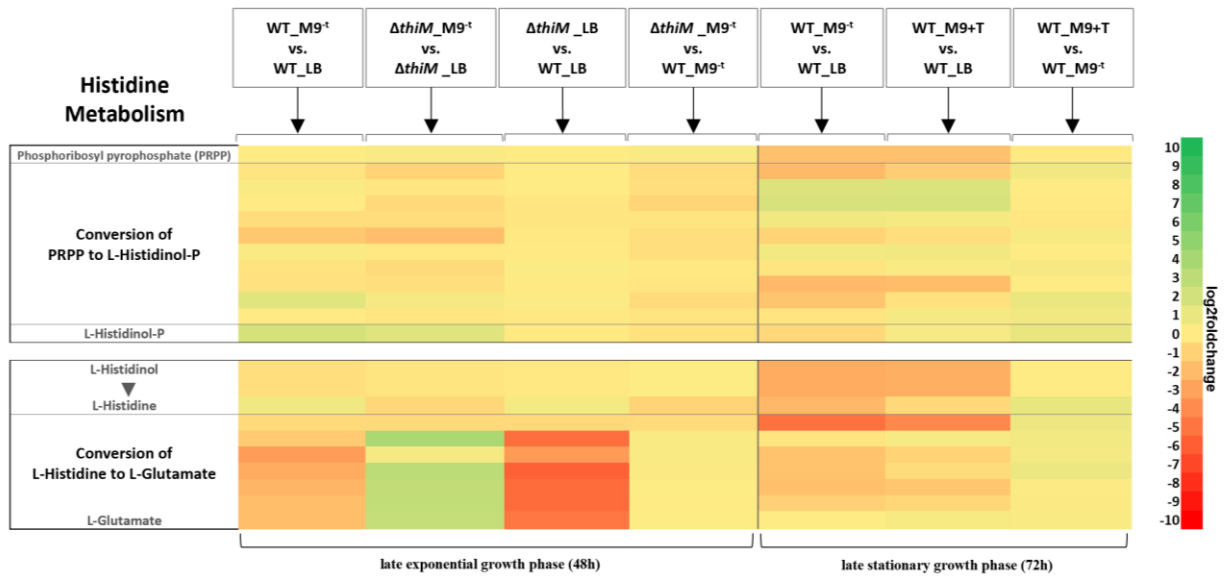
Figure 27: Heat map of expression pattern distribution of the histidine metabolism in *B. plantarii* PG1 strains. The metabolic processes of the histidine metabolism were represented by the conversion of phosphoribosyl pyrophosphate (PRPP) to L-histidinol-P and the conversion of L-histidine to L-glutamate. Log2foldchanges are displayed.

The metabolic network analysis of the comparative transcriptome analyses revealed metabolic changes but no unexpected highly differences with exception of the histidine metabolism. Here it was observed that the conversion of L-histidine to L-glutamate was down-regulated in the comparison of the wildtype BpPG1 in M9 medium without thiamine to LB medium as well as in the comparison of the deletion mutant BpPG1Δ*thiM* to the wildtype BpPG1 in LB medium in the late exponential growth phase (48h). In contrast, the comparison of the deletion mutant BpPG1Δ*thiM* in M9 medium without thiamine to LB medium showed an up-regulation to a value of 3.81 log2fold here (Figure 27). Histidine metabolism is important for the synthesis of PRPP which is part of essential metabolic processes. Additionally, histidine represents an important component of amino acid metabolism and is essential for the formation of glutamates which close the metabolic cycle here.
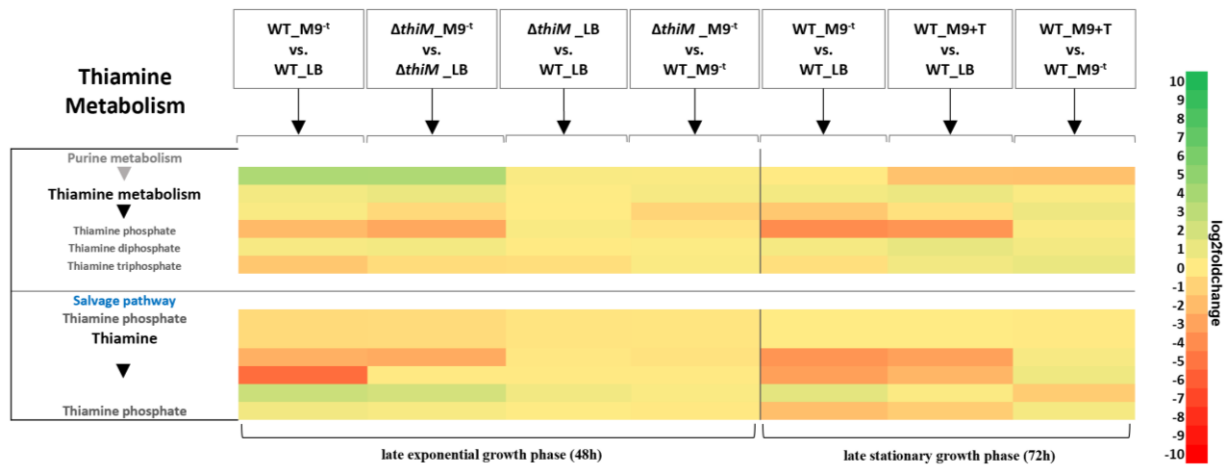
Figure 28: Heat map of expression pattern distribution of the thiamine metabolism in *B. plantarii* PG1 strains. The thiamine metabolism is separated in the main metabolism and salvage pathway. Log2foldchanges are displayed.

As previously mentioned, the kinase ThiM is part of the salvage pathway. To determine the role of ThiM and thiamine in metabolic processes in the *B. plantarii* PG1, the thiamine metabolism was further investigated. As expected, the salvage pathway revealed a down-regulation in the conversion of thiamine to thiamine phosphate in the comparison of M9 medium without thiamine to LB medium in the late exponential (48h) as well as in the late stationary growth phase (72h). Additionally, the thiamine biosynthesis protein ThiC was significant up-regulated here and in the comparison of the wildtype BpPG1 in M9 medium without thiamine to LB medium, the kinase ThiM was significant down-regulated in the salvage pathway. Further, no significant transcriptional differences were detected (Figure 28). In addition, the transcription levels of the CRISPR/CAS system were investigated.
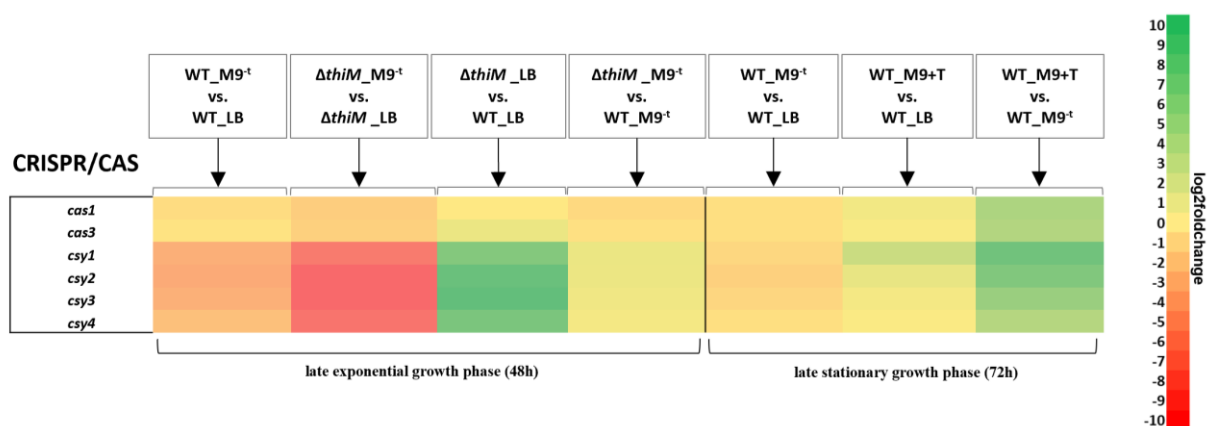

Figure 29: Heat map of expression pattern distribution of the CRISPR/CAS system in *B. plantarii* PG1 strains. Log2foldchanges are displayed.

Here the same effects were observed as mentioned in the previous chapter. The comparison of the deletion mutant BpPG1Δ*thiM* in LB medium to the wildtype BpPG1 in LB medium revealed an up-regulation of the csy complex with values of 1.5 to 2.2 log2fold whereas in the comparison of the deletion mutant BpPG1Δ*thiM* and the wildtype BpPG1 in M9 medium without thiamine to LB medium a reducing effect was detected with values of -2.7 to -6.6 log2fold in the exponential growth phase (48h). In the analysis of the late stationary growth phase (72h) a slight but not significant increase of the csy complex was observed in the comparison of the wildtype BpPG1 in M9 medium with supplemented thiamine to M9 medium without thiamine to values of 0.6 to 1.9 log2fold (Figure 29).

In addition to the metabolic pathways that require thiamine as essential cofactor, other metabolic pathways also indicated transcriptional changes. Due to the changing media and limitations of the thiamine salvage pathway, adaptations of other metabolic processes occurred as reaction of changing environmental conditions. Therefore, it was observed that the changing conditions led to an increase in the oxidative stress response and the iron metabolism which are closely connected to each other and play an important role in metabolic processes of the cell life cycle.
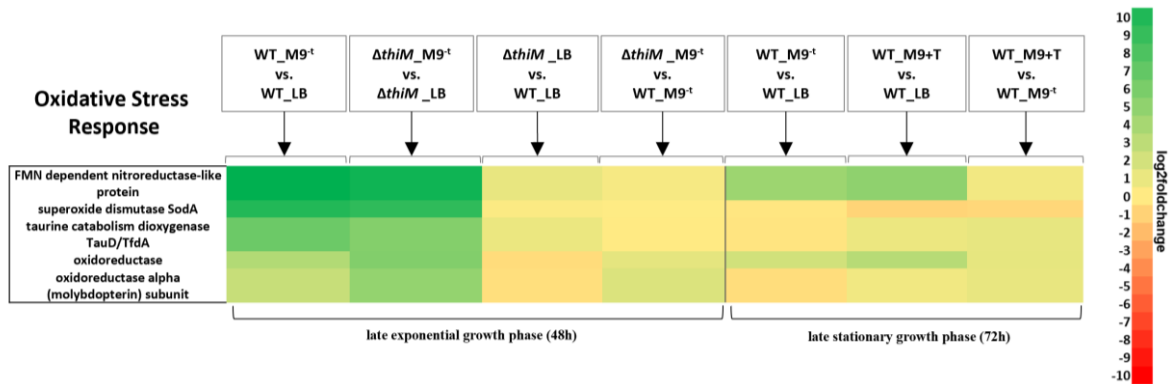

Figure 30: Heat map of expression pattern distribution of oxidative stress regulation in *B. plantarii* PG1 strains. Log2foldchanges are displayed.

The comparative transcriptome analysis determined that the associated oxidative stress response genes were up-regulated to high values of 11.38 log2fold in the late exponential growth phase (48h) and slightly increased of values of 4.42 to 5.05 log2fold in the late stationary growth phase (72h) in the comparison of the wildtype BpPG1 and the deletion mutant BpPG1Δ*thiM* in M9 medium without thiamine to LB medium. The oxidative stress response is separating in the reaction to peroxide or superoxide. In this case the present stress was mediated by superoxide anion due to the activation of the superoxide dismutase SodA (Figure 30).
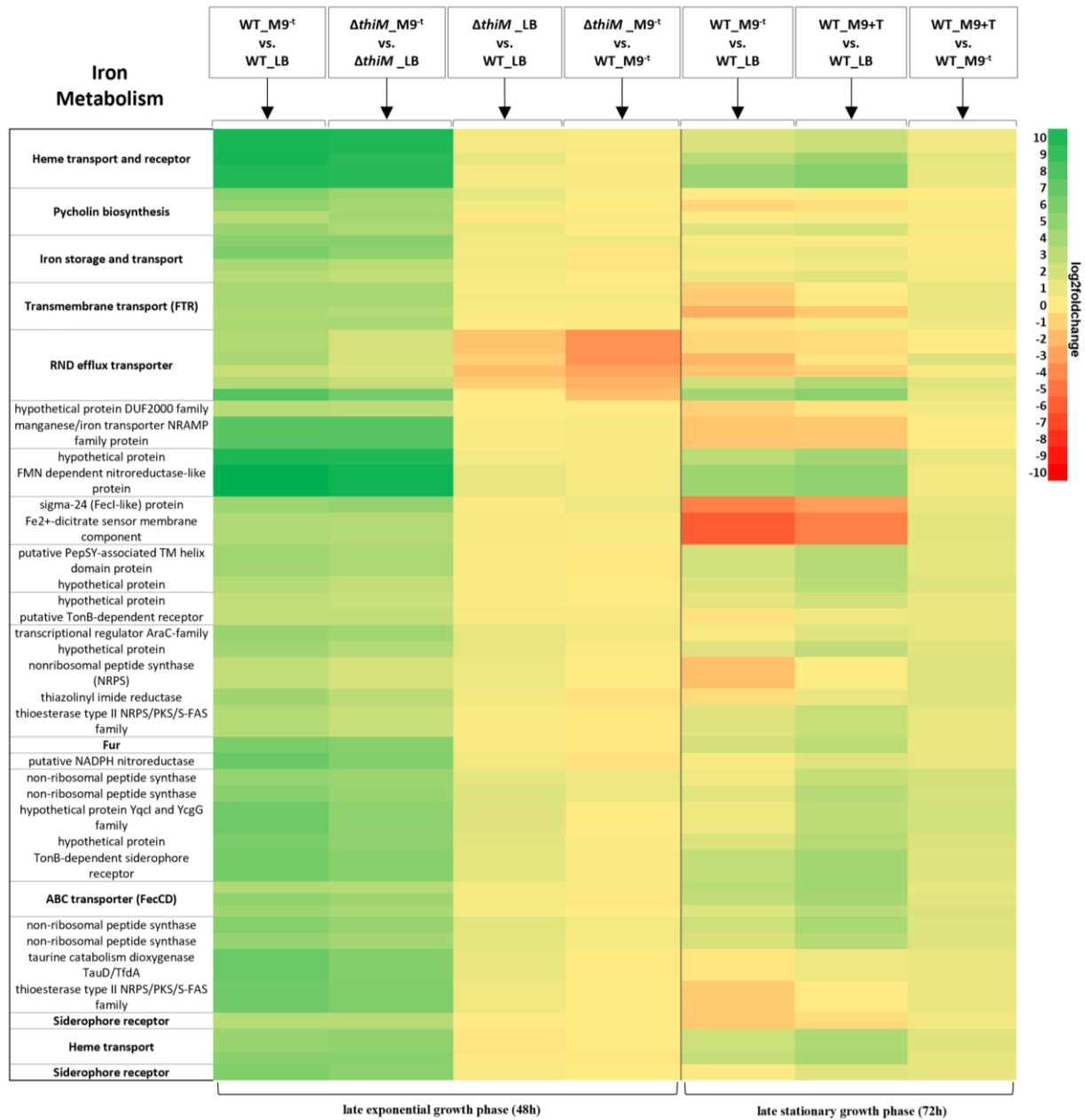
Figure 31: Heat map of expression pattern distribution of iron metabolism in *B. plantarii* PG1 strains. Log2foldchanges are displayed.

The oxidative stress response is closely connected to the iron metabolism. An imbalance of the iron concentration in the cell leads to the activation of the oxidative stress response to avoid toxic levels (Farr and Kogoma, 1991). Here an up-regulation of the iron metabolism was observed especially in the comparison of wildtype BpPG1 and the deletion mutant BpPG1Δ*thiM* in M9 medium without thiamine to LB medium in the late exponential growth phase (48h) and slightly reduced in the late stationary growth phase (72h). This led to the

assumption that additionally to the thiamine, another effect occurred resulting in an imbalance of iron concentration and the activation of the oxidative stress response (Figure 31).
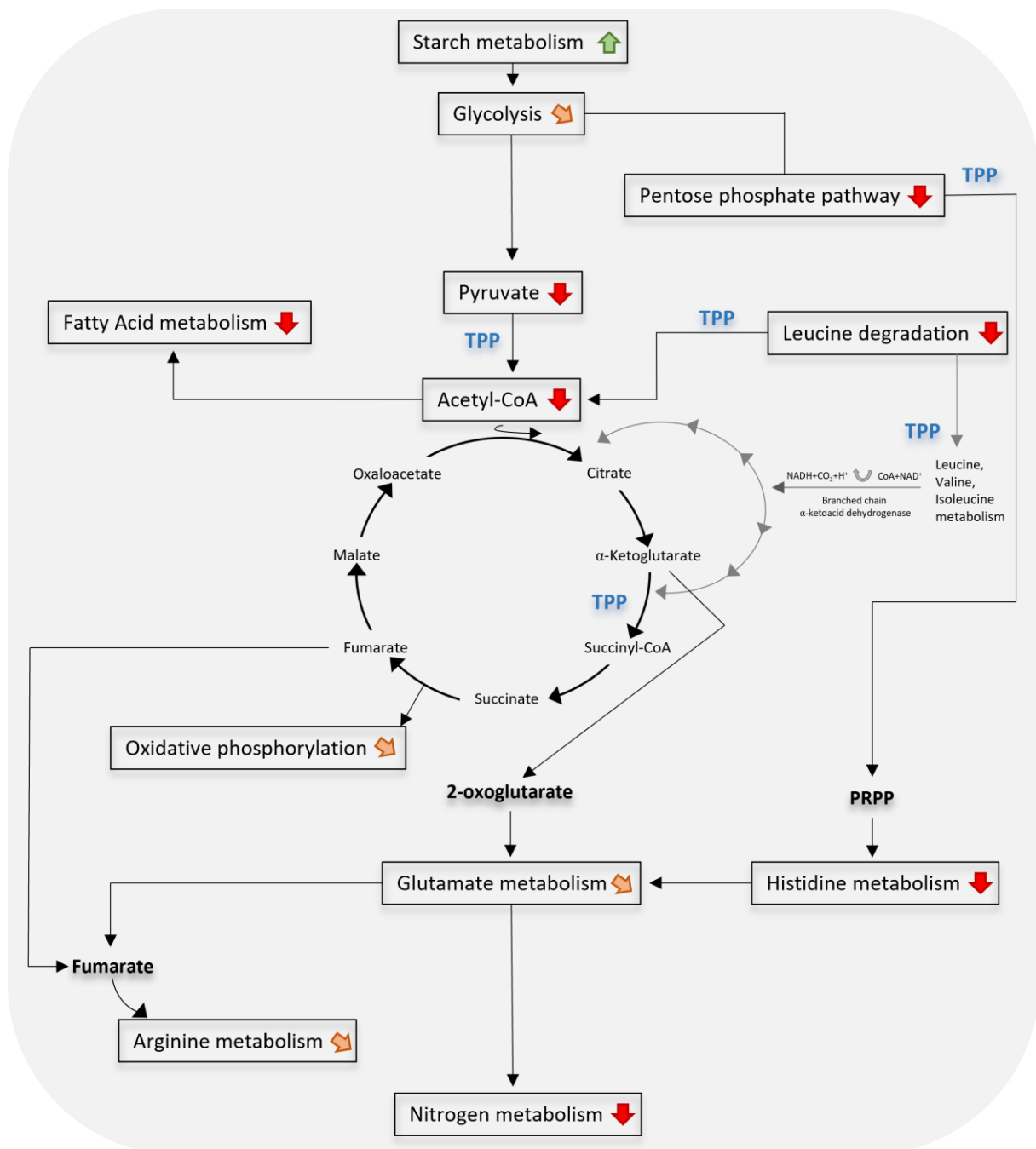

Figure 32: Metabolic network of TPP-dependent processes related to up- and down-regulated genes in the wildtype BpPG1 and the deletion mutant BpPG1Δ*thiM* in comparison of M9 medium without thiamine to LB medium and display of TPP-independent metabolic processes with observed transcriptional changes.

In conclusion, the transcriptome analysis revealed differences in all compared analyses, however the most striking changes were observed in the compared transcriptome analyses

between the strains in M9 medium without thiamine to LB medium. Here the M9 medium was additional limited by lacking thiamine which led to changes in the metabolic processes. As already mentioned, thiamine is an essential co-factor in metabolic processes and its limitation resulted in metabolic adaptations. In the beginning, glucose precursors for glycolysis were provided from the starch metabolism. The glycolysis pathway was followed by the pentose phosphate pathway, which used TPP as co-factor and were observed as first metabolic pathway which was down-regulated, followed by the pyruvate and acetyl-CoA metabolism. Due to the absence of produced precursors for the branched chain amino acid metabolism, a decrease in expression was detected in the leucine degradation, histidine metabolism, glutamate metabolism, arginine metabolism, nitrogen metabolism, oxidative phosphorylation, and fatty acid metabolism. This clearly revealed the steps at which the TPP exerts an essential effect on the metabolism, so that the corresponding metabolic pathways resulted in a down-regulation (Figure 32). Additionally, further metabolic pathways showed adaptations beside of TPP effects, resulting in an up-regulation of oxidative stress response and iron metabolism. Here another impact factor must be considered which will be discussed in the discussion chapter.

3.3 Investigation of possible regulation mechanisms of the CRISPR/CAS system

First transcriptome analysis of the wildtype BpPG1 in the early exponential growth phase (28h) in LB medium collected in the study of Rong Gao in 2015 revealed different transcription levels of the CRISPR/CAS genes which led to the assumption that the immune system is differently regulated, and more than one promoter site could be present in this system (Figure 33a).
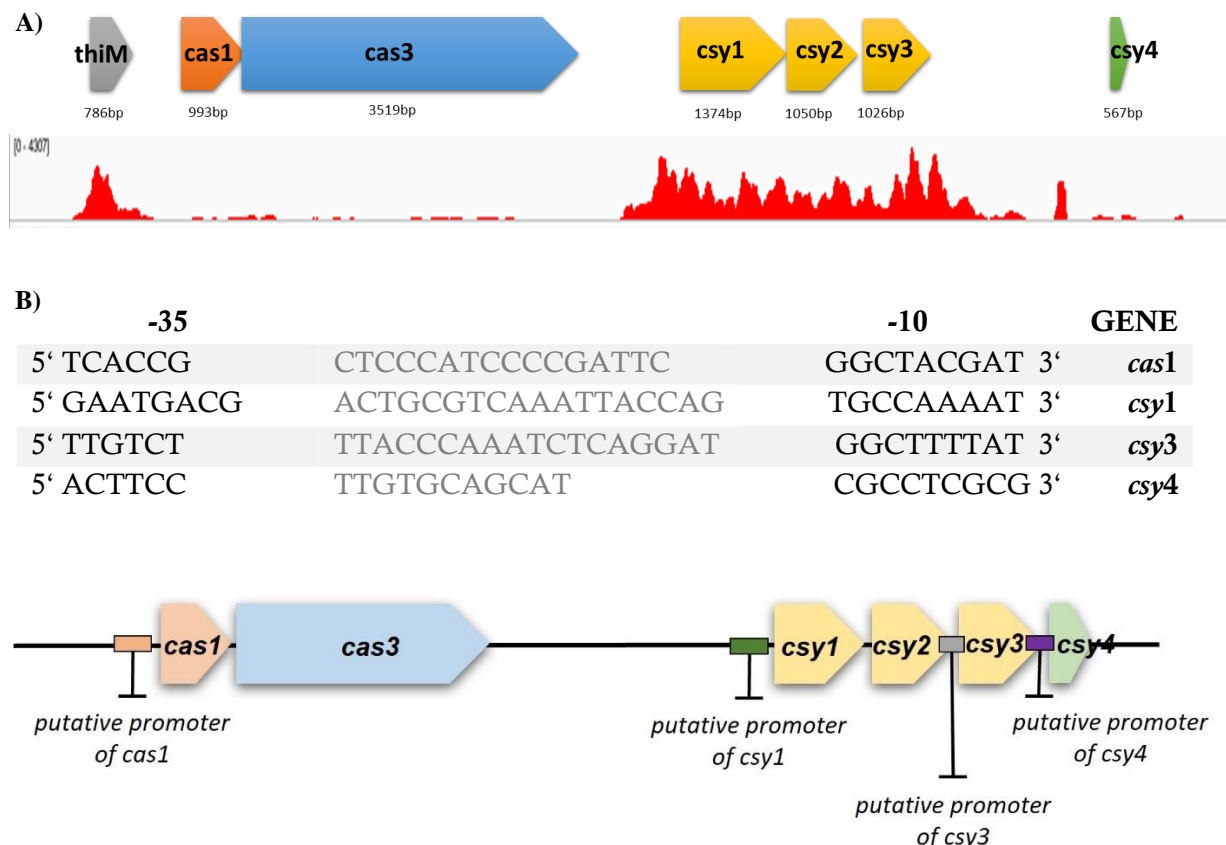

Figure 33: Different transcription level and putative promoter sites of the CRISPR/CAS system. (a) Different transcription level of the genes of the CRISPR/CAS system in the exponential growth phase (28h) based on the transcriptomic data of Rong Gao. (b) Identification of putative promoter sites predicted with softberry analysis.

For further insights, a promoter prediction search was performed. By softberry analysis, it was possible to identify four putative promoter sequences in the CRISPR/CAS system. Regarding to the different transcription levels, the putative promoter sequences of *cas1*, *csy1* and *csy4* were evaluated as possible promoter sites of the CRISPR/CAS system (Figure 33b).
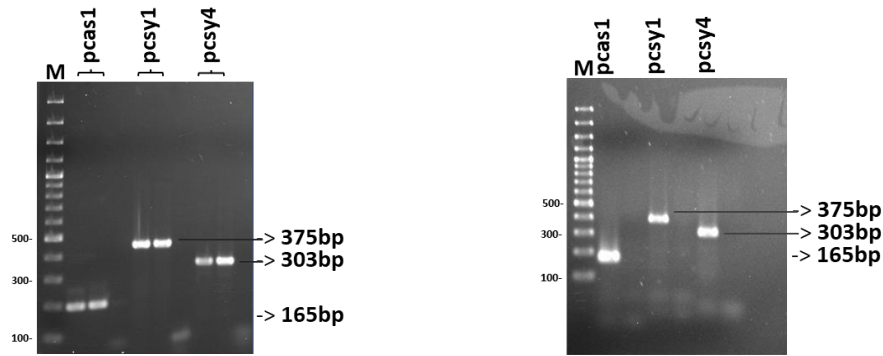
Figure 34: Amplification of the putative promoter regions of *cas1* (165bp), *csy1* (375bp) and *csy4* (303bp) on gDNA of PG1 (left). Control PCR with specific primer at the plasmid constructs with pBBR1MCS-2 with the promoter regions of *cas1*, *csy1* and *csy4* (right). p= promoter region, 2% agarose gel, 100bp+ O'GeneRuler™ DNA Marker (Thermo Scientific™ SM1153), 5µl per sample

For experimental examination, a promoter-mcherry fusion on the plasmid pBBR1MCS-2 were created and quantified at the plate reader. The putative promoter sites of *cas1* (165bp), *csy1* (375bp) and *csy4* (303bp) were amplified with specific primers on genomic DNA of *B. plantarii* PG1. The promoter sites as well as the plasmid were digested with restriction enzymes and ligated to the final construct. Further, the construct was transformed to *E. coli* DH5α for replication. The final plasmid was isolated and introduced into the respective Burkholderia strains by electroporation (Figure 34). As positive control the *rpoD* promoter of the BpPG1 wildtype was fused with mcherry and as negative control mcherry was fused with a promoter of NGR234 in reverse direction on the plasmid pBBR1MCS-2 provided by Katrin Petersen.
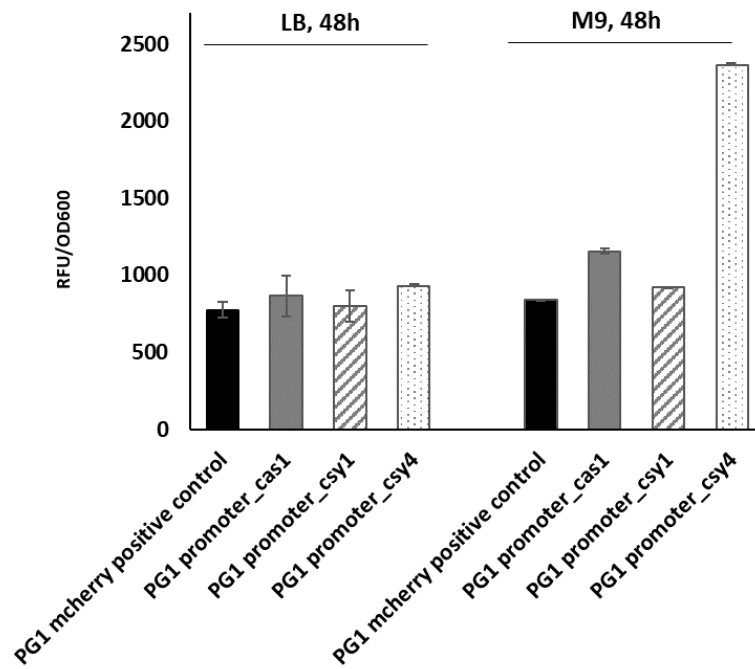
Figure 35: RFU/OD600 evaluation of the created promotor constructs in BpPG1 WT in LB and M9 medium. Evaluation of the relative fluorescence level normalized to the optical density (RFU/OD600) of the promoter-mcherry fusion strains with the putative promoter sites of *cas1*, *csy1* and *csy4* and the positive control (plate reader with monochromator). The mean values of three replicates are represented and bars indicate relative standard deviation.

The created strains were validated over a time period of 72h in biological and technical triplicates in LB and M9 medium (with thiamine, Chapter 2.2 Cultivation and storage of bacteria) at the plate reader with a monochromator. Here, the fluorescence values were normalised to the OD_{600} and the *B. plantarii* PG1 WT strain was used as a non-fluorescent strain as control (blank). The strongest fluorescence signal was detected at 48h, the late exponential growth phase and was used as optimal time point in the following experiments. In the first measurements no significant differences between the positive control and the strains with the promoter fusions of the putative promoter of *cas1*, *csy1* and csy4 were observed in LB medium. However, the reporter strain with the putative promoter site of *cas1* showed a slight increase and with the promoter site of *csy4* a high increase of the fluorescence level in M9 medium (Figure 35). In the next step the detected fluorescence levels of the different reporter strains were examined under the confocal microscope in M9 medium to avoid a possible medium effect of the LB medium at the late exponential growth phase (48h). Here, a sufficient mcherry fluorescence level was recorded in all strains and the cells were additionally stained with Dapi as control (Figure 36).
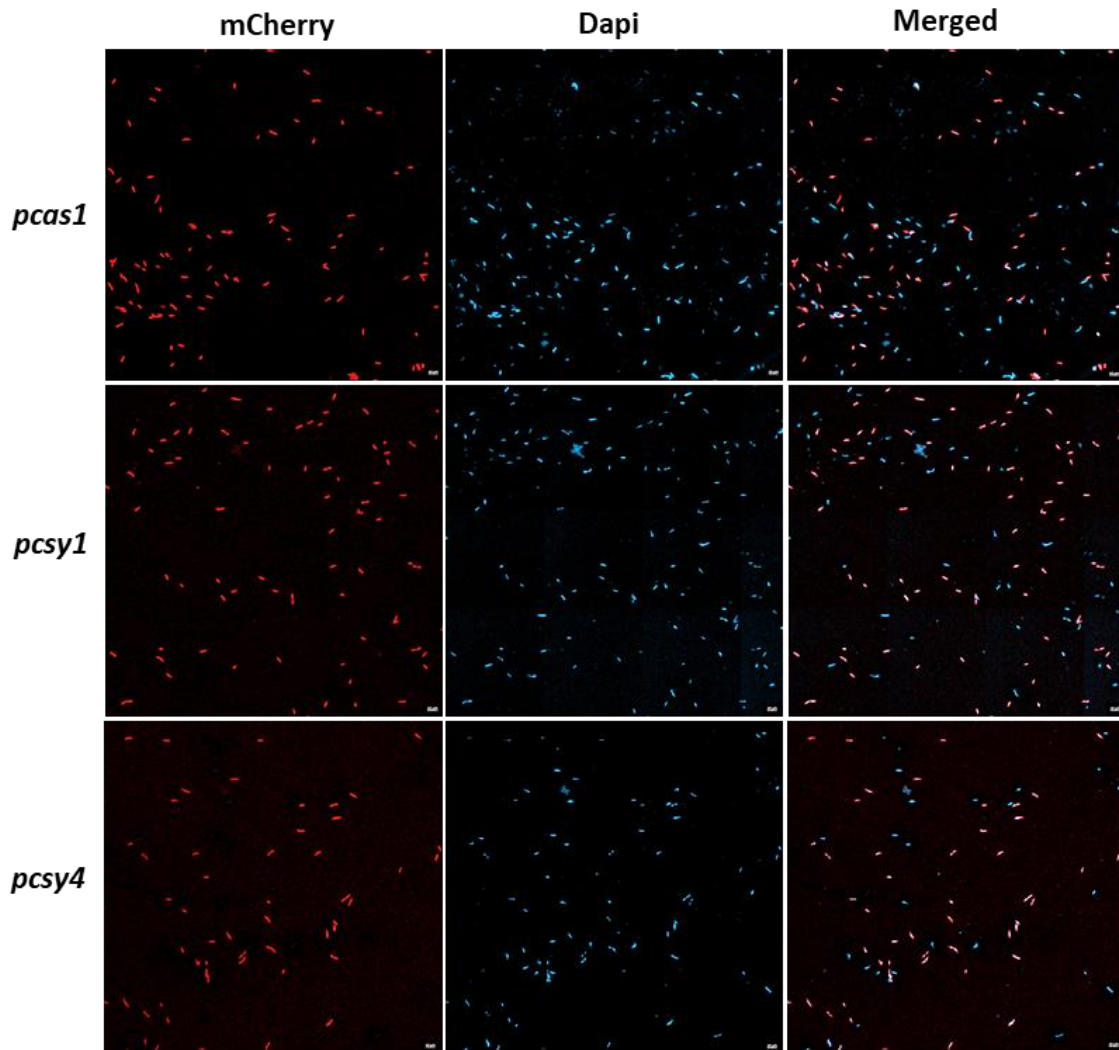
Figure 36: Confocal microscope images of the different mcherry promoter fusion strains in the wildtype BpPG1 in M9 medium in the late exponential growth phase (48h). *pcas1* = putative promoter site of *cas1*, *pcsy1*= putative promoter site of *csy1*, *pcsy4*= putative promoter site of *csy4*. Dapi stained. Settings can be found in Chapter 2.11, Table 9.

During further analysis of the transcriptome data, transcriptional changes regarding to possible regulators of the CRISPR/CAS system emerged. In order to identify known regulators for the CRISPR/CAS system, a literature search was performed. Here it was described that the existing CRISPR/CAS systems are regulated very differently depending on the organism. For further investigations of possible regulators, a genome search was performed for known regulators of the CRISPR/CAS I-F system in *B. plantarii* PG1. Here, the following possible regulators were detected: *LysR1* (BGL_1c18180), *LysR2* (BGL_1c18920), *LysR3* (BGL_2c03670), *LRP* (BGL_1c12270), *H-NS* (BGL_1c01520), *GalM* (BGL_1c13130), *CRP1* (BGL_2c00710), *CRP2* (BGL_2c19310), *CRP3* (BGL_2c22980) and *HtpG* (BGL_1c28680). In the following the transcriptome levels of the possible regulators were displayed (Figure 37).
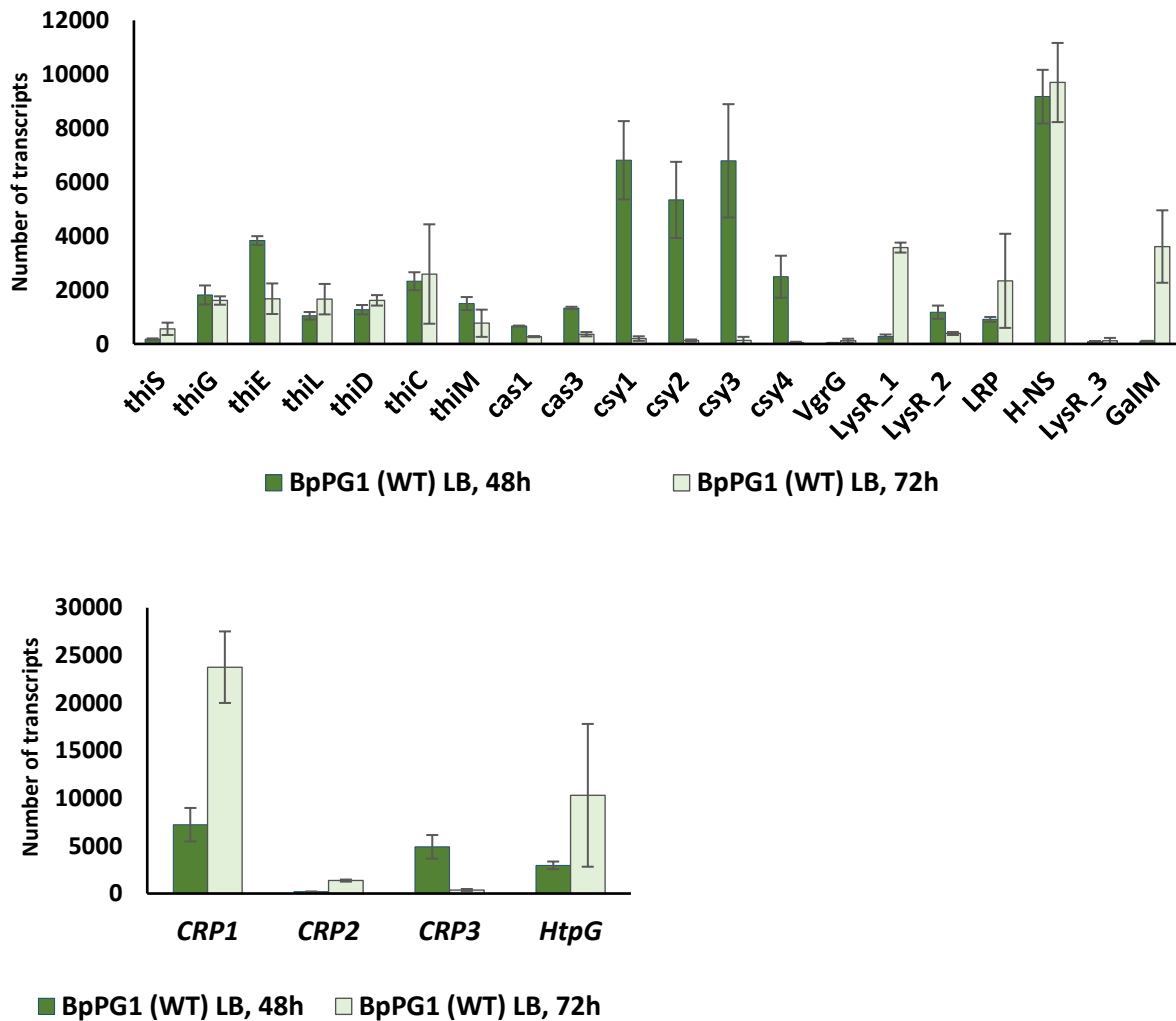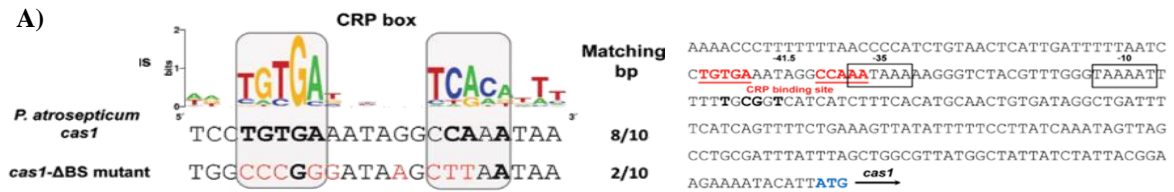
Figure 37: Different expression levels of selected possible regulators of the CRISPR/CAS system in the wildtype BpPG1. Number of transcripts of possible regulators of the CRISPR/CAS system in BpPG1 WT in LB medium at the late exponential growth phase (48h) and the late stationary growth phase (72h). The first graph is limited to 12000 transcripts and the second graph to 30000 transcripts. The mean values of three replicates are represented and bars indicate relative standard deviation.

In comparison, the genes of the thiamine metabolism *thiS* (BGL_1c03110), *thiG* (BGL_1c03120), *thiE* (BGL_1c03130), *thiL* (BGL_1c05130), *thiD* (BGL_1c07140), *thiC* (BGL_1c10790) and *thiM* (BGL_1c18800) revealed no highly differences from the late exponential (48h) to the late stationary growth phase (72h), except of *thiE*, here an increase of the transcription level was detected in the late exponential growth phase (48h). Regarding to the CRISPR/CAS system, the csy complex showed a higher transcription level in the late exponential growth phase (48h). Possible chosen regulators revealed different expression levels. Here, the transcription levels of the regulators *LysR*1, *GalM*, *CRP*1 and *HtpG* were increased in the late stationary growth phase (72h) whereas the other regulators exposed no

highly differences, except of *CRP*3 with an increased transcription level in the late exponential growth phase (48h). This led to the suggestion that *LsyR*1, *GalM*, *CRP*1, *CRP*3 and *HtpG* could have an influence on the CRISPR/CAS system.

A)

B)

DNA fragment	pilL2P		piLS2P
-10	**aaataaaag**	gcgtaacat	**tggtatcta**
-35	**ttgaaa**	ttccca	**ttgcca**
Crp binding site	AAATAACA	NA	NA

Table SA4. Putative promoters of *pilL2* and *pilS2* genes

Figure 38: Identification of the CRP binding site A) in *E.coli* K12 and B) in *P. aeruginosa* PAO1 (Patterson *et al*., 2015, Carter *et al*., 2010).

Due to this observation, a binding motif prediction search was performed. Here, two possible regulators of the CRISPR/CAS system were identified, the cAMP receptor proteins CRP1 and CRP3 which are dependent on the glucose metabolism and known as possible regulators of the CRISPR/CAS I-F system in other organisms. In literature different CRP binding motifs are described. The binding motif of *E. coli* K12 and *P. aeruginosa* PAO1 were compared to the CRISPR/CAS system to identify CRP binding motifs (Figure 38 and 39).
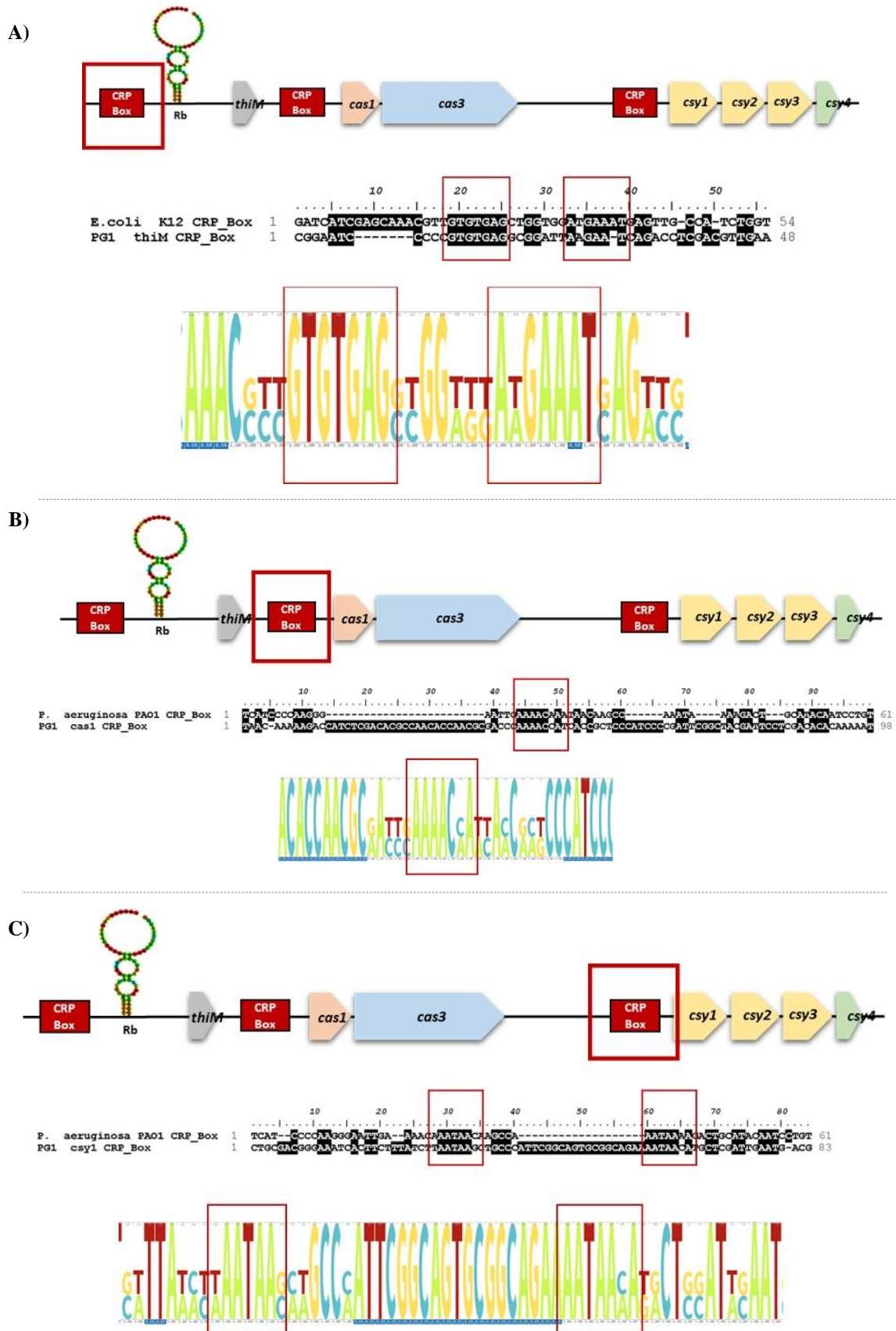
Figure 39: Alignments of CRP binding motifs from *E. coli* K12 and *P. aeruginosa* PAO1 to the CRISPR/CAS cluster. Identification of three putative CRP binding motifs upstream of A) *thiM*, B) *cas1* and C) *csy1*. Alignments were performed with Bioedit and displayed with LogoMaker.

57

The performed alignments revealed three putative CRP binding motifs in the CRISPR/CAS system. The first binding motif (GTGTGAG-AAGAA-T) was located upstream of the putative riboswitch structure of the hydroxyethylthiazole kinase ThiM. The second binding motif (AAAACCA) was located upstream of the endonuclease Cas1 and the third one (AATAA-AATAACA) was located upstream of the endonuclease Csy1 (Figure 39).
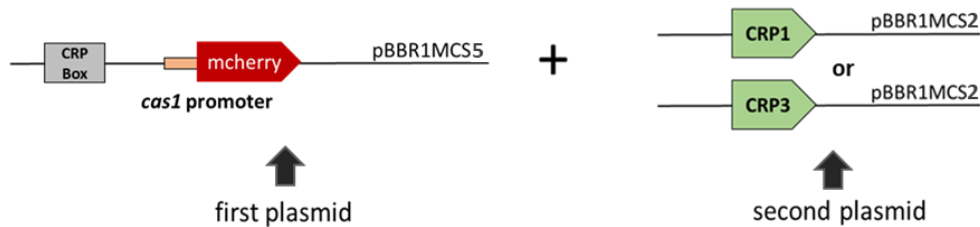

Figure 40: Scheme of experimental approach to the mcherry promoter fusion constructs and regulator constructs. Plasmid mcherry and regulator constructs to investigate the possible role of the regulators CRP1 and CRP3 with a second plasmid insertion in the promoter fusion strain with the putative promoter of *cas1*.

To further investigate CRP as possible regulator for the CRISPR/CAS system, CRP1 and CRP3 were inserted in the pBBR1MCS-2 plasmid and transferred to the promoter reporter strain of *cas1*. Thus, *CRP*1 (787bp) and *CRP*3 (825bp) were amplified with specific primers on genomic DNA of the wildtype BpPG1 and digested with restriction enzymes for the following ligation into the pBBR1MCS-2 plasmid (Figure 40). The construct was transformed to *E. coli* DH5α for replication and isolation of the final plasmid. The receptor protein CRP2 was not investigated more in detail due to it proved to be cytotoxic in experimental approaches.
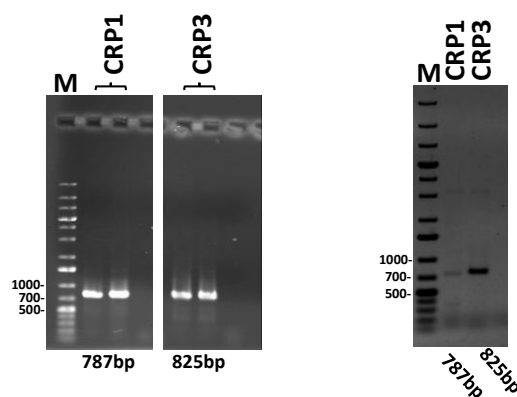

Figure 41: Amplification of the possible regulators *CRP1* (787bp) and *CRP3* (825bp) on gDNA of the wildtype BpPG1 (left). Control PCR with specific primer at the plasmid constructs with pBBR1MCS-2 with the possible regulators *CRP1* and *CRP3* (right). p= promoter region, 0,8% agarose gel, 1kb+ O'GeneRuler™ DNA Marker (Thermo Scientific™ SM1343), 5µl per sample

The final plasmid was isolated and introduced into the promoter fusion strain of the putative promoter site of *cas1* in the wildtype BpPG1 by electroporation. In this approach two plasmids are available in the wildtype BpPG1 at the same time. To evaluate the possible influence of the receptor protein CRP1 and CRP3 the fluorescence level was measured at the plate reader to the late exponential growth phase (48h) in LB medium.
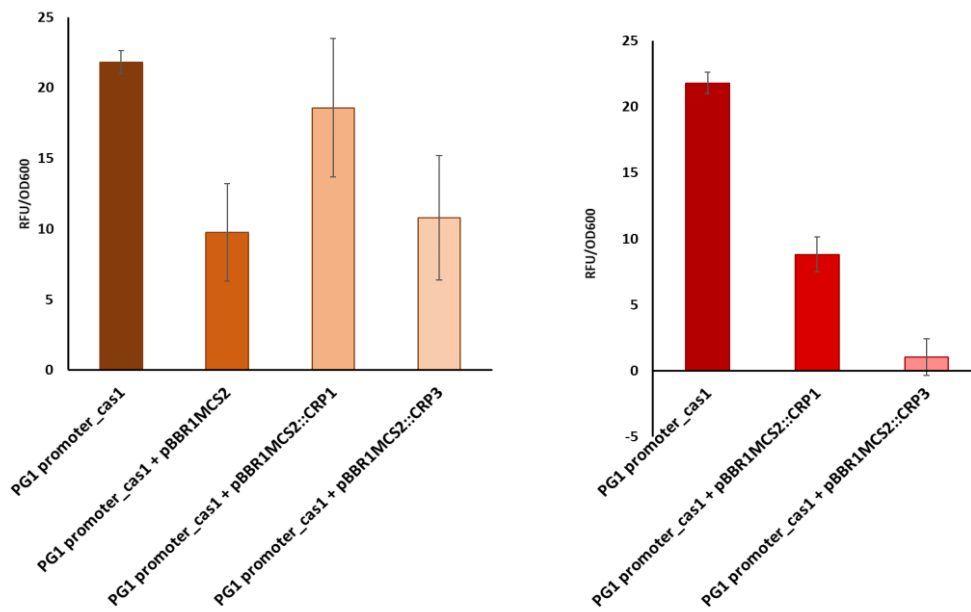

Figure 42: RFU/OD600 evaluation of the mcherry promoter fusion strains in combination with the possible regulators. Evaluation of the relative fluorescence level normalized to the optical density (RFU/OD600) of the promoter-mcherry fusion strains with the putative promoter sites of *cas1* and the positive control, a fusion of the house-keeping gene *rpoD* with mcherry and the second plasmid insertion with the possible regulator of *CRP1* or *CRP3* (left). Control of a possible second plasmid effect by normalising the first measurement of the RFU/OD600 level with the positive control of BpPG1 pBBR2MCS-2 without regulator (right). The mean values of three replicates are represented and bars indicate relative standard deviation.

The strains were measured for 48h to the late exponential growth phases in biological and technical triplicates. The fluorescence values were normalised to the OD_{600} and *B. plantarii* PG1 WT strain was used as a non-fluorescent strain as control (blank). To avoid an effect on the fluorescence level due to the second plasmid in the organism, as additional control the measured data were normalized to a *B. plantarii* PG1 strain with a second plasmid of pBBR1MCS-2 without regulator. The insertion of the second plasmid with the regulator of CRP1 and CRP3 led to a significant decreased RFU/OD_{600} level, which led to the assumption that CRP1 and CRP3 could act as repressor of the CRISPR/CAS system (Figure 42).
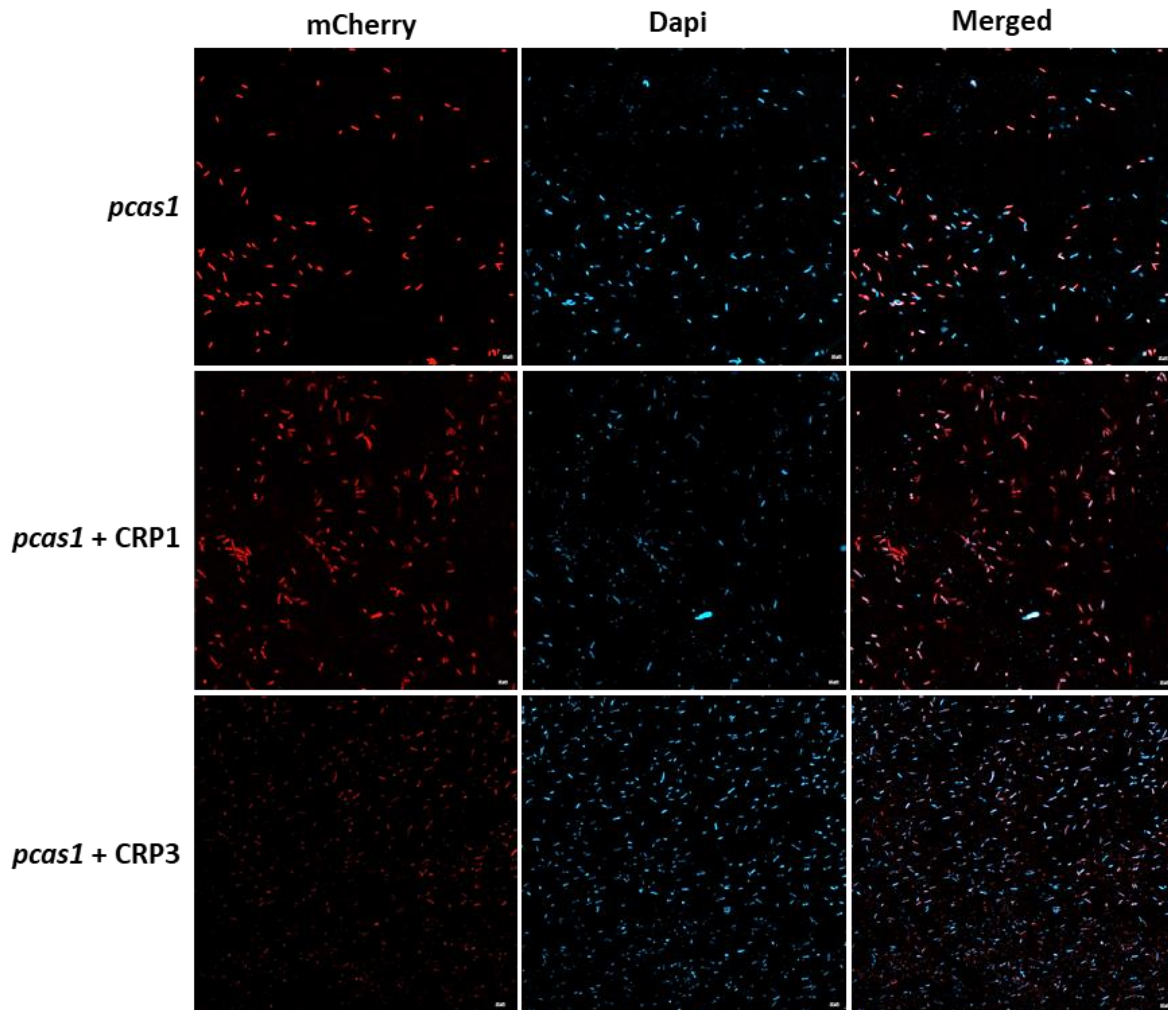
Figure 43: Confocal microscope images of the two-plasmid approach in BpPG1 WT in M9 medium in the late exponential growth phase (48h) in the promoter fusion strain of *cas1* to evaluate the role of CRP1 and CRP3 as possible regulators of the CRISPR/CAS system. *pcas1* = putative promoter site of *cas1*. Dapi stained. Settings can be found in Chapter 2.11, Table 9.

Subsequently, the bacterial strains with the two plasmids were examined under the confocal microscope in LB medium at the late exponential growth phase (48h). Here a similar effect as in the plate reader measurements were observed. The fluorescence level was reduced by the insertion of the possible regulator CRP1 and especially with the possible regulator CRP3 (Figure 43). In the next step transcriptome analyses were performed. Here the wildtype BpPG1 with an inserted plasmid pBBR1MCS-2 as control were compared to the expression levels of the wildtype BpPG1 with pBBR1MCS-2 and the possible regulators CRP1 and CRP3.
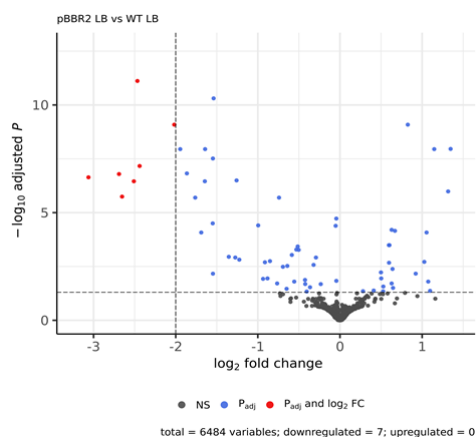
Locus Tag	Annotation	log2foldchange	p-value
BGL_1c15240	3D-(3,5/4)-trihydoxycyclohexane-1,2-dione hydrolase IolD	-2.02	6.61E-13
BGL_1c26810	putative acyl-CoA dehydrogenase HutD	-2.44	1.3708E-10
BGL_1c00500	phenylalanine-4-hydoxylase PhhA	-2.47	1.54E-15
BGL_1c26790	formimidoylglutamate deiminase HutF	-2.51	1.0966E-09
BGL_1c26840	histidine ammonia-lyase HutH	-2.65	6.5233E-09
BGL_1c26800	imidazolone propionase HutI	-2.69	3.8859E-10
BGL_1c26820	urocanate hydratase HutU	-3.06	5.9772E-10

Figure 44: Comparison of different expression analysis of RNA-seq data between BpPG1 pBBR1MCS-2 and the wildtype BpPG1 in LB medium in the late exponential growth phase (48h). Volcano plot of gene distribution of significant up- and down-regulated genes. Table of significant down-regulated genes.

The transcriptome analysis of the control strain BpPG1 pBBR1MCS-2 displayed only small transcriptional changes. No up-regulated genes were represented and only a small number of genes were down-regulated. The down-regulated genes were allocated to the histidine metabolism (Figure 44). This change in metabolism could be interpreted as a stress response, due to the introduction of a plasmid into the organism. In the environment, the introduction of a plasmid into the cell is used to adapt features such as antibiotic resistance or to utilise components for internal metabolism. Therefore, the histidine metabolism is an essential pathway to generate precursors for the amino acid metabolism and further important for the control of the citrate cycle and following reaction leading, for example to the alpha-ketoglutarate in citrate cycle (Lemire *et al*., 2010, Bender, 2012).
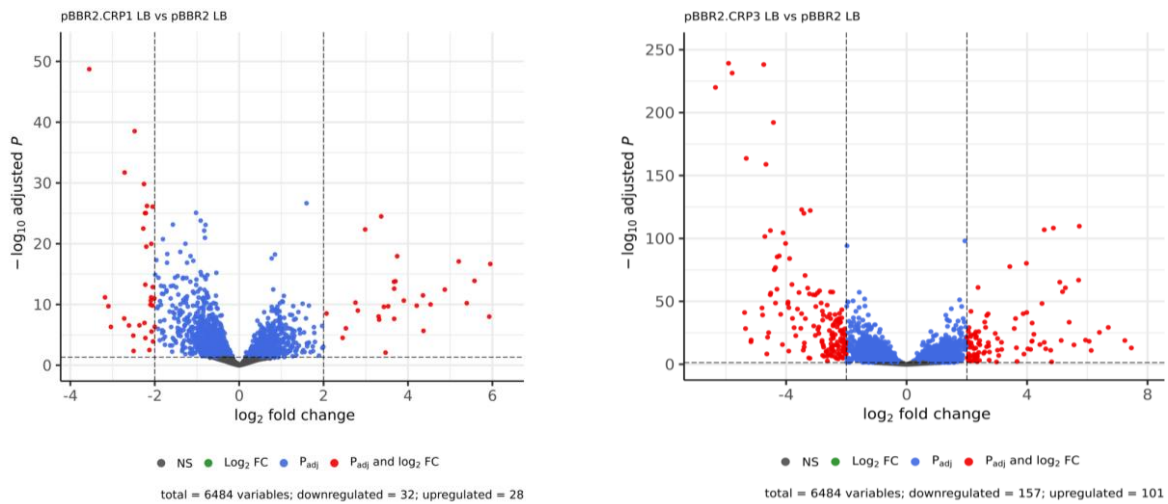
Figure 45: Comparison of the gene distribution of the possible regulators CRP1 and CRP3. Volcano plots of significant up- and down-regulated genes in the different expression analyses of RNA-seq data of BpPG1 pBBR1MCS-2::CRP1 and CRP3 to BpPG1 pBBR1MCS-2 in LB medium in the late exponential growth phase (48h).

The comparison of the expression levels of the transcriptome analysis of BpPG1 pBBR1MCS-2::CRP1 and BpPG1 pBBR1MCS-2::CRP3 revealed a small number of regulated genes. In total 6483 genes were transcribed (Figure 45). A BlastKOALA analysis displayed in the examination of CRP1 that nine out of 28 up-regulated and 16 out of 33 down-regulated detected genes were allocated to KEGG pathways. Here, especially the fatty acid metabolism, drug resistance genes and efflux pumps were up-regulated and the amino acid transport and metabolism, particularly for glutamate and tyrosine and the nitrogen metabolism were down-regulated. In contrast, no significant effects were observed when considering selected genes of the thiamine metabolism, the CRISPR/CAS system and other possible regulators (Figure 46).
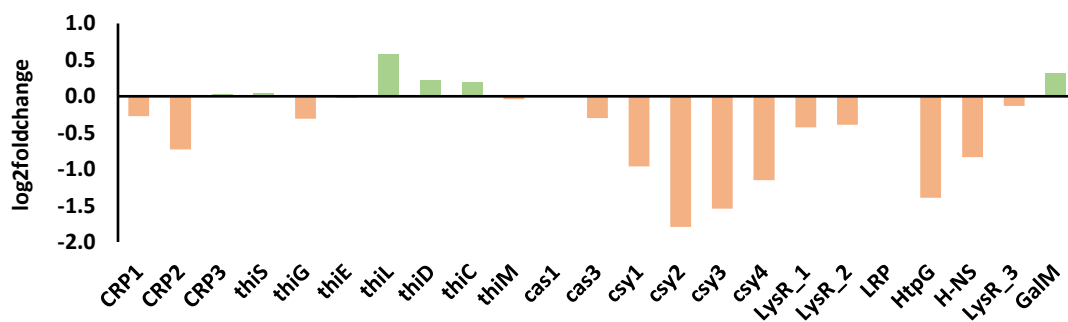

Figure 46: Expression levels of possible regulators, the thiamine metabolism and CRISPR/CAS system in BpPG1 pBBR1MCS-2::CRP1 in comparison to PG1 pBBR1MCS-2 in LB medium in the late exponential growth phase (48h).

The different expression analysis of RNA-seq data of BpPG1 pBBR1MCS-2::CRP3 to BpPG1 pBBR1MCS-2 in LB medium revealed 101 up-regulated and 160 down-regulated genes due to the total amount of 6483 transcribed genes. Here, 46 out of 101 up-regulated and 96 out of 160 down-regulated genes were allocated to KEGG pathways according to BlastKOALA analysis. Thus, it was observed that the fatty acid metabolism, sugar transport, carbohydrate metabolism and coenzyme transport were up-regulated. The energy production and conversion, amino acid transport and metabolism as well as the phenylacetic acid degradative pathway were down-regulated. Additionally, no significant changing transcription levels of the possible regulators were observed except of *galM*. A significant decrease of the transcription level of *csy2-4* and *HtpG* were observed which confirmed the results of the previous promoter studies (Figure 47).
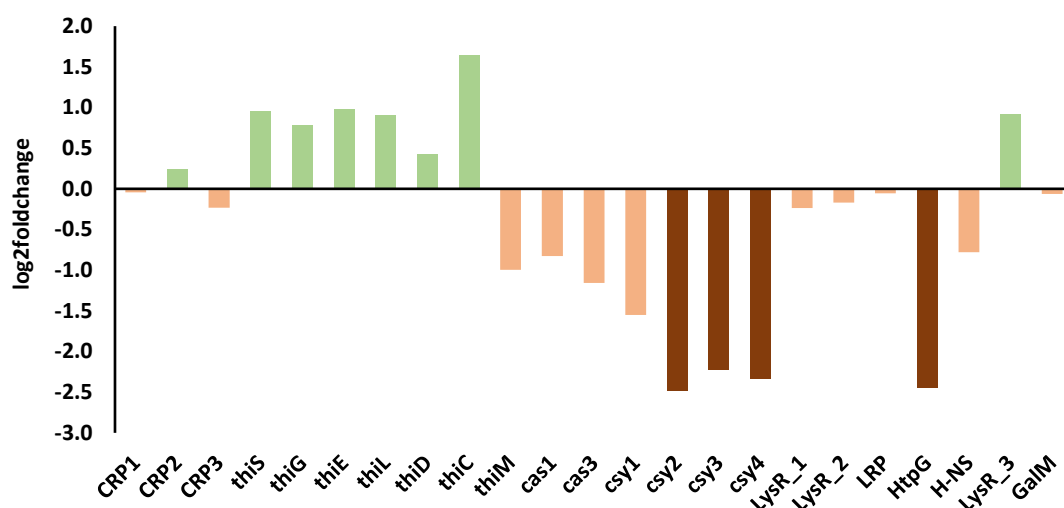
Figure 47: Expression levels of possible regulators, genes of thiamine metabolism and CRISPR/CAS. Distribution of up- and down-regulated genes in BpPG1 pBBR1MCS-2::CRP3 in comparison to BpPG1 pBBR1MCS-2 in LB medium in the late exponential growth phase (48h). Light bars = not significant, dark bars = significant.

In conclusion, in both transcriptome analyses of CRP1 and CRP3, the fatty acid metabolism was up-regulated, especially in the transcriptome analysis of CRP3 the sugar transport and carbohydrate metabolism were up-regulated as well. Here it was striking that in both transcriptome analyses the amino acid transport and metabolism was down-regulated and in the transcriptome analysis of CRP3 several genes responsible for the phenylacetic acid degradative pathway were down-regulated which is a central pathway for the degradation of aromatic compounds.

Other influences on the CRISPR/CAS system

In literature it is described that the CRISPR/CAS system is regulated by the Quorum sensing system. In 2015 a study was published which revealed that the special QS system in *B. plantarii* PG1 has an influence on the CRISPR/CAS system (Gao *et al.*, 2015). To investigate the observed effect on the CRISPR/CAS system the created promoter fusion constructs were introduced by electroporation into the in the previous study of Rong Gao created QS deletion mutant BpPG2, BpPG3 and BpPG4 (formerly *glumae* = BgPG2-4).
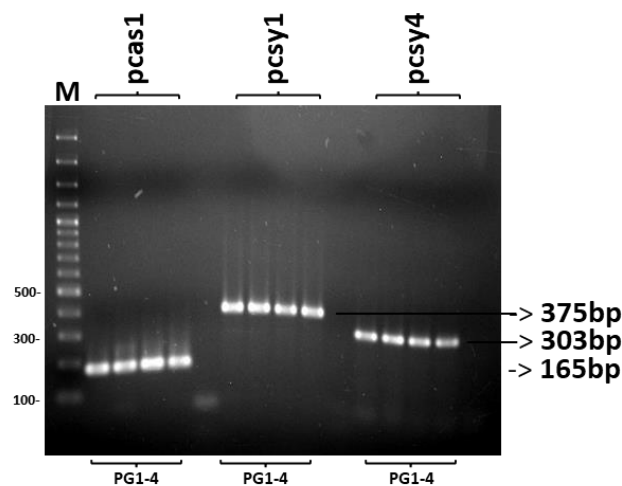
Figure 48: Control PCR with specific primer on the plasmid constructs with pBBR1MCS-2 with the putative promoter sites of *cas1* (165bp), *csy1* (375bp) and *csy4* (303bp) on the isolated plasmids of BpPG1(WT), BpPG2(Δ*bgal*1), BpPG3(Δ*bgal*2) and BpPG4(Δ*bgal*3); p= promoter region, 0,8% agarose gel, 1kb+ O'GeneRuler™ DNA Marker (Thermo Scientific™ SM1343), 5µl per sample

In the next step, the promoter fusion plasmids were isolated from the different strains and controlled via PCR with specific primers (Figure 48). To evaluate the influence of the lacking QS AHL synthases the strains were measured for 48h to the late exponential growth phase in biological and technical triplicates at the plate reader with a monochromator in LB and M9 medium (thiamine added). The fluorescence values were normalised to the OD_{600} and to the *B. plantarii* PG1 wildtype strain as non-fluorescent strain as control (blank).
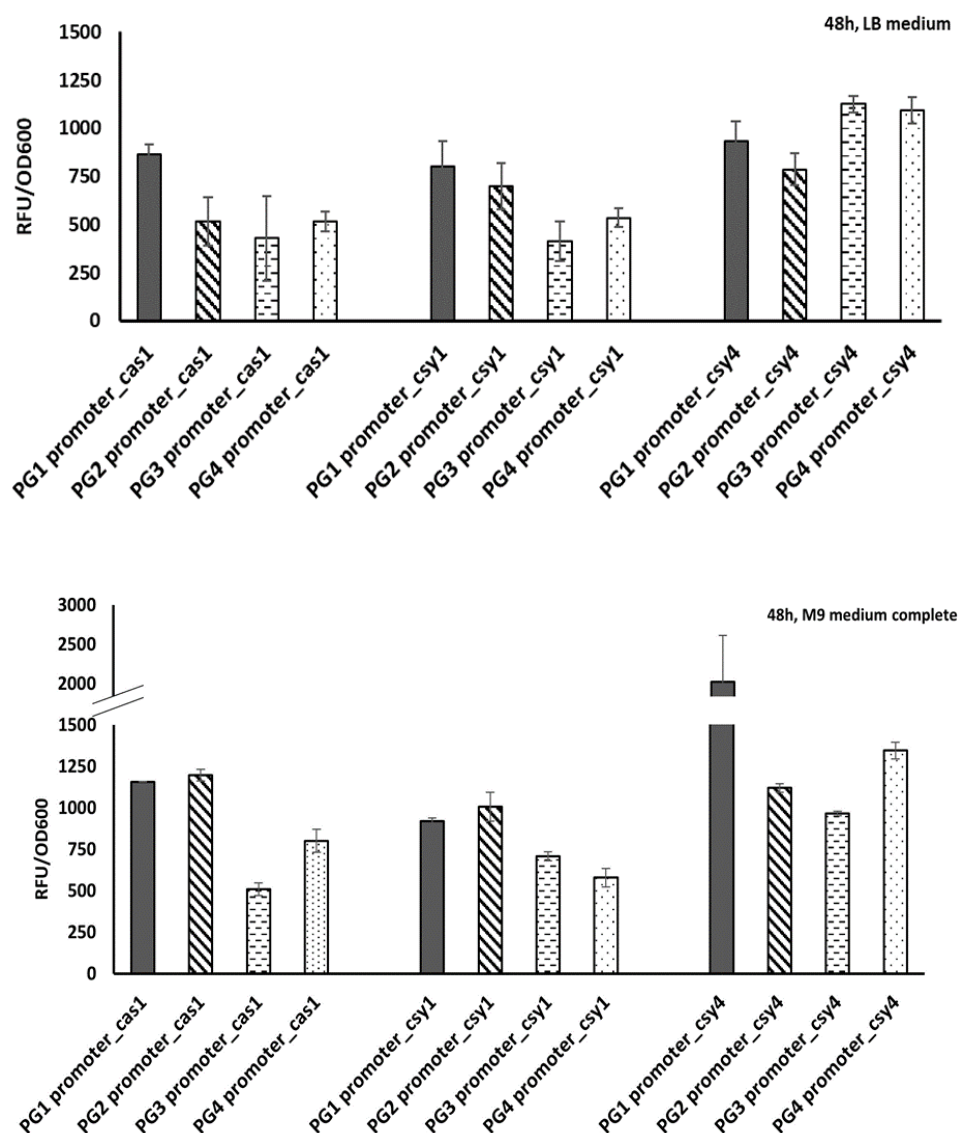
Figure 49: Relative fluorescence level of the reporter constructs in BpPG1-4. RFU normalised to the optical density at 600 nm of the reporter constructs with the putative promoter sites of *cas1*, *csy1* and *csy4* with mcherry in the QS-deletion mutant BpPG1-4 measured in LB and M9 medium at the exponential growth phase (48h) at 28°C at the plate reader (monochromator). The mean values of three replicates are represented and bars indicate relative standard deviation.

The strains were evaluated in LB and M9 medium (thiamine added). Here, significant differences were observed between the different strains and in the different media. The fluorescence values of the wildtype reporter strains revealed slight increased differences, especially with the promoter of *csy4* in comparison of LB to M9 medium. In contrast to this observation, in the QS deletion mutants BpPG3 and BpPG4, a reduction of the fluorescence level was observed in all strains, except the promoter fusion of the promoter of *csy4* in LB medium (Figure 49).
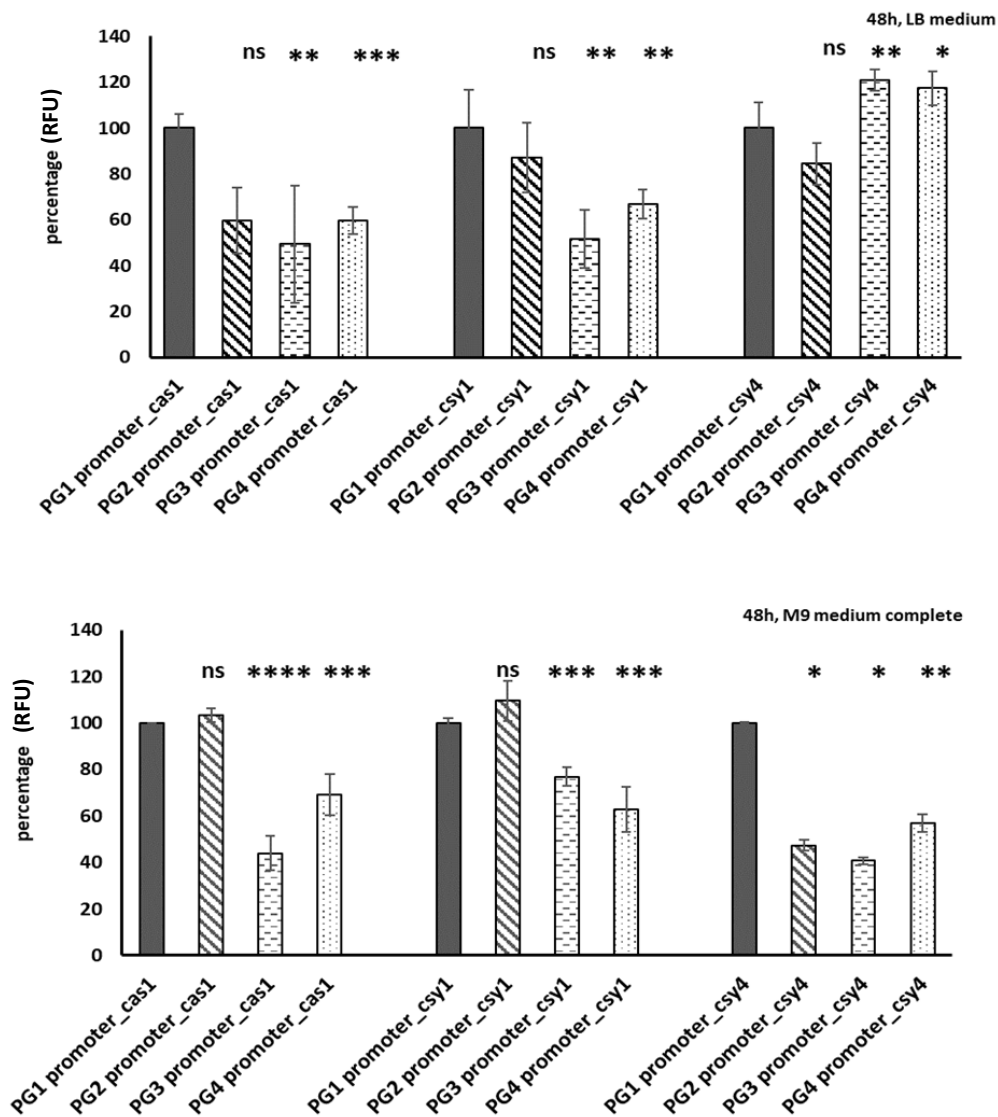
Figure 50: Percentage representation of the relative fluorescence level of the reporter constructs in BpPG1-4. Relative fluorescence level (RFU) normalised to the optical density at 600 nm of the reporter constructs with the putative promoter sites of *cas1*, *csy1* and *csy4* with mcherry in the QS-deletion mutant BpPG1-4 measured in LB and M9 medium at the exponential growth phase (48h) at 28°C at the plate reader (monochromator). ns = not significant, *= p ≤ 0.05, **= p ≤ 0.01, ***= p≤0.001, ****= p ≤ 0.0001. The mean values of three replicates are represented and bars indicate relative standard deviation.

Additionally, the measured results were displayed in percentage regarding to the wildtype reporter strains for enhanced verification and proving the significance (Figure 50). Here again it was striking that the promoter fusions showed a decreased fluorescence values in the QS deletion mutants of BpPG3 and BpPG4 with the promotor sites of *cas1* and *csy1* in LB and M9 medium. In contrast the *csy4* promoter sites displayed an increased fluorescence level in the

different strains in LB medium but a decreased fluorescence value in M9 medium. Summarised, the nutrient change from LB to M9 medium showed an effect on the QS system and the CRISPR/CAS system. To explore this type of network-like behaviour in more detail, different salt and glucose concentrations were tested in addition. The QS reporter strains were cultivated in M9 medium with and without salt and with and without glucose depending on the experimental testing conditions.
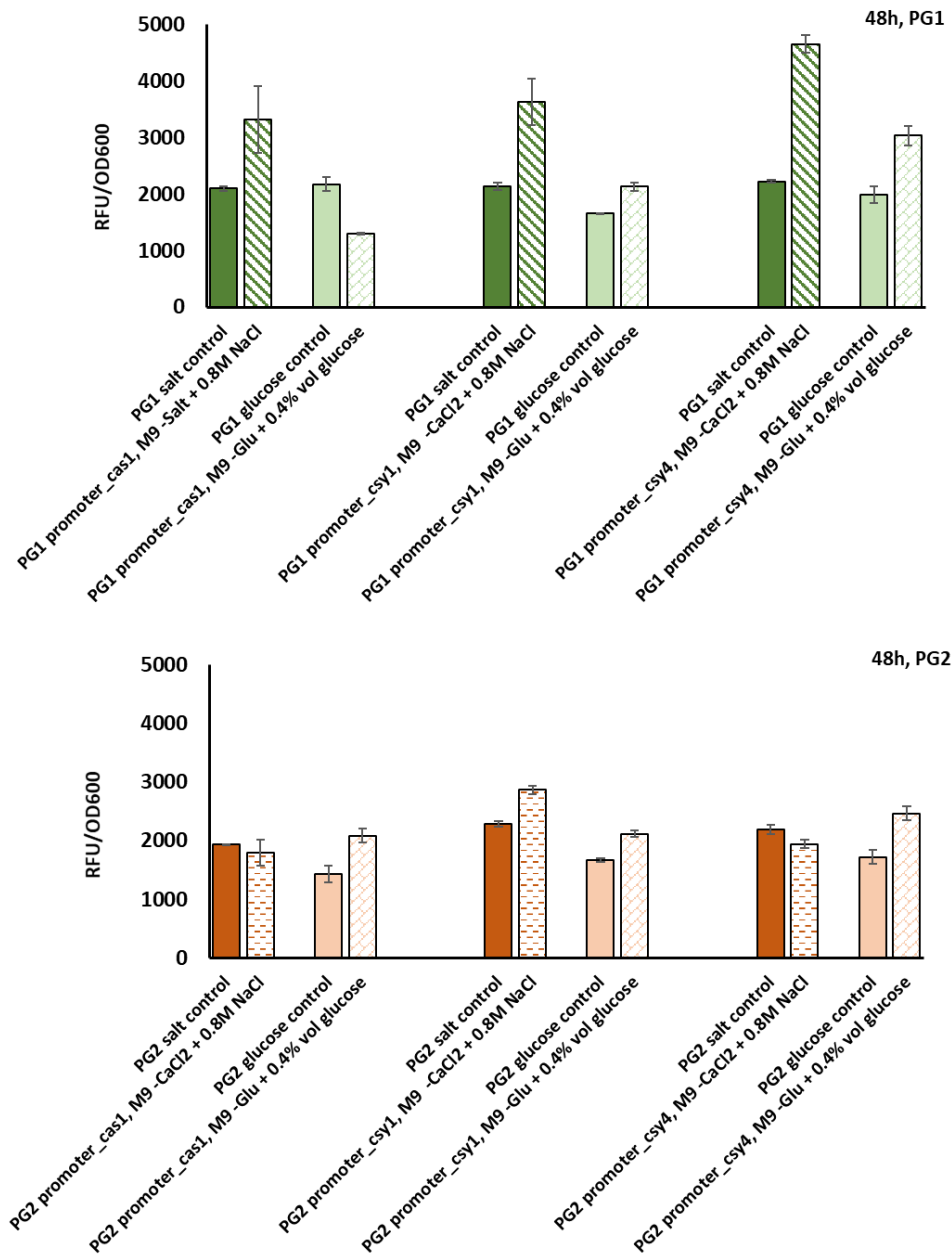
Figure 51: Salt and glucose stress test in BpPG1 and BpPG2 promoter fusion strains. Relative fluorescence level (RFU) normalised to the optical density at 600 nm of the reporter constructs with the putative promoter sites of *cas1*, *csy1* and *csy4* with mcherry in the QS-deletion mutant BpPG1-2 measured in M9 medium under different salt and glucose concentrations at the exponential growth phase (48h) at 28°C at the plate reader (monochromator). The mean values of three replicates are represented and bars indicate relative standard deviation.
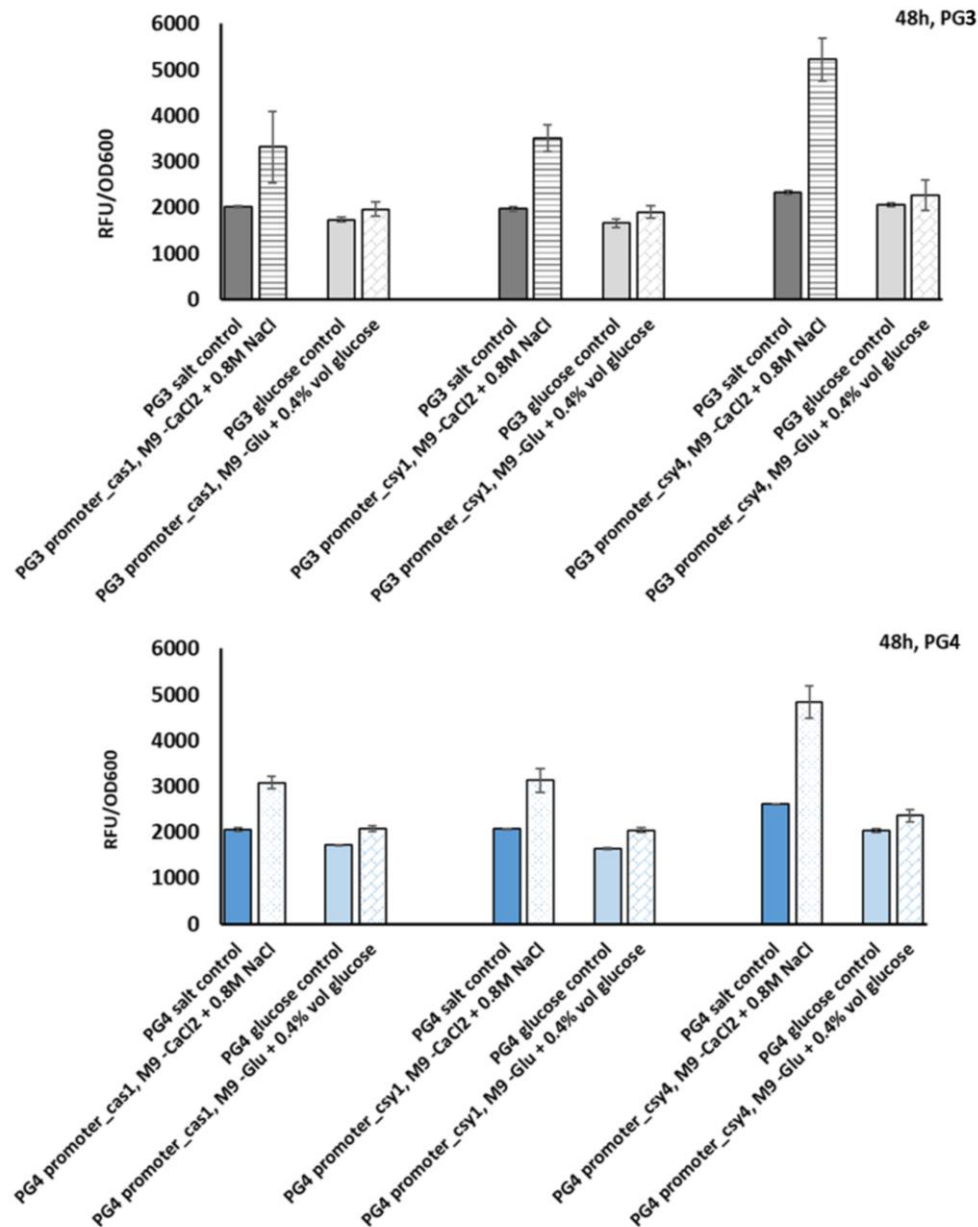
Figure 52: Salt and glucose stress test in BpPG3 and BpPG4 promoter fusion strains. RFU normalised to the optical density at 600 nm of the reporter constructs with the putative promoter sites of *cas1*, *csy1* and *csy4* with mcherry in the QS-deletion mutant BpPG3-4 measured in M9 medium under different salt and glucose concentrations at the exponential growth phase (48h) at 28°C at the plate reader (monochromator). The mean values of three replicates are represented and bars indicate relative standard deviation.

The fluorescence levels of the different strains were measured in the late exponential growth phase (48) in biological and technical triplicates at the plate reader with a monochromator. The fluorescence values were normalised to the OD_{600} and to the *B. plantarii* PG1 wildtype strain as non-fluorescent strain as control (blank). In preliminary tests, different glucose and salt concentrations were tested. In the salt tests, a change was perceived from a concentration of 0.8M NaCl. In the preliminary glucose tests no highly changes were observed, so the highest concentration which were tested and was displayed here in the amount of 0.4% vol glucose and showed small differences. In the wildtype BpPG1 an increase of the fluorescence level was observed in all promoter strains under the salt stress condition. The glucose condition revealed a decrease of fluorescence level in the reporter strain of *cas1*, whereas a slight increase of fluorescence level was detected in the reporter strain of *csy4*. In contrast, no significant differences were measured in the QS deletion mutant BpPG2 independent of the promoter site and the salt and glucose concentration (Figure 51). In the comparison to the QS deletion mutant strains BpPG3 and BpPG4 an increased fluorescence level was detected applying 0.8M NaCl in all promoter strains. In contrast no significant differences were detected under glucose stress conditions (Figure 52). For further investigations, the static biofilm formation of the different reporter constructs in the wildtype BpPG1 were investigated under salt stress conditions in LB medium to compare biofilm growth under natural nutrient saturated conditions with imitation salinisation.
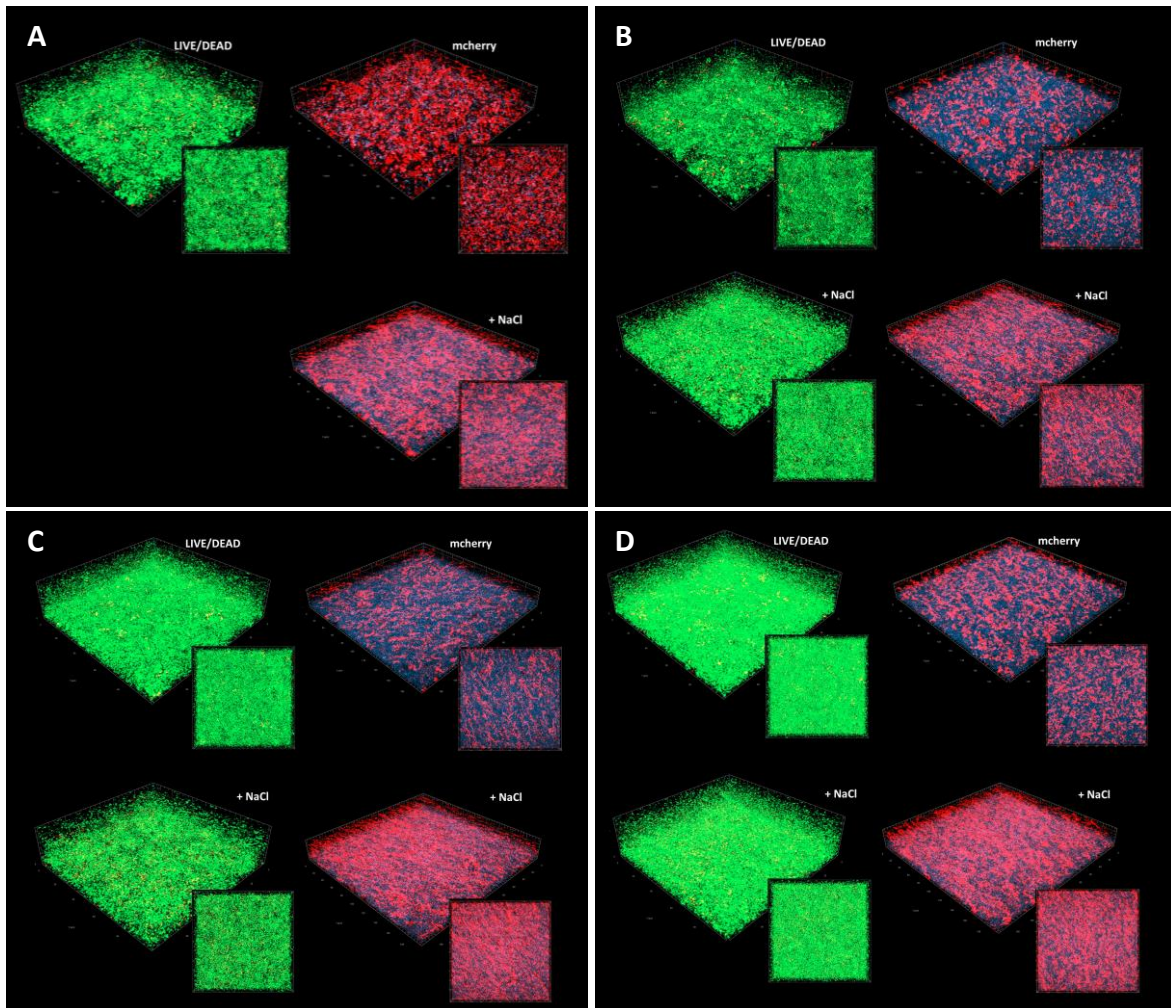
Figure 53: Confocal microscope images of static biofilm formations of BpPG1 strains under salt stress conditions in LB medium in the late exponential growth phase (48h).
(A) BpPG1 positive control mcherry. (B) BpPG1 pBBR1MCS-2 prom*cas1*::mcherry (promoter of *cas1*). (C) BpPG1 pBBR1MCS-2 prom*csy1*::mcherry (promoter of *csy1*). (D) BpPG1 pBBR1MCS-2 prom*csy4*::mcherry (promoter of *csy4*). All strains were cultivated to the late exponential growth phase (48h) in LB medium and LB medium with supplemented 0.8M NaCl. The biofilms were stained with Dapi (blue) and Live/Dead staining (left, green). In addition, the mcherry fluorescence level (red) were detected and displayed on the right side of each sample. Settings can be found in Chapter 2.11, Table 10-11.

The bacterial strains were cultivated with a starting OD_{600} of 0.05 with and without 0.8M NaCl in LB medium to the late exponential growth phase (48h). In the following, the samples were dyed with LIVE/DEAD staining (red) and Dapi (blue) and analysed under the confocal microscope. Here, an increasing fluorescence level were observed in all promoter fusion strains supplying 0.8M NaCl which confirmed the previous measured results at the plate reader in M9 medium (Figure 53).

4 Discussion & Outlook

4.1 A hydroxyethylthiazole kinase as possible regulator of the CRISPR/CAS I-F system

Thiamine plays an important role in the metabolism of bacteria as well as of plants. It represents an essential co-factor for the regulation of several metabolic processes (Yuan X *et al.*, 2021). In *B. plantarii* PG1 the genomic location of the hydroxyethylthiazole kinase ThiM upstream of the endonuclease Cas1 of the CRISPR/CAS system is unique and its relation to it is still unknown. The CRISPR/CAS system is an adaptive bacterial immune system and in literature it is described that the regulation mechanism of CRISPR/CAS systems are very diverse and organism specific (Patterson *et al.*, 2017). To investigate a possible relation of the kinase ThiM to the CRISPR/CAS system the unique position of ThiM first had to be validated. The gene neighbourhood region searches by IMG in other relatives confirmed the unique position of the kinase ThiM upstream of the endonuclease Cas1 (Figure 2). First transcriptome analyses revealed different expression activities of the kinase ThiM and the genes *csy1-3* of the CRISPR/CAS system compared to the endonucleases Cas1, Cas3 and Csy4 in the wildtype BpPG1 in the early exponential growth phase (28h) in LB medium (Figure 11). In further analyses the wildtype BpPG1 were compared to the deletion mutant BpPG1Δ*thiM* in LB medium and in M9 medium without thiamine in the late exponential growth phase (48h) and in LB medium in the late stationary growth phase (72h). In the comparison of the wildtype BpPG1 to the deletion mutant BpPG1Δ*thiM* in LB medium in the late exponential growth phase (48h) an increased number of transcripts of *csy1-3* were observed in the deletion mutant BpPG1Δ*thiM* (Figure 13). In contrast, the number of transcripts of the CRISPR/CAS system in M9 medium without thiamine showed no significant activity (Figure 14). In the following log2foldchange analysis of the wildtype BpPG1 and the deletion mutant BpPG1Δ*thiM* in LB and M9 medium without thiamine confirmed the results of the comparison of the number of transcripts (Table 12). The comparison of the different media demonstrated significant transcriptional changes in both strains but the comparison of the different strains in the same media revealed no significant changes.

In conclusion, a direct regulation of the CRISPR/CAS system by the kinase ThiM could not be determined here. Nevertheless, changing medium conditions caused transcriptional changes in the deletion mutant BpPG1Δ*thiM* as well as in the wildtype BpPG1. However, it was demonstrated that the activity of the CRISPR/CAS system in the exponential growth phase (48h) was increased compared to the stationary growth phase (72h). Additionally, slight differences in the CRISPR/CAS genes of *csy2* and *csy3* were detected in the deletion mutant BpPG1Δ*thiM* as well as in LB and M9 medium without supplemented thiamine. This led to the

suggestion of a possible co-regulation of the thiamine metabolism and the CRISPR/CAS system. Additionally, the analysis indicated an influence on the activity of the CRISPR/CAS system by changing environmental conditions via different media (LB to M9 medium without thiamine). Based on these results, a metabolic network analysis was performed to identify expression patterns and evaluate the role of thiamine in the regulation of the CRISPR/CAS system and in metabolic processes of the wildtype BpPG1 and the deletion mutant BpPG1Δ*thiM*. In literature it is described that the CRISPR/CAS system is influenced by environmental changes. For example, a study investigated the influence of environmental signals in *Flavobacterium columnare* related to eukaryotic hosts. Here it was discovered that the CRISPR spacer acquisition increased in the presence of mucin, a eukaryotic host signal. Additionally low nutrient conditions led to a higher level of spacer acquisitions in the bacterium (de Freitas Almeida *et al*., 2022). Other studies have also shown the effect of changing temperature and induced oxidative stress at CRISPR immunity (Weissman *et al*., 2019). The stress induced activity of CRISPR/CAS immunity in *Myxococcus xanthus* during sporulation has also been demonstrated (Louwen *et al*., 2014). This implies that the CRISPR/CAS system is very sensitive to external signals and involved in molecular signalling processes which indicates that it would not be surprising if there were a co-regulation of thiamine metabolism and CRISPR/CAS system in *B. plantarii* PG1. Thiamine could have an influence due to its function as secondary metabolites in plants and can be used for example, as messenger signal under changing environmental conditions as stress response or in the event of an attack to activate the CRISPR/CAS system (Jurgenson *et al*., 2009). A direct effect of thiamine was not observed from the transcriptome analysis, but further experiments could evaluate the unique position of ThiM in more detail.

For future insights, to investigate a possible co-regulation of the thiamine metabolism and CRISPR/CAS system, a thiamine auxotroph mutant could be generated, and a phenotypic characterisation could lead to new perceptions. Additionally, the insertion of a fluorescence marker in the CRISPR/CAS system could be valuable for further studies in future experiments to monitor changes in the CRISPR/CAS system. On the other hand, the literature suggests that Burkholderia will not be able to maintain its metabolism without thiamine biosynthesis, as it is an essential co-factor, which makes it a difficult challenge (Koenigsknecht *et al*., 2010). At the same time, however other studies show that thiamine auxotrophic mutants are possible (Sannino *et al*., 2018). Nevertheless, by generating different thiamine mutants, the limits of thiamine auxotrophy could be determined and used for further experiments to elucidate a possible co-regulation of thiamine metabolism and the CRISPR/CAS system.

4.2 Evaluation of metabolic changes by transcriptome profiling analysis

Since prokaryotes, in contrast to eukaryotes, do not have separate cell compartments in which metabolic processes can proceed independently to other cellular processes, prokaryotes had to build up a complex network of regulatory cascades through which metabolic processes can be coordinated and conducted efficiently. For this purpose, there are different mechanisms to build and maintain an optimal cost-benefit life cycle. In this way, important functions are activated, and non-required functions are regulated. Changes in gene regulation are mainly caused by abiotic as well as biotic factors. *B. plantarii* PG1 is a soil bacterium whose life cycle is closely related to plants. Studies have shown that plants influence their microbiome by secreting metabolites and that the microbiome influences the plant. These signalling are used for the defence against pathogens, pests and herbivores and enable a response to environmental stresses (Zhiqiang Pang *et al.*, 2021). In fact, the plant microbiome is defined as plant health providing community. *B. plantarii* PG1 in turn is a plant pathogen that causes great damage in agriculture and leads to the death of infected plants. Here it senses the signals of the environment as well as of the plants and induces adaptations in its metabolic processes. As already mentioned, thiamine plays an important role in bacteria as well as in plants and represents an essential co-factor in metabolic pathways. So far it is known that most bacteria require thiamine as co-factor. But in contrast there are also bacteria known which are not limited by the amount of thiamine. *Borrelia burgdorferi*, the causative agent of Lyme disease in human do not possesses any genes for thiamine biosynthesis or transport and has evolved alternative pathways to synthesise acetyl-CoA and ATP (Zhang *et al.*, 2017). Despite to the challenging limitation due to its importance in metabolic pathways thiamine biosynthesis and transport is well studied in literature.

In the performed metabolic network analysis in this work, the wildtype BpPG1 were compared to the deletion mutant BpPG1Δ*thiM* under different conditions. The bacterial strains were cultivated in the nutritionally rich LB-medium, in a mineral M9 medium without thiamine and a mineral M9 medium supplemented with 7.5 mM thiamine at the late exponential (48h) and the late stationary growth phase (72h). Volcano plots of the distribution of significant up- and down-regulated genes in the late exponential growth phase (48h) revealed several regulated genes in the comparison of the strains in M9 medium without thiamine to LB medium (Figure 16a, b). In the comparison of the deletion mutant BpPG1Δ*thiM* to the BpPG1 wildtype in the same medium a small number of genes were regulated (Figure 16c, d). The same effect was observed in the previous transcriptome analysis of Chapter 3.1. For obtaining first insights regarding to the highly regulated genes, PATRIC analyses of the transcriptome analysis of the late exponential (48h) and late stationary growth phase (72h) were performed (Figure 17, 18).

In the following, the regulated genes were classified according to the respective metabolic pathways and displayed in heat maps. Transcriptional changes were observed in several metabolic pathways; however, the most striking changes were observed in the compared transcriptome analyses in M9 medium without thiamine to LB medium in all strains.
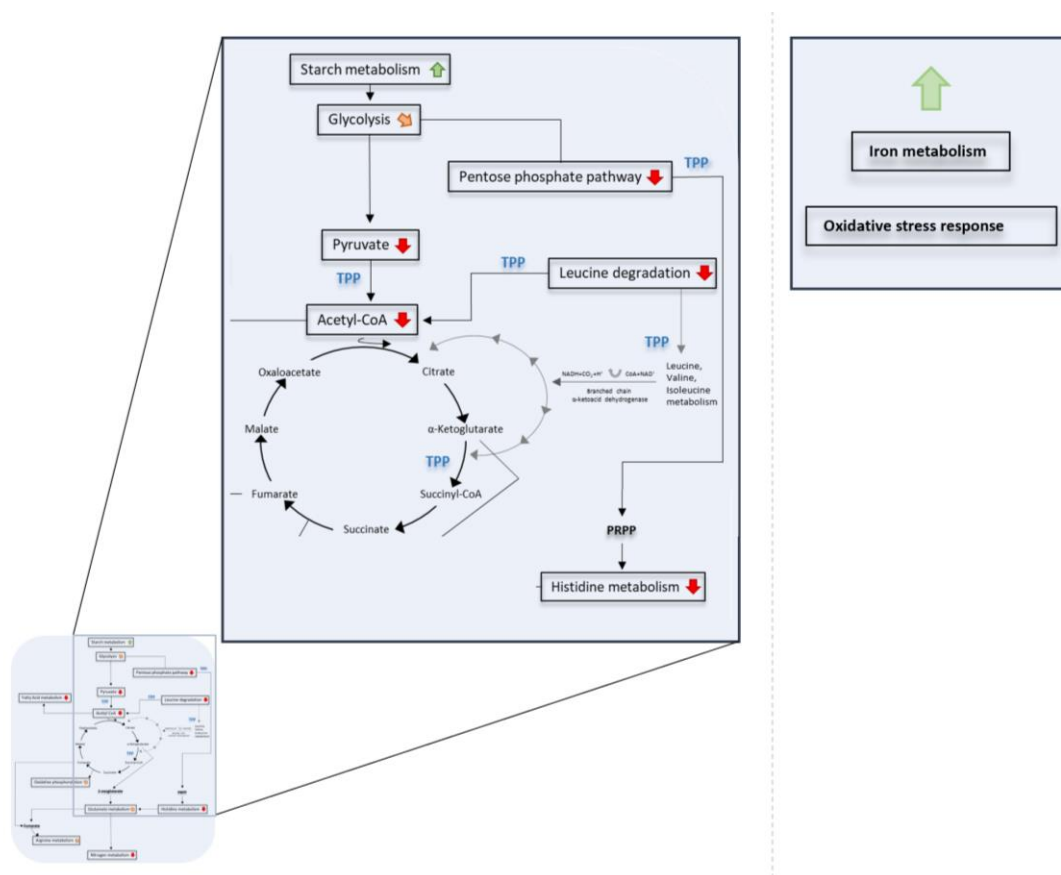
Figure 54: Final summary of the TPP-dependent metabolic processes related to up- and down-regulated genes in the wildtype BpPG1 and the deletion mutant BpPG1Δ*thiM* in comparison of M9 medium without thiamine to LB medium and display of TPP-independent metabolic processes with observed transcriptional changes. The limitation of TPP caused a down-regulation of several metabolic processes. In addition, the changing medium conditions resulted to an up-regulation of the iron metabolism and oxidative stress response caused by an induced disbalance of nutrients in the organism.

In the metabolic network analysis different effects were recognized which revealed an efficient connected system to regulate metabolic processes and responses to environmental changes in *B. plantarii* PG1 (Figure 54). The absence of the hydroxyethylthiazole kinase ThiM and the limitation of thiamine by using M9 medium without thiamine revealed a down-regulation of the metabolic pathways of the glycolysis, the citrate cycle, oxidative phosphorylation, leucine degradation, arginine biosynthesis, histidine metabolism, thiamine metabolism, nitrogen

metabolism and fatty acid metabolism. In addition, the changing medium conditions resulted to an up-regulation of the iron metabolism and oxidative stress response.

In the beginning, the glycolysis is required for the conversion of glucose to cellular energy by providing ATP and NADH. Glucose precursors for glycolysis are provided from the starch metabolism (Cohen, 2010). However, in the glycolysis metabolism, important precursors are formed, essential for other metabolic pathways (Radlinski *et al.*, 2018). In the metabolic network analysis, an up-regulation of the glycogen/starch synthase was observed in the compared strains in M9 medium without thiamine to LB medium in the late exponential growth phase (48h) (displayed in the heat map of the oxidative phosphorylation, Figure 22). In the comparative analysis of M9 medium without thiamine to LB medium, a down-regulation of several processes of the glycolysis were observed caused by the thiamine limitations and requirements of TPP as co-factor in essential reaction steps. The TPP-dependent transition from pyruvate to hydroxyethyl-THPP by the pyruvate dehydrogenase were significant down-regulated in the late exponential growth phase (48h). A greater down-regulation were observed in the late stationary growth phase (72h), which can be explained by the depletion of existing precursors and substrates over time. In the exponential growth phase of bacteria activated genes are associated to the translation, energy metabolism and the synthesis of amino acids. In the stationary growth phase, the regulation changes to processes of defense and environmental stress response mechanisms (Veselovsky *et al*., 2022). Additionally regarding to processes of glycolysis, in the pentose phosphate pathway, NADPH and ribose-5-phosphate are released, which is essential for energy conversion and the downstream production of amino acids, nucleic acids and fatty acids. Especially the phosphoribosyl pyrophosphate (PRPP), formed from ribose-5-phosphate, plays an important role as active compound in histidine metabolism, which is essential for the formation of amino acids. Acetyl-CoA is formed from pyruvate and represents the transition into the citrate cycle (Krivoruchko *et al*., 2015). Further, acetyl-CoA represents the building block for fatty acid synthesis and is synthesised by fatty acid degradation (Fujita *et al.,* 2007).

In the metabolic network analysis, due to the lack of TPP as active thiamine form, the production of acetyl-CoA was down-regulated which led to a subsequent down-regulation of the fatty acid metabolism (Figure 20, 24). In the next step the glycolysis proceeds via the pentose phosphate pathway to the pyruvate pathway to the citrate cycle. In the citrate cycle, acetyl-CoA is converted into carbon dioxide and water, releasing energy indirectly as ATP and directly as intermediates and precursors for other metabolic pathways (Radlinski *et al.*, 2018, Martin, 2020).

In the metabolic network analysis, a more specific regulation of TPP-dependent reactions was observed. The transit reaction of 2-oxo-glutarate to dihydrolipoamide-E were down-regulated due to the lacking TPP in the comparison of M9 medium without thiamine to LB medium in both growth phases. Additionally, the transit reaction of succinyl-CoA to succinate was down-regulated in the late exponential growth phase (48h) but not significant regulated in the late stationary growth phase (72h) (Figure 21). The reaction step of 2-oxo-glutarate to dihydrolipoamide-E represents a crucial control point of the citrate cycle for its regulation and leads to the suggestion that the citrate cycle between acetyl-CoA and 2-oxo-glutarate (more often referred to as α-ketoglutarate) is delayed due to the lacking NADH from valine, leucine and isoleucine metabolism (Richardson *et al*., 2015, Gorissen and Phillips, 2019). Here, through the down-regulation of the leucine degradation, in the metabolic network analysis, the synthesis of acetyl-CoA was limited. The leucine, valine and isoleucine metabolism provided the release of NADH, CO_2 and H^+ ions, which was missing in the next metabolic processes which was additionally influenced by the amount of succinate. Succinate represents the passage from the citrate cycle into the respiratory cycle. The respiration is the process of oxidative phosphorylation in which a series of oxidation and reduction reactions catalyse an electron transfer reaction for the conversion of ADP and phosphate to ATP for energy production (Jurtshuk, 1996).

The metabolic network analysis revealed in the comparison of M9 medium without thiamine to LB medium a down-regulation of complex I in the oxidative phosphorylation caused through the decreased synthesis of NADH of the previous metabolic pathways. Complex II were similar down-regulated, catalysing the conversion of succinate to fumarate. The complex III and IV were not significant regulated, whereas in the cytochrome bd complex up- and down-regulated expression patterns were detected (Figure 22). In literature it is described, Complex I is responsible for the conversion of NADH to NAD^+ and H^+ (Friedrich and Scheide, 2000). Complex II includes the conversion of succinate to fumarate. Fumarate at the same time leads to the next connected metabolic pathway of the arginine biosynthesis (Hägerhäll, 1997, Rutter *et al*., 2010). The cytochrome bd complex is activated to counteract oxidative stress in bacteria. In literature it is described that the tolerance to oxidative stress and nitrosative stress conditions is increased by the bd complex (Giuffrè *et al*., 2014). This could explain the different expression patterns of the cytochrome bd complex in the metabolic network analysis regarding to the up-regulation of the oxidative stress response.

In addition, in the metabolic network analysis, the histidine metabolism showed differences in the expression patterns of the conversion of L-histidine to L-glutamate in the late exponential

growth phase (48h). The compared transcriptome analyses of the wildtype BpPG1 in M9 medium without thiamine to LB medium as well as the comparison of the deletion mutant BpPG1Δ*thiM* in LB medium to the wildtype BpPG1 in LB medium revealed a down-regulation of the conversion of L-histidine to L-glutamate. In contrast, in the comparison the deletion mutant BpPG1Δ*thiM* in M9 medium without thiamine to LB medium an up-regulation were detected (Figure 27).

In literature it is described that the synthesis of aminoimidazole carboxyamide ribotide belongs to the histidine metabolism in *Salmonella enterica* and that the lack of it leads to a decrease in the synthesis of HMP moiety of thiamine (Bazurto and Downs, 2014). These insights lead to the possible explanation that the lack of thiamine caused the reduction of the transcription of 4-imidazole-5-propanoate and led to the down-regulation of the conversion of L-histidine to L-glutamate, observed in the metabolic network analysis. Additionally, the lack of TPP in the pentose phosphate pathway led to an insufficient synthesis of phosphoribosyl pyrophosphate (PRPP), which in turn resulted in an increased regulation of histidine metabolism. In the metabolic network analysis, it was observed that the histidine metabolism as well as the subsequent metabolic pathways of glutamate, arginine and nitrogen were down-regulated (Figure 25, 26). Histidine is an important component of amino acid metabolism and essential for the formation of glutamates (Bender, 2012).

At least the thiamine metabolic pathway and the expression pattern of the CRISPR/CAS system were analysed in the metabolic network analysis. In the comparison of the wildtype BpPG1 in M9 medium without thiamine to LB medium in the late exponential growth phase (48h), the thiamine biosynthesis protein ThiC was significant up-regulated, whereas the following process of the phosphorylation of thiamine phosphate to thiamine diphosphate was down-regulated. Additionally, the kinase ThiM was significant down-regulated in the salvage pathway. Further significant expression patterns were not observed in the thiamine metabolism. These observations were expected regarding to the previous results (Figure 28).

In the comparison of the wildtype BpPG1 in M9 medium without thiamine to LB medium in the late exponential growth phase (48h), in the CRISPR/CAS system the same effects were observed as mentioned in the previous chapter. The comparison of the deletion mutant BpPG1Δ*thiM* to the wildtype BpPG1 in LB medium revealed an up-regulation of the csy complex whereas in the comparison of the deletion mutant BpPG1Δ*thiM* and the wildtype BpPG1 in M9 medium without thiamine to LB medium a reducing effect was observed (Figure 29).

Moreover, some other effects were occurring in the metabolic network analysis which led to the assumption of another influence on the metabolism of *B. plantarii* PG1 through the changing media conditions. The metabolic network analysis determined that the associated oxidative stress response genes were highly up-regulated in the comparison of M9 medium without thiamine to LB medium in the late exponential growth phase (48h) (Figure 30). The oxidative stress response is separated in the reaction to peroxide or superoxide (Seixas *et al.*, 2022). In this case the present stress was mediated by superoxide anion due to the activation of the superoxide dismutase SodA, displayed in the heat map. In contrast, the oxidative stress response is closely connected to the iron metabolism. An imbalance of the iron concentration in the cell leads to the activation of the oxidative stress response to avoid toxic levels (Tardat and Touati, 1991). Here an up-regulation of the iron metabolism was observed especially in the comparison M9 medium without thiamine to LB medium in the late exponential growth phase (48h) (Figure 31).

The metabolism of iron and oxidative stress response is closely related to each other. Iron is an essential micronutrient for bacterial processes, but free iron can lead to DNA, protein and lipid damage and up to cell death (Frawley and Fang, 2014). Free iron can activate the Fenton reaction and Haber-Weiss reactions which leads to oxygen free radicals referred to as reactive oxygen species (ROS) (Wardman *et al.*, 1996, Kehrer, 2000).

$$Fe^{3+} + O_2^{\cdot -} \longleftrightarrow Fe^{2+} + O_2$$

$$Fe^{2+} + H_2O_2 \longrightarrow Fe^{3+} + HO^{\cdot} + OH^-$$
$$\text{(Fenton reaction)}$$

$$O_2^{\cdot -} + H_2O_2 \longleftrightarrow O_2 + HO^{\cdot} + OH^-$$
$$\text{(Haber-Weiss reaction)}$$
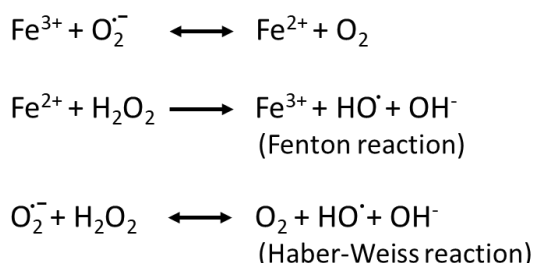
Figure 55: Reaction scheme of Fenton and Haber-Weiss reaction.

To detoxify reactive oxygen species, bacteria have protective enzymes such as superoxide dismutases (SODs), catalyses and peroxidases. *B. plantarii* PG1 possesses a superoxide dismutase sodA with iron as co-factor (FeSOD) that perform the following reaction for detoxifying ROS:

$$O_2^- + O_2^- + 2H^+ \longrightarrow H_2O_2 + O_2$$
$$\text{(SOD reaction)}$$
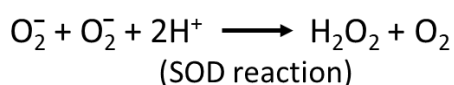
Figure 56: Scheme of reaction of superoxide dismutase (SOD).

FeSOD is expressed under high levels of iron and explain the iron induced oxidative stress which can be observed here (Nóbrega and Pauleta, 2019). In the metabolic network analysis, the up-regulation of the iron metabolism was mainly present in the comparison of the transcriptomic data of M9 medium without thiamine to LB medium in the late exponential growth phase (48h). But no additional iron was supplemented to the M9 medium. One ready-to-use component of the used M9 medium was the casamino acid by ThermoFisher. In the manufactures documents it was declared that the casamino acid includes small amounts of iron and nitrogen (Bacto™ Casaminosäuren (#223050). This may explain the up-regulation of the iron metabolism and the subsequent activation of the oxidative stress response.

For further knowledge, a detailed analysis of the reaction steps could provide profound insights of the observed effects. In addition, further environmental factors in particular iron, nitrogen and pH values should be investigated. With regard to the thiamine metabolism, a thiamine auxotrophic mutant could contribute to a better understanding of the metabolic processes, additionally with regard to a possible co-regulation with the CRISPR/CAS system.

In conclusion, the regulatory network for monitoring metabolic processes in bacteria is very complex and continues to be perfected over generations, since these organisms must constantly adapt to new environmental conditions in order to survive. The detailed elucidation of the metabolic processes and dependencies is a major challenge, as it is to adapt to changing environmental conditions for an organism.

4.3 Regulation mechanism of the CRISPR/CAS I-F system

In literature, the regulation of the CRISPR/CAS system is described as diverse and organism specific. To investigate the regulation of the CRISPR/CAS I-F system in *B. plantarii* PG1 different transcriptome analysis were performed. Here the first analysis revealed different transcription levels of the individual genes of the CRISPR/CAS system which led to the suggestion that the CRISPR/CAS system is not regulated as an operon in this strain. In further analysis three putative promoter sites were identified located upstream of *cas1*, *csy1* and *csy4* (Figure 33). The activity was experimentally evaluated by constructed reporter strains with the red fluorescent protein mcherry, determining the fluorescence level in LB and M9 medium (with thiamine) in the late exponential growth phase (48h). In LB medium no significant differences were detected whereas the reporter strain with the putative promoter site of *cas1* showed a slight increase and the promoter site of *csy4* a high increase of the fluorescence level in M9 medium (Figure 35). In literature it is described that the endonuclease *csy4* shows

independent activities (Wiedenheft *et al.,* 2011, Guido Papa *et al*., 2020). So, the higher fluorescence level may be explained by a stress reaction of the organism to the M9 medium due to changing nutrient conditions. The endonuclease *csy4* is responsible for the precr-RNA processing and part of the first step in the CRISPR/CAS immunity (Przybilski *et al*., 2011). Endonucleases as well as restriction enzymes are essential for the protection against foreign DNA such as bacteriophages and activated in environmental stress situations (Vasu *et al.,* 2013, Isaev *et al*., 2021). Further investigations could lead to additional insights regarding to the application of the endonuclease, for the use in biotechnology or to examine a role of CRISPR/CAS beyond immunity (Ding *et al.,* 2020).

To determine the regulation of the CRISPR/CAS system in *B. plantarii* PG1 the transcriptomic analysis was investigated regarding to possible regulators of the CRISPR/CAS system. In literature several regulators were identified but show different regulatory potentials in different organisms, so in order to find a regulator especially for the regulation of the CRISPR/CAS I-F system in *B. plantarii* PG1, several possible regulators were selected and investigated. Finally, two possible regulators of the CRISPR/CAS system were identified, the cAMP receptor proteins CRP1 and CRP3 which are dependent on the glucose metabolism and known as possible regulators of the CRISPR/CAS I-F system in other organisms. At a low glucose concentration in the cell, ATP is converted into cAMP by the adenylate cyclase and synthesised into CRP-cAMP. At a high glucose concentration this process is inhibited, which led to the assumption that different glucose concentration could have an influence on the CRISPR/CAS system. In the following, the possible regulators were investigated in a two-plasmid approach in the wildtype BpPG1 by transferring a plasmid with the possible regulator in the previous created promoter reporter strain of *cas1*. Here, a repressive effect of the possible regulators of CRP1 and CRP3 on the CRISPR/CAS promoter site of *cas1* were detected (Figure 43). Additionally, transcriptome analyses of the possible regulators in the wildtype BpPG1 confirmed the observed results (Figure 49). For the final evaluation of the role of the possible regulators of the CRISPR/CAS system further experiments are required. The creation of deletion mutants of CRP1 and CRP3 could lead to further perceptions to determine the role of the possible regulators of the CRISPR/CAS system in *B. plantarii* PG1. In literature several studies examine the elucidation of the regulation of the CRISPR/CAS system. A review specifically on the CRISPR/CAS I-F system by Adrian Patterson in 2017 has shown that transcription regulators as well as signalling molecules from metabolic pathways directly or indirectly regulate the CRISPR/CAS I-F system. For example, in *Pectobacterium atrosepticum* the cAMP receptor protein CRP which is part of the glucose metabolism acts as an activator

whereas it is an inhibitor of the system in *E. coli* (Patterson *et al.*, 2015, Yang C-D *et al.*, 2014). In *Salmonella enterica* serovar Typhi the regulation of the CRISPR/CAS system is dependent of the LysR-type transcriptional regulator LeuO which is controlled by the histone-like nucleoid-structuring DNA-binding protein H-NS and leucine-responsive regulatory protein LRP. In *E. coli* the H-NS and LRP however has no influence on the regulation of the CRISPR/CAS system (L. Medina-Aparicio *et al.*, 2011, Ü. Pul *et al.*, 2010). Another interesting protein is the heat shock protein G (HtpG) which is activated as a cellular stress response of phage infection and promotes the stability of Cas3 in *E. coli* CRISPR/CAS I-E system (Yosef *et al.*, 2011). This leads to the assumption that the regulation of the CRISPR/CAS systems has evolved independently in different strains and thereby making the identification of possible regulators a challenging task. Additionally, it has been shown that the cell-cell communication through QS plays an important role in the regulation of CRISPR/CAS systems. For example, in *Pseudomonas aeruginosa* it could be observed that the QS system activates the adaptation process of the CRISPR/CAS system. Interestingly, however, for CRISPR/CAS inhibition to occur, more than one component of the QS system must be dysfunctional (Høyland-Kroghsbo *et al.*, 2017).

Furthermore, in literature it is described that the CRISPR/CAS system is regulated in an QS-dependent manner (Gao *et al.*, 2015). For further analyses, the created promoter fusion constructs were introduced into the QS deletion mutant BpPG2, BpPG3 and BpPG4. The QS-promoter-reporter strains were cultivated in LB and M9 medium (with thiamine) to the late exponential growth phase (48h) and the fluorescence levels were subsequently determined. Here, the wildtype BpPG1 reporter strains revealed slight increased differences in the fluorescence values, especially with the promoter of *csy4* in comparison of LB to M9 medium. In the QS deletion mutants BpPG3 and BpPG4, a reduction of the fluorescence level was observed in all strains, except the promoter fusion of the promoter of *csy4* in LB medium (Figure 49). Summarised, the nutrient change from LB to M9 medium showed an effect on the QS system and the CRISPR/CAS system. In literature it is commonly known that the QS system is dependent of the environmental changes and used for the inner cell and outer cell to cell communication to sense environmental changes, so this observation was not surprising (Ng WL and Bassler, 2009, Moreno-Gámez *et al.*, 2017). To investigate environmental stress condition different salt and glucose concentration were analysed. Here, an increased fluorescence level in the wildtype BpPG1 was observed in all promoter strains applying 0.8M NaCl. Changing glucose concentration to a 0.4% vol glucose caused a decreased fluorescence level in the reporter strain of *cas1* and a slight increased fluorescence level in the reporter strain of *csy4*.

However, no significant differences were measured in the QS deletion mutant BpPG2 independent of the promoter site and the salt and glucose concentration (Figure 51). The QS deletion mutant strains BpPG3 and BpPG4 revealed an increased fluorescence level under salt stress conditions in all promoter strains, but no significant differences were detected under glucose stress conditions (Figure 52).

Salt and glucose compounds represent two essential elements of bacterial life cycle. Salt maintains the cells osmolarity and can be used to sense environmental changes whereas glucose is an important carbon sources for metabolic processes (Sleator and Hill, 2002, Ernesto and McKinney, 2006). In future studies, further salt and glucose concentrations as well as other environmental stress conditions such as temperature or pH could be investigated here to determine the influence of environmental changes on the CRISPR/CAS system. Additionally, to liquid cultures, the behaviour of the biofilm formation of *B. plantarii* PG1 and the generated strains were investigated. *B. plantarii* PG1 was confirmed to produce biofilm in preliminary experiments under dynamic conditions in flow cell chambers as well as static conditions. Here the static biofilm formation was investigated under salt stress conditions in LB medium. In the wildtype BpPG1 promoter-reporter strains the formation of a stable biofilm with a high number of living cells were observed in all strains in LB medium at the late exponential growth phase (48h). In the comparative analysis of changing mcherry fluorescence values under salt stress conditions, an increased fluorescence level was detected in all strains which leads to the assumption that changing salt conditions activate the CRISPR/CAS system (Figure 53). To evaluate these results further experiments are required. For further advances, the biofilm formation should be verified in M9 medium with and without supplemented thiamine. Here, other salt concentrations as well as other salts could be evaluated in order to examine their influence. In addition, further transcriptome analysis of the static biofilms could provide further insights. Biofilm formation is dependent of environmental abiotic stress factors like temperature, nutrients deficiency, pH, salinity, oxidation and desiccation (Goller and Romeo, 2008, Li *et al.*, 2021). Especially, salt causes different effects in environment, so in *Clostridium ljungdahlii* for example sodium chloride leads to a 20 times higher biofilm biomass (Jo Philips *et al.,* 2017) whereas in *E. coli* elevated concentrations decrease growth and biofilm formation (Li *et al*., 2021). In a study of *Burkholderia pseudomallei* it is described that the biofilm growth supplemented with salt or not had no effect on biofilm formation (Pumirat *et al.,* 2017). Both salt and glucose are two major stress and limiting factors for microbial communities in the environment. In particular, soil salination of agricultural land is a serious threat to ecosystems worldwide. Already 15-50% of utilised land is affected by salination.

Resulting in a reduced productivity and resistance of plants (Yuan Qin *et al*., 2016). *B. plantarii* PG1 is known as a rice pathogen which causes great damage in agriculture. Rice is one of the most important crops in the world and feeds the majority of people on our planet (Fukagawa NK *et al*., 2019) Therefore, a joint consideration of abiotic factors as well as pathogenic microbial factors is necessary to find a solution against plant pathogens for providing food and to advance research in this field.

References

Alessandro Giuffrè, Vitaliy B. Borisov, Marzia Arese, Paolo Sarti, Elena Forte. "Cytochrome bd oxidase and bacterial tolerance to oxidative and nitrosative stress." Biochimica et Biophysica Acta (BBA) - Bioenergetics, Vol1837, Issue 7, (2014), https://doi.org/10.1016/j.bbabio.2014.01.016.

Alexander Wittmann, Beatrix Suess. "Engineered riboswitches: Expanding researchers' toolbox with synthetic RNA regulators." FEBS Letters 586, (2012), https://doi.org/10.1016/j.febslet.2012.02.038

Alkhnbashi OS, Shah SA, Garrett RA, Saunders SJ, Costa F, Backofen R. "Characterizing leader sequences of CRISPR loci." Bioinformatics. 2016 Sep 1;32(17):i576-i585. (2016) https://doi.org/10.1093/bioinformatics/btw454. PMID: 27587677.

Anastasia Krivoruchko, Yiming Zhang, Verena Siewers, Yun Chen, Jens Nielsen. "Microbial acetyl-CoA metabolism and metabolic engineering." Metabolic Engineering, Vol28, Pages 28-42, ISSN 1096-7176 (2015), https://doi.org/10.1016/j.ymben.2014.11.009.

Andreas Knapp, Sonja Voget, Rong Gao, Nestor Zaburannyi, Dagmar Krysciak, Michael Breuer, Bernhard Hauer, Wolfgang R. Streit, Rolf Müller, Rolf Daniel, Karl-Erich Jaeger. „Mutations improving production and secretion of extracellular lipase by *Burkholderia glumae* PG1." Appl Microbiol Biotechnol. 2016; 100: 1265–1273. Published online (2015) Oct 17. https://doi.org/10.1007/s00253-015-7041-z, PMCID: PMC4717159

Barrick JE, Breaker RR. "The distributions, mechanisms, and structures of metabolite-binding riboswitches." Genome Biol 8: R239, (2007)

Bassler, B. L. & R. Losick. "Bacterially speaking." Cell 125(2): 237-246, (2006)

Begley TP, Downs DM, Ealick SE, McLafferty FW, Van Loon AP, Taylor S, Campobasso N, Chiu HJ, Kinsland C, Reddick JJ, Xi J. "Thiamin biosynthesis in prokaryotes." Arch Microbiol. 1999 Apr;171(5):293-300. (1999) https://doi.org/10.1007/s002030050713. PMID: 10382260.

Bender RA. "Regulation of the histidine utilization (hut) system in bacteria." Microbiol Mol Biol Rev. (2012);76(3):565-584. https://doi.org/10.1128/MMBR.00014-12

Blake Wiedenheft, Esther van Duijn, Jelle B. Bultema, Sakharam P. Waghmare, Kaihong Zhou, Arjan Barendregt, Wiebke Westphal, Albert J. R. Heck, Egbert J. Boekema, Mark J. Dickman, and Jennifer A. Doudna. "RNA-guided complex from a bacterial immune system enhances target recognition through seed sequence interactions.", PNAS Vol. 108, (2011) https://doi.org/10.1073/pnas.1102716108

Boekema, B.K.H.L., Beselin, A., Breuer, M., Hauer, B., Koster, M., Rosenau, F., Jaeger,K.-E., Tommassen, J., „Hexadecane and Tween 80 stimulate lipase production in *Burkholderia glumae* by different mechanisms." Appl. Environ. Microbiol.73, 3838–3844, (2007) https://doi.org/10.1128/AEM.00097-07.

Breaker RR. "Riboswitches and the RNA World." Cold Spring Harb Perspect Biol 4: a003566, (2012)

C. C. Goller and T. Romeo. "Environmental Influences on Buiofilm Development." Current Topics in Microbiology and Immunology 322, (2008)

C. S. Heil, S. S. Wehrheim, K. S. Paithankar, M. Grininger. „Fatty Acid Biosynthesis: Chain-Length Regulation and Control." ChemBioChem, 20, 2298. (2019) https://doi.org/10.1002/cbic.201800809

C. S. Kim *et al*. "Characterization of Autoinducer-3 Structure and Biosynthesis in *E.coli*." ACS Cent. Sci. 6, 197–206, (2020)

C.E. Kraft, E.R. Angert. „Competition for vitamin B1 (thiamin) structures numerous ecological interactions." Q. Rev. Biol., 92 (2017)

Cady KC, White AS, Hammond JH, Abendroth MD, Karthikeyan RS, Lalitha P, Zegans ME, O'Toole GA. "Prevalence, conservation and functional analysis of Yersinia and Escherichia CRISPR regions in clinical *Pseudomonas aeruginosa* isolates." Microbiology (Reading). Feb;157(2):430-437. (2011) https://doi.org/10.1099/mic.0.045732-0. PMID: 28206903.

Carter MQ, Chen J, Lory S. "The *Pseudomonas aeruginosa* pathogenicity island PAPI-1 is transferred via a novel type IV pilus." J Bacteriol. 2010;192(13):3249-3258. (2010) https://doi.org/10.1128/JB.00041-10

Cecilia Hägerhäll, "Succinate: quinone oxidoreductases: Variations on a conserved theme." Biochimica et Biophysica Acta (BBA) - Bioenergetics, Vol1320, (1997), https://doi.org/10.1016/S0005-2728(97)00019-4.

Chien & Chang. „The susceptibility of rice plants at different groth stages and of 21 commercial rice varieties of *Pseudomonas glumae*." J. Agric. Res China 36, 302-310, (1987)

Christopher T. Jurgenson,1 Tadhg P. Begley and Steven E. Ealick. "The Structural and Biochemical Foundations of Thiamin Biosynthesis." Annu. Rev. Biochem. 78:569–603, 10.1146/annurev.biochem.78.072407.102340, (2009)

Cláudia S. Nóbrega and Sofia R. Pauleta. "Reduction of hydrogen peroxide in gram-negative bacteria – bacterial peroxidases." Advances in Microbial Physiology, Vol74, ISSN 0065-2911, (2019) https://doi.org/10.1016/bs.ampbs.2019.02.006

Cohen, G.N. "Glycolysis, Gluconeogenesis and Glycogen Synthesis." Microbial Biochemistry. Springer, Dordrecht. (2010) https://doi.org/10.1007/978-90-481-9437-7_6

Cottyn, B., Regalado, E., Lanoot, B., De Cleene, M., Mew, T.W. and Swings, J. „Bacterial diseases of rice. Characterization of pathogenic bacteria associated with sheath rot complex and grain discoloration of rice in the Philippines" Plant Dis.61, (1996)

References
_____

David R. Sannino Clifford E. Kraft Katie A. Edwards Esther R. Angert." Thiaminase I Provides a Growth Advantage by Salvaging Precursors from Environmental Thiamine and Its Analogs in *Burkholderia thailandensis*." ASM Journal, Vol84, (2018) https://doi.org/10.1128/AEM.01268-18

de Freitas Almeida, G.M., Hoikkala, V., Ravantti, J. et al. "Mucin induces CRISPR-Cas defense in an opportunistic pathogen." Nat Commun 13, 3653 (2022). https://doi.org/10.1038/s41467-022-31330-3

Devashish Rath, Lina Amlinger, Archana Rath, Magnus Lundgren. "The CRISPR-Cas immune system: Biology, mechanisms and applications." Biochimie, Volume 117, Pages 119-128, ISSN 0300-9084, (2015) https://doi.org/10.1016/j.biochi.2015.03.025.

Ding Wentao, Zhang Yang, Shi Shuobo, "Development and Application of CRISPR/Cas in Microbial Biotechnology." Frontiers in Bioengineering and Biotechnology. Vol. 8, (2020) https://doi.org/10.3389/fbioe.2020.00711

Ernesto J. Muñoz-Elías and John D. McKinney. "Carbon metabolism of intracellular bacteria." Cellular Microbiology (2006) https://doi.org/10.1111/j.1462-5822.2005.00648.x

Ethan Settembre, Tadhg P Begley, Steven E Ealick, "Structural biology of enzymes of the thiamin biosynthesis pathway." Current Opinion in Structural Biology, Volume 13, Issue 6, (2003) https://doi.org/10.1016/j.sbi.2003.10.006.

Farr SB, Kogoma T. "Oxidative stress responses in Escherichia coli and Salmonella typhimurium." Microbiol Rev. 1991 Dec;55(4):561-85. (1991) https://doi.org/10.1128/mr.55.4.561-585.1991. PMID: 1779927; PMCID: PMC372838.

Frawley ER, Fang FC. "The ins and outs of bacterial iron metabolism." Mol Microbiol. 2014;93(4):609-616. (2014) https://doi.org/10.1111/mmi.12709

Fukagawa NK, Ziska LH. "Rice: Importance for Global Nutrition." J Nutr Sci Vitaminol (Tokyo). 2019;65(Supplement):S2-S3, (2019) https://doi.org/10.3177/jnsv.65.S2. PMID: 31619630.

Fuqua C., Winans S.C., Greenberg E.P. "Quorum Sensing in Bacteria: The LuxR-LuxI Family of Cell Density-Responsive Transcriptional Regulators." J Bacteriol 176(2): 269-275, (1994)

Gao R, Krysciak D, Petersen K, Utpatel C, Knapp A, Schmeisser C, Daniel R, Voget S, Jaeger KE, Streit WR. "Genome-wide RNA sequencing analysis of quorum sensing-controlled regulons in the plant-associated *Burkholderia glumae* PG1 strain." Appl Environ Microbiol. 2015 Dec;81(23):7993-8007. (2015) https://doi.org/10.1128/AEM.01043-15. Epub 2015 Sep 11. PMID: 26362987; PMCID: PMC4651095.

Garst AD, Edwards AL, Batey RT. "Riboswitches: structures and mechanisms." Cold Spring Harb Perspect Biol 3: a003533, (2011)

Gigliobianco, T., Lakaye, B., Wins, P., Benaïssa El Moualij, Willy Zorzi & Lucien Bettendorff. "Adenosine thiamine triphosphate accumulates in *Escherichia coli* cells in response to specific conditions of metabolic stress." BMC Microbiol 10, 148 (2010). https://doi.org/10.1186/1471-2180-10-148

Guido Papa, Luca Venditti, Luca Braga, Edoardo Schneider, Mauro Giacca, Gianluca Petris, Oscar R. Burrone. "CRISPR-Csy4-Mediated Editing of Rotavirus Double-Stranded RNA Genome", Cell Reports, Volume 32, (2020) https://doi.org/10.1016/j.celrep.2020.108205.

Haft, D. H., Selengut, J., Mongodin, E. F. & Nelson, K. E. A guild of 45 "CRISPR-associated (Cas) protein families and multiple CRISPR/Cas subtypes exist in prokaryotic genomes." PLoS Comput. Biol. 1, e60–e60 (2005).

He X., Chang W., Pierce D.L., Seib L.O., Wagner J., Fuqua C. "Quorum Sensing in Rhizobium sp. Strain NGR234 Regulates Conjugal Transfer (tra) Gene Expression and Influences Growth Rate." J Bacteriol 185(3): 809-822, (2003)

Hidalgo-Cantabrana, C., Goh, Y. J. & Barrangou, R. "Characterization and repurposing of type I and type II CRISPR-Cas systems in bacteria." J. Mol. Biol. 431, 21–33 (2019).

Horvath P, Barrangou R. "CRISPR/Cas, the immune system of bacteria and archaea." Science. 2010 Jan 8;327(5962):167-70. (2010) https://doi.org/10.1126/science.1179555. PMID: 20056882.

Høyland-Kroghsbo NM, Paczkowski J, Mukherjee S, Broniewski J, Westra E, Bondy-Denomy J, Bassler BL. "Quorum sensing controls the *Pseudomonas aeruginosa* CRISPR-Cas adaptive immune system." Proc Natl Acad Sci U S A. 2017 Jan 3;114(1):131-135. Epub 2016 Nov 14 https://doi.org/10.1073/pnas.1617415113. PMID: 27849583; PMCID: PMC5224376.

I. Yosef, M.G. Goren, R. Kiro, R. Edgar, U. Qimron. "High-temperature protein G is essential for activity of the *Escherichia coli* clustered regularly interspaced short palindromic repeats (CRISPR)/Cas system." Proc Natl Acad Sci U S A, 108 (2011)

Isaev, A.B., Musharova, O.S. & Severinov, K.V. "Microbial Arsenal of Antiviral Defenses – Part I." Biochemistry Moscow 86, 319–337 (2021). https://doi.org/10.1134/S0006297921030081

Ishino Y, Shinagawa H, Makino K, Amemura M, Nakata A. "Nucleotide sequence of the iap gene, responsible for alkaline phosphatase isozyme conversion in *Escherichia coli*, and identification of the gene product." J Bacteriol. (1987) Dec;169(12):5429-33. https://doi.org/10.1128/jb.169.12.5429-5433.1987. PMID: 3316184; PMCID: PMC213968.

J.C. Nshogozabahizi, K.L. Aubrey, J.A. Ross, N. Thakor, "Applications and limitations of regulatory RNA elements in synthetic biology and biotechnology." Journal of Applied Microbiology, (2019) https://doi.org/10.1111/jam.14270

James P Kehrer, "The Haber–Weiss reaction and mechanisms of toxicity." Toxicology, Vol149, (2000) https://doi.org/10.1016/S0300-483X(00)00231-6.

Jannell V. Bazurto, Diana M. Downs. "Amino-4-Imidazolecarboxamide Ribotide Directly Inhibits Coenzyme A Biosynthesis in *Salmonella enterica*." ASM Journal, Vol196, (2014) https://doi.org/10.1128/JB.01087-13

Jansen R, Embden JD, Gaastra W, Schouls LM. "Identification of genes that are associated with DNA repeats in prokaryotes." Mol Microbiol. (2002) Mar;43(6):1565-75. https://doi.org/10.1046/j.1365-2958.2002.02839.x. PMID: 11952905.

Jeong, J Kim, S Kim, Kang, Nagamatsu, Hwang, „Toxoflavin produced by *Burkholderia glumae* causing rice grain rot is responsible for inducing bacterial wilt in many field crops." Plant Dis. 87, 890-895, (2003)

Jinek M, Chylinski K, Fonfara I, Hauer M, Doudna JA, Charpentier E. "A programmable dual-RNA-guided DNA endonuclease in adaptive bacterial immunity." Science. 2012 Aug 17;337(6096):816-21. (2012) https://doi.org/10.1126/science.1225829. Epub 2012 Jun 28. PMID: 22745249; PMCID: PMC6286148.

Jo Philips, Korneel Rabaey, Derek R. Lovley, Madeline Vargas. "Biofilm Formation by *Clostridium ljungdahlii* Is Induced by Sodium Chloride Stress: Experimental Evaluation and Transcriptome Analysis." PLOS, (2017) https://doi.org/10.1371/journal.pone.0170406

Jurgenson CT, Begley TP, Ealick SE. "The structural and biochemical foundations of thiamin biosynthesis." Annu Rev Biochem 78: 569–603, (2009)

Jurtshuk P Jr.. "Bacterial Metabolism." In: Baron S, editor. Medical Microbiology. 4th edition. Galveston (TX): University of Texas Medical Branch at Galveston; (1996). Chapter 4.

Karunakaran R, Ebert K, Harvey S, Leonard ME, Ramachandran V, Poole PS. "Thiamine is synthesized by a salvage pathway in *Rhizobium leguminosarum* bv. viciae strain 3841." J Bacteriol. 2006 Sep;188(18):6661-8. (2006) https://doi.org/10.1128/JB.00641-06. PMID: 16952958; PMCID: PMC1595474.

Kim AD, Baker AS, Dunaway-Mariano D, Metcalf WW, Wanner BL, Martin BM. "The 2-aminoethylphosphonate-specific transaminase of the 2-aminoethylphosphonate degradation pathway." J Bacteriol. 2002 Aug;184(15):4134-40. (2002) https://doi.org/10.1128/JB.184.15.4134-4140.2002. PMID: 12107130; PMCID: PMC135204.

Koenigsknecht MJ, Downs DM. "Thiamine biosynthesis can be used to dissect metabolic integration." Trends Microbiol. 2010;18(6):240-247. (2010) https://doi.org/10.1016/j.tim.2010.03.003

Koji Azegami, Koushi Nishiyama, Yasumasa Watanabe, Ikuo Kadota, Akira Ohuchi, Chikafusa Fukazawa. "*Pseudomonas plantarii* sp. nov., the Causal Agent of Rice Seedling

Blight." International Journal of systematic and evolutionary microbiology. Vol 37, (1987) https://doi.org/10.1099/00207713-37-2-144

Kurita and Tabei, (1967). "On the pathogenic bacterium of bacterial grain rot of rice." Ann. Phytopathol. Soc. Jpn. 33, 111, (1967)

L. Medina-Aparicio, J. E. Rebollar-Flores, A. L. Gallego-Hernández, A. Vázquez, L. Olvera, R. M. Gutiérrez-Ríos, E. Calva, and I. Hernández-Lucas. "The CRISPR/Cas Immune System Is an Operon Regulated by LeuO, H-NS, and Leucine-Responsive Regulatory Protein in *Salmonella enterica Serovar* Typhi." American Society for Microbiology Journal of BacteriologyVolume 193, Issue 10, 15 May 2011, Pages 2396-2407 (2011) https://doi.org/10.1128/JB.01480-10

Laura Ortega and Clemencia M. Rojas, "Bacterial Panicle Blight and *Burkholderia glumae*: From Pathogen Biology to Disease Control." The American Phytopathological Society, (2021) http://doi.org/10.1094/PHYTO-09-20-0401-RVW

Lemire J, Milandu Y, Auger C, Bignucolo A, Appanna VP, Appanna VD. "Histidine is a source of the antioxidant, alpha-ketoglutarate, in *Pseudomonas fluorescens* challenged by oxidative stress." FEMS Microbiol Lett. 2010 Aug 1;309(2):170-7. Epub 2010 Jun 9 https://doi.org/10.1111/j.1574-6968.2010.02034.x. PMID: 20597986.

Leo Eberl, "Quorum sensing in the genus Burkholderia." International Journal of Medical Microbiology, Vol.296, Issues 2–3, (2006) https://doi.org/10.1016/j.ijmm.2006.01.035.

Li Fen, Xiong Xue-Song, Yang Ying-Ying, Wang Jun-Jiao, Wang Meng-Meng, Tang Jia-Wei, Liu Qing-Hua, Wang Liang, Gu Bing. "Effects of NaCl Concentrations on Growth Patterns, Phenotypes Associated With Virulence, and Energy Metabolism in *Escherichia coli* BW25113." Frontiers in Microbiology, Vol.12, (2021) https://doi.org/10.3389/fmicb.2021.705326

Louwen R, Staals RH, Endtz HP, van Baarlen P, van der Oost J. "The role of CRISPR-Cas systems in virulence of pathogenic bacteria." Microbiol Mol Biol Rev. (2014) Mar;78(1):74-88. https://doi.org/10.1128/MMBR.00039-13. PMID: 24600041; PMCID: PMC3957734.

Lucien Bettendorff, Pierre Wins, "Thiamin diphosphate in biological chemistry: new aspects of thiamin metabolism, especially triphosphate derivatives acting other than as cofactors." The Febs Journal, (2009) https://doi.org/10.1111/j.1742-4658.2009.07019.x

Luo J, Xie G, Li B, Lihui X. "First Report of *Burkholderia glumae* Isolated from Symptomless Rice Seeds in China." Plant Dis. (2007) Oct;91(10):1363. https://doi.org/10.1094/PDIS-91-10-1363B. PMID: 30780540.

Makarova KS, Wolf YI, Alkhnbashi OS, Costa F, Shah SA, Saunders SJ, Barrangou R, Brouns SJ, Charpentier E, Haft DH, Horvath P, Moineau S, Mojica FJ, Terns RM, Terns MP, White MF, Yakunin AF, Garrett RA, van der Oost J, Backofen R, Koonin EV. "An updated evolutionary classification of CRISPR-Cas systems." Nat Rev Microbiol. 2015

References

Nov;13(11):722-36. Epub (2015) Sep 28. https://doi.org/10.1038/nrmicro3569. PMID: 26411297; PMCID: PMC5426118.

Makarova, K.S., Wolf, Y.I., Iranzo, J. et al. "Evolutionary classification of CRISPR–Cas systems: a burst of class 2 and derived variants." Nat Rev Microbiol 18, 67–83 (2020). https://doi.org/10.1038/s41579-019-0299-x

Martin WF. "Older Than Genes: The Acetyl CoA Pathway and Origins." Front Microbiol. 2020;11:817. Published (2020) Jun 4. https://doi.org/10.3389/fmicb.2020.00817

Medina-Aparicio L., Rebollar-Flores J.E., Gallego-Hernández A.L., Vázquez A., Olvera L., Gutiérrez-Ríos R.M., Calva E., Hernández-Lucas I. "The CRISPR/Cas immune system is an operon regulated by LeuO, H-NS, and leucine-responsive regulatory protein in *Salmonella enterica serovar* Typhi." J. Bacteriol. 2011;193:2396–2407 (2011)

Mojica FJ, Díez-Villaseñor C, Soria E, Juez G. "Biological significance of a family of regularly spaced repeats in the genomes of Archaea, Bacteria and mitochondria." Mol Microbiol. 2000 Apr;36(1):244-6. (2000) https://doi.org/10.1046/j.1365-2958.2000.01838.x. PMID: 10760181.

Mojica FJM, Ferrer C, Juez G, Rodrı́guez-Valera F, "Long stretches of short tandem repeats are present in the largest replicons of the Archaea *Haloferax mediterranei* and *Haloferax volcanii* and could be involved in replicon partitioning." MolMicrobiol 17:85–93, (1995)

Mojica MJ, Juez G, Rodríguez-Valera F. "Transcription at different salinities of Haloferax mediterranei sequences adjacent to partially modified PstI sites." Mol Microbiol 9:613–621. (1993) https://doi.org/10.1111/j.1365-2958.1993.tb01721.x

Moreno-Gámez, S., Sorg, R.A., Domenech, A. et al. "Quorum sensing integrates environmental cues, cell density and cell history to control bacterial competence." Nat Commun 8, 854 (2017). https://doi.org/10.1038/s41467-017-00903-y

Nandakumar R, Rush MC, Correa F. "Association of *Burkholderia glumae* and *B. gladioli* with Panicle Blight Symptoms on Rice in Panama." Plant Dis. (2007) Jun;91(6):767. https://doi.org/10.1094/PDIS-91-6-0767C. PMID: 30780491.

Ng WL, Bassler BL. "Bacterial quorum-sensing network architectures." Annu Rev Genet. 2009;43:197-222. (2009) https://doi.org/10.1146/annurev-genet-102108-134304

Nina M. Høyland-Kroghsbo, Jon Paczkowski, Sampriti Mukherjee, Jenny Broniewski, Edze Westra, Joseph Bondy-Denomy, Bonnie L. Bassler. "Quorum sensing controls the *Pseudomonas aruginosa* CRISPR/CAS adaptive immune system." Proceedings of the National Academy of Sciences Jan (2017), 114 (1) 131-135; https://doi.org/10.1073/pnas.1617415113

Pang Zhiqiang, Chen Jia, Wang Tuhong, Gao Chunsheng, Li Zhimin, Guo Litao, Xu Jianping, Cheng Yi. "Linking Plant Secondary Metabolites and Plant Microbiomes: A Review." Frontiers in Plant Science, VOL12, (2021) https://doi.org/10.3389/fpls.2021.621276

Patterson AG, Chang JT, Taylor C, Fineran PC. "Regulation of the Type I-F CRISPR-Cas system by CRP-cAMP and GalM controls spacer acquisition and interference." Nucleic Acids Res. 2015 Jul 13;43(12):6038-48. Epub 2015 May 24. https://doi.org/10.1093/nar/gkv517. PMID: 26007654; PMCID: PMC4499141.

Paulsen IT, Park JH, Choi PS, Saier MH Jr. "A family of gram-negative bacterial outer membrane factors that function in the export of proteins, carbohydrates, drugs and heavy metals from gram-negative bacteria." FEMS Microbiol Lett. (1997) https://doi.org/10.1111/j.1574-6968.1997.tb12697.x. PMID: 9368353.

Pul U, Wurm R, Arslan Z, Geissen R, Hofmann N, Wagner R. "Identification and characterization of *E. coli* CRISPR-cas promoters and their silencing by H-NS." Mol Microbiol. 2010 Mar;75(6):1495-512. Epub 2010 Feb 1. https://doi.org/10.1111/j.1365-2958.2010.07073.x PMID: 20132443.

Pul U., Wurm R., Arslan Z., Geissen R., Hofmann N., Wagner R. "Identification and characterization of *E. coli* CRISPR-cas promoters and their silencing by H-NS." Mol. Microbiol. 2010;75:1495–1512 (2010)

Pumirat P, Vanaporn M, Boonyuen U, Indrawattana N, Rungruengkitkun A, Chantratita N. "Effects of sodium chloride on heat resistance, oxidative susceptibility, motility, biofilm and plaque formation of Burkholderia pseudomallei." Microbiologyopen. (2017) Aug;6(4):e00493. https://doi.org/10.1002/mbo3.493. PMID: 28643413; PMCID: PMC5552950.

Radlinski LC, Brunton J, Steele S, Taft-Benz S, Kawula TH. "Defining the Metabolic Pathways and Host-Derived Carbon Substrates Required for *Francisella tularensis* Intracellular Growth." mBio. 2018;9(6):e01471-18. Published (2018) https://doi.org/10.1128/mBio.01471-18

Rath D, Amlinger L, Rath A, Lundgren M. "The CRISPR-Cas immune system: biology, mechanisms and applications." Biochimie. (2015) Oct;117:119-28. https://doi.org/10.1016/j.biochi.2015.03.025. Epub 2015 Apr 10. PMID: 25868999.

Rath, D., Amlinger, L., Hoekzema, M., Devulapally, P. R., and Lundgren, M. "Efficient programmable gene silencing by Cascade." Nucleic Acids Res. 43, 237–246. (2015) https://doi.org/10.1093/nar/gku1257

Rhea G. Abisado, Saida Benomar, Jennifer R. Klaus, Ajai A. Dandekar and Josephine R. Chandler, "Bacterial Quorum Sensing and Microbial Community Interactions." ASM Journal, mbio, Vol.9, (2018) https://doi.org/10.1128/mBio.02331-17

Richardson AR, Somerville GA, Sonenshein AL. "Regulating the Intersection of Metabolism and Pathogenesis in Gram-positive Bacteria." Microbiol Spectr. 2015;3(3):10.1128/microbiolspec.MBP-0004-2014. https://doi.org/10.1128/microbiolspec.MBP-0004-2014

Rita Przybilski, Corinna Richter, Tamzin Gristwood, James S. Clulow, Reuben, B. Vercoe & Peter C. Fineran, "Csy4 is responsible for CRISPR RNA processing in *Pectobacterium atrosepticum*." RNA Biology, 8:3, 517-528, (2011) https://doi.org/10.4161/rna.8.3.15190

Ritsuko Mizobuchi, Shuichi Fukuoka, Chikako Tsuiki, Seiya Tsushima and Hiroyuki Sato (2020) "Evaluation of major rice cultivars for resistance to bacterial seedling rot caused by *Burkholderia glumae* and identification of Japanese standard cultivars for resistance assessments." Breeding Science 70: 221–230 (2020), https://doi.org/10.1270/jsbbs.19117

Rodionov DA, Vitreschak AG, Mironov AA, Gelfand MS. "Comparative genomics of thiamin biosynthesis in procaryotes. New genes and regulatory mechanisms." J Biol Chem. 2002 Dec 13;277(50):48949-59. Epub 2002 Oct 9. https://doi.org/10.1074/jbc.M208965200. PMID: 12376536.

Roy D. Sleator, Colin Hill. "Bacterial osmoadaptation: the role of osmolytes in bacterial stress and virulence." FEMS Microbiology Reviews, Volume 26, Issue 1, March (2002), Pages 49–71, https://doi.org/10.1111/j.1574-6976.2002.tb00598.x

Rutter J, Winge DR, Schiffman JD. „Succinate dehydrogenase - Assembly, regulation and role in human disease. Mitochondrion." (2010);10(4):393-401. https://doi.org/10.1016/j.mito.2010.03.001

S. Kim, J. Park, J. Lee, D. Shin, D.S. Park, J.S. Lim, I.Y. Choi, Y.S. Seo. "Understanding pathogenic *Burkholderia glumae* metabolic and signaling pathways within rice tissues through in vivo transcriptome analyses." Gene, 547 (1) (2014)

S. Voget, A. Knapp, A. Poehlein, C. Vollstedt, W. Streit, R. Daniel, K.E. Jaeger. „Complete genome sequence of the lipase producing strain *Burkholderia glumae* PG1." J Biotechnol, 204 (2015)

Sannino DR, Kraft CE, Edwards KA, Angert ER. „Thiaminase I Provides a Growth Advantage by Salvaging Precursors from Environmental Thiamine and Its Analogs in *Burkholderia thailandensis*." Appl Environ Microbiol. 2018;84(18):e01268-18. Published (2018) Aug 31. https://doi.org/10.1128/AEM.01268-18

Sato F, Kumagai H. "Microbial production of isoquinoline alkaloids as plant secondary metabolites based on metabolic engineering research." Proc Jpn Acad Ser B Phys Biol Sci. 2013;89(5):165-182. (2013) https://doi.org/10.2183/pjab.89.165

Seixas André F., Quendera Ana P., Sousa João P., Silva Alda F. Q., Arraiano Cecília M., Andrade José M. "Bacterial Response to Oxidative Stress and RNA Oxidation." Frontiers in Genetics, VOL 12, (2022) https://doi.org/10.3389/fgene.2021.821535

Seo, Lim, Park, Kim, Lee, Cheong, Kim, Moon, Hwang. "Comparative genome analysis of rice-pathogenic Burkholderia provides insight into capacity to adapt to different environments and hosts." BMC Genomics 16, (2015)

Silke Leimkühler, Chantal Iobbi-Nivol, "Bacterial molybdoenzymes: old enzymes for new purposes." FEMS Microbiology Reviews, Volume 40, Issue 1, January (2016), Pages 1–18, https://doi.org/10.1093/femsre/fuv043

Škerlová, J., Berndtsson, J., Nolte, H. et al. „Structure of the native pyruvate dehydrogenase complex reveals the mechanism of substrate insertion." Nat Commun 12, 5277 (2021). https://doi.org/10.1038/s41467-021-25570-y

Stefan H.M. Gorissen, Stuart M. Phillips, Chapter 17 – "Branched-Chain Amino Acids (Leucine, Isoleucine, and Valine) and Skeletal Muscle." Nutrition and Skeletal Muscle, Academic Press, (2019) https://doi.org/10.1016/B978-0-12-810422-4.00016-6.

Suárez-Moreno ZR, Caballero-Mellado J, Coutinho BG, Mendonça-Previato L, James EK, Venturi V. (2012) "Common features of environmental and potentially beneficial plant-associated Burkholderia.", Microb Ecol. 2012 Feb;63(2):249-66. Epub 2011 Aug 18. https://doi.org/10.1007/s00248-011-9929-1. PMID: 21850446.

Sudarsan N, Cohen-Chalamish S, Nakamura S, Emilsson GM, Breaker RR. "Thiamine pyrophosphate riboswitches are targets for the antimicrobial compound pyrithiamine." Chem Biol. 2005 Dec;12(12):1325-35. (2005) https://doi.org/10.1016/j.chembiol.2005.10.007. PMID: 16356850.

Tardat, B., and Touati, D. "Two Global Regulators Repress the Anaerobic Expression of MnSOD in *Escherichia coli*: Fur (Ferric Uptake Regulation) and Arc (Aerobic Respiration Control)." Mol. Microbiol. 5, 455–465. (1991) https://doi.org/10.1111/j.1365-2958.1991.tb02129.x

Teufel R, Mascaraque V, Ismail W, et al. "Bacterial phenylalanine and phenylacetate catabolic pathway revealed." Proc Natl Acad Sci U S A. 2010;107(32):14390-14395. (2010) https://doi.org/10.1073/pnas.1005399107

Thorsten Friedrich, Dierk Scheide. "The respiratory complex I of bacteria, archaea and eukarya and its module common with membrane-bound multisubunit hydrogenases." Letters, Volume 479, Issues 1–2, Pages 1-5, ISSN 0014-5793, (2000) https://doi.org/10.1016/S0014-5793(00)01867-6.

Trung & Van. „Occurance of rice grain rot disease in Vietnam." Int. Rice Res Notes 18, (1993)

Urakami T., Itl-Yoshida C., Araki H., Kijima T., Suzuki K.I., Komagata K., „Transfer of *Pseudomonas plantarii* and *Pseudomonas glumae* to Burkholderia as Burkholderia spp. and description of *Burkholderia vandii* sp. nov." Int. J. Syst. Bacteriol. 44, 235-245, (1944)

Vasu K, Nagaraja V. "Diverse functions of restriction-modification systems in addition to cellular defense." Microbiol Mol Biol Rev. 2013;77(1):53-72. (2013) https://doi.org/10.1128/MMBR.00044-12

Veselovsky VA, Dyachkova MS, Bespiatykh DA, et al. "The Gene Expression Profile Differs in Growth Phases of the Bifidobacterium Longum Culture." Microorganisms. 2022;10(8):1683. Published (2022) Aug 21. https://doi.org/10.3390/microorganisms10081683

Verbeke F, De Craemer S, Debunne N, "Peptides as Quorum Sensing Molecules: Measurement Techniques and Obtained Levels In vitro and In vivo." Front Neurosci. 2017;11:183. Published (2017) Apr 12. https://doi.org/10.3389/fnins.2017.00183

Vial L, Groleau MC, Dekimpe V, Déziel E. Burkholderia diversity and versatility: an inventory of the extracellular products. J Microbiol Biotechnol. (2007) Sep;17(9):1407-29. PMID: 18062218.

Walsh CT, Wencewicz TA. "Flavoenzymes: versatile catalysts in biosynthetic pathways." Nat Prod Rep. 2013;30(1):175-200. doi:10.1039/c2np20069d

Wardman, Peter, and Luis P. Candeias. "Fenton Chemistry: An Introduction." Radiation Research, vol. 145, no. 5, pp. 523–31. JSTOR, (1996) https://doi.org/10.2307/3579270. Accessed 23 Jul. 2022.

Weinberg JB, Alexander BD, Majure JM, "*Burkholderia glumae* infection in an infant with chronic granulomatous disease." J Clin Microbiol. 2007;45(2):662-665. https://doi.org/10.1128/JCM.02058-06

Weissman JL, Laljani RMR, Fagan WF, Johnson PLF. "Visualization and prediction of CRISPR incidence in microbial trait-space to identify drivers of antiviral immune strategy." ISME J. 2019 Oct;13(10):2589-2602. Epub 2019 Jun 25. https://doi.org/10.1038/s41396-019-0411-2. PMID: 31239539; PMCID: PMC6776019.

Westra ER, van Erp PB, Künne T, Wong SP, Staals RH, Seegers CL, Bollen S, Jore MM, Semenova E, Severinov K, de Vos WM, Dame RT, de Vries R, Brouns SJ, van der Oost J. "CRISPR immunity relies on the consecutive binding and degradation of negatively supercoiled invader DNA by Cascade and Cas3." Mol Cell. 2012 Jun 8;46(5):595-605. Epub 2012 Apr 19. https://doi.org/10.1016/j.molcel.2012.03.018. PMID: 22521689; PMCID: PMC3372689.

Y.S. Seo, J.Y. Lim, J. Park, S. Kim, H.H. Lee, H. Cheong, S.M. Kim, J.S. Moon, I. Hwang. "Comparative genome analysis of rice-pathogenic Burkholderia provides insight into capacity to adapt to different environments and hosts" BMC Genom, 16 (2015), p. 349

Yabuuchi E, Kosako Y, Oyaizu H, Yano I, Hotta H, Hashimoto Y, Ezaki T, Arakawa M. "Proposal of Burkholderia gen. nov. and transfer of seven species of the genus Pseudomonas homology group II to the new genus, with the type species *Burkholderia cepacian* (Palleroni and Holmes 1981) comb. nov." Microbiol Immunol. 1992;36(12):1251-75. https://doi.org/10.1111/j.1348-0421.1992.tb02129.x. Erratum in: Microbiol Immunol 1993;37(4):335. PMID: 1283774.

Yang C.-D., Chen Y.-H., Huang H.-Y., Huang H.-D., Tseng C.-P. "CRP represses the CRISPR/Cas system in *Escherichia coli*: evidence that endogenous CRISPR spacers impede phage P1 replication." Mol. Microbiol. 2014;92:1072–1091. (2014)

Yanli Zheng, Jiamei Han, Baiyang Wang, Xiaoyun Hu, Runxia Li, Wei Shen, Xiangdong Ma, Lixin Ma, Li Yi, Shihui Yang, Wenfang Peng, "Characterization and repurposing of the endogenous Type I-F CRISPR–Cas system of Zymomonas mobilis for genome engineering." Nucleic Acids Research, Volume 47, Issue 21, 02 December (2019), Pages 11461–11475, https://doi.org/10.1093/nar/gkz940

Yasutaro Fujita, Hiroshi Matsuoka, Kazutake Hirooka. "Regulation of fatty acid metabolism in bacteria." Molecular Microbiology Vol66, (2007) https://doi.org/10.1111/j.1365-2958.2007.05947.x

Yuan Qin, Irina S. Druzhinina, Xueyu Pan, Zhilin Yuan. "Microbially Mediated Plant Salt Tolerance and Microbiome-based Solutions for Saline Agriculture." Biotechnology Advances, Vol. 34, (2016) https://doi.org/10.1016/j.biotechadv2016.08.005.

Yuan X, McGhee GC, Slack SM, Sundin GW. "A Novel Signaling Pathway Connects Thiamine Biosynthesis, Bacterial Respiration, and Production of the Exopolysaccharide Amylovoran in Erwinia amylovora." Mol Plant Microbe Interact. 2021 Oct;34(10):1193-1208. Epub 2021 Oct 28. https://doi.org/10.1094/MPMI-04-21-0095-R. PMID: 34081536.

Zhang, K., Bian, J., Deng, Y. "Lyme disease spirochaete *Borrelia burgdorferi* does not require thiamin." Nat Microbiol 2, 16213 (2017) https://doi.org/10.1038/nmicrobiol.2016.213

Zheng Yanli, Li Jie, Wang Baiyang, Han Jiamei, Hao Yile, Wang Shengchen, Ma Xiangdong, Yang Shihui, Ma Lixin, Yi Li, Peng Wenfang. "Endogenous Type I CRISPR-Cas: From Foreign DNA Defense to Prokaryotic Engineering." Frontiers in Bioengineering and Biotechnology, Vol. 8, (2020) https://doi.org/10.3389/fbioe.2020.00062

Zhou, „First report of bacterial panicle blight of rice caused by *Burkholderia glumae* in South Africa." Plant Dis. 98, (2013)

Ziegler & Alvarez, „Grain discoloration of rice caused by *Pseudomonas glumae* in Latin America." Plant Dis. 73, (1989)

Abbreviations

%	Percentage
°C	Centigrade
µg	Microgram (10^{-6})
µl	Microlitre (10^{-6})
AHL	*N*-Acyl-homoserine lactone
AI	Autoinducer
Amp	Ampicillin
BGL_1c	*Burkholderia plantarii* PG1 first chromosome
BGL_2c	*Burkholderia plantarii* PG1 second chromosome
BpPG1	*Burkholderia plantarii* PG1 wildtype
BpPG2	*Burkholderia plantarii* PG2 (Δ*bgal*1)
BpPG3	*Burkholderia plantarii* PG3 (Δ*bgal*2)
BpPG4	*Burkholderia plantarii* PG4 (Δ*bgal*3)
bp	Base pair
Cm	Chloramphenicol
DNA	Desoxyribonucleic acid
DMF	Dimethylformamide
DMSO	Dimethyl sulfoxide
dNTP	Deoxyribonucleoside triphosphate
et al.	And others
EtOH	Ethanol
EtBr	Ethidium bromide
g	Gram
Gent	Gentamycin
h	Hour
H_2O	Water
H-NS	Histone-like nucleid structuring protein
Kan	Kanamycin
kb	Kilo base
kDa	Kilodalton
LB	Luria-Bertani medium
m	Milli (10^{-3})

M	Molar (mol/l)
mg	Milligram
min	Minute
ml	millilitre
$MgSO_4$	Magnesium sulphate
Na_2PO_4	Disodium phosphate
NCBI	National Center of Biotechnology Information
NaCl	Sodium chloride
NaOH	Sodium hydroxide
OD	Optical density
OD_{600}	Optical density to $\lambda = 600$ nm
PCR	Polymerase chain reaction
pH	Decimal logarithm of the reciprocal of the hydrogen ion activity
qPCR	Quantitative Real-Time PCR
QS	Quorum sensing
RT	Room temperature
RNA	Ribonucleic acid
rRNA	Ribosomal RNA
rpm	Round per minute
sec	Second
ThiM	Hydroxyethylthiazole kinase ThiM
Tm	Melting temperature
WT	Wildtype
Δ	Deletion
λ	Wavelength (lambda)

Table of Figures

Table of Tables

Appendix

Figure A1: 100bp+ O'GeneRuler™ DNA Marker (Thermo Scientific™ SM1153)
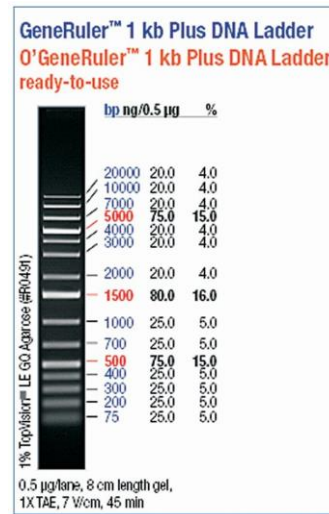
Figure A2: 1kb+ O'GeneRuler™ DNA Marker (Thermo Scientific™ SM1343
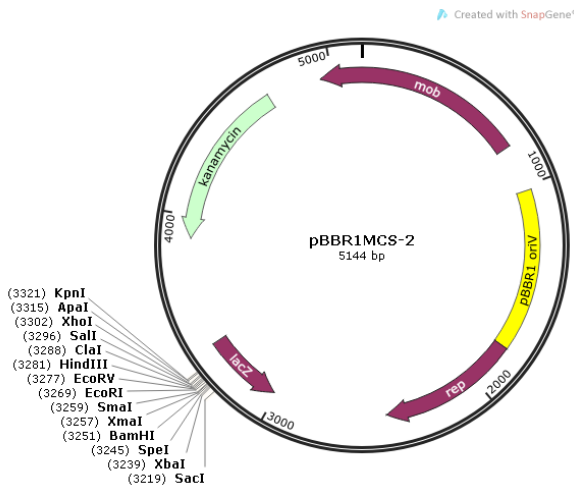
Figure A3: Vector map of pBBR1MCS-2
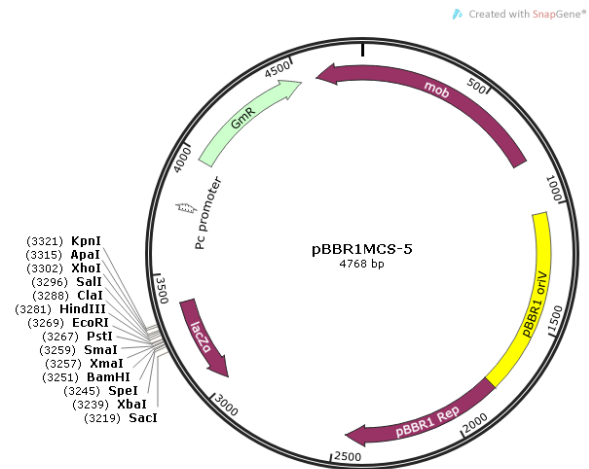
Figure A4: Vector map of pBBR1MCS-5

Table A1: Alignment sequences of the CRP binding motives

>P. aeruginosa PAO1 CRP_Box
TCATCCCCAAGGGAATTGAAAACAAATAACAAGCCAAATAAAAGACTGCATACAATCCTGT

>PG1 *cas1* CRP_Box
TAACAAAAAGACCATCTCGACACGCCAACACCAACGCGACCCAAAACCATCACCGCTCCCATCCCC
GATTCGGCTACGATTCCTCGACACACAAAAAT

>P. aeruginosa PAO1 CRP_Box
TCATCCCCAAGGGAATTGAAAACAAATAACAAGCCAAATAAAAGACTGCATACAATCCTGT

>PG1 *csy1* CRP_Box
CTGCGACGGGAAATCACTTCTTTATCTTAATAAGCTGCCCATTCGGCAGTGCGGCAGAAAATAACA
TGCTCGATTGAATGACG

>E.coli K12 CRP_Box
GATCATCGAGCAAACGTTGTGTGAGCTGGTGGATGAAATGAGTTGCCATCTGGT

>PG1 *thiM* CRP_Box
CGGAATCCCCCGTGTGAGGCGGATTAAGAATCAGACCTCGACGTTGAA

Table A2: Sequences of the promoter mcherry fusion constructs and CRP1 and CRP3 constructs

>pBBR1MCS-2::promcas1::mcherry, M13 primer

CGGTGGAGTGGCGGCCCTCGGCGCGTTCGTACTGTTCCACGATGGNGTAGNCCTCGNTGNGGGAGG
TGATGTCCAACTTGATGTTGACGTTGTAGGCGCCGGGCAGCTGCACGGGCTTCTTGGCCTTGTAGGT
GGTCTTGACCTCANCGTCGTAGTGGCCGCCGTCCTTCAGCTTCAGCCTCTGCTTGATCTCGCCCTTC
NGGGCGCCGTCCTCGGGGTACATCCGCTCGGAGGAGGCCTCCCAGCCCATGGTCTTCTTCTGCNTT
ACGGGGCCGTCGGAGGGGAAGTTGGTGCCGCGCAGCTTCACCTTGNAGATGAACTCGCCGTCCTGC
NAGGAGGAGTCCTGNGTCACGGTCACCACGCCGCCGTCCTCNAAGTTCNTCACGCGCTCCCACTTG
AAGCCCTCGGGGAAGGACAGCTTCAAGTAGTCGGGGATGTCGGCGGGGTGCTTCACGTAGGCCTT
GGAGCCGTACATGAACTGAGGGGACAGGATGTCCCAGGCGAAGGGCAGGGGGCCACCCTTGNTCA
CCTTCAGNTTGGCGGTCTGGGTGCCCTCGTAGGGGCGGCCCTCGCCCTCGCCCTCGATCTCGAACTC
NTGNCCGTTCACGGAGCCCTCCATGTGCACCTTGAAGNGCATGAACTCCTTGATGATGGCCATGTT
ATCCTCCTCGCCCTTGCTCACCATCTCGAGGGGGGGGCCCGGTA

>pBBR1MCS-2::promcsy1::mcherry, M13 primer

GCTTACTTGTACAGCTCGTCCATGCCGCCGGTGGAGTGGCGGCCCTCGGCGCGNTCGTACTGTTCC
ACGATGGNGTAGTCCTCGTTGNGGGAGGTGATGTCCAACTTGATGTTGACGTTGTNNGCGCCGGGC
AGCTGCACGGGCTTCTTGGCCTTGTANGTGGTCTTGACCTCAGCGTCGTAGTGGCCGCCGTCCTTCA
NCTTCAGCCTCTGCTTGATNTCNCCCTTCNGGGNGCCGNCCTCGGGGTACATCCGCTCGGAGGAGG
CCTCCCANCCCATGGTCTTCTTCTGCATTACGGGGCCGTCGGAGGGGAAGTTGGTGCCGCGCANCT
TCACCTTGTAGATGAACTCGCCGTCCTGCNAGGAGGAGTCCTGNGKCNCGGTCACCACGCCGCCGT
CCTCGAAGTTCATCACGCGCTCCCACTTGAAGCCCTCGGGGAANGACAGCTTCAAGTAGTCGGGGA
TGTCGGCGGGGTGCTTCACGTANGCCTTGGAGCCGTACATGAACTGAGGGGACAGGATGTCCCAG
GNGAAGGGNAGGGGGCCACCCTTGGTCACCTTCAGCTTGGCGGTCTGGGTGCCCTCGTAGGGGCG
GCCCTCGCCCTCGCCCTCGATCTCGAACTCGTGGCCGTTCACGGAGCCCTCCATGTGCACCTTGAAG
CGCATGAACTCCTTGATGATGGCCATGTTATCCTCCTCGCCCTTGCTCACCATCTCGAGGGGGGGCC
CGGTACCCAGCTTTTGTTCCCTTTAGTGAGGGNTAATTGCGCGCTTTGGCGTAATCATGGTCATAGC
TGTTTCCTGTGTGAAATTGTTATCCGCTCAC

>pBBR1MCS-2::promcsy4::mcherry, M13 primer

ACTASTGGATCCCTGTCGCGCAAAAGTACAACGTGTTTGCTGCCGGATAGGCAGCTTAGAAATCGT
GAGCCTGGACGACAAGCCGGGCACAAGAGTTTGCTGCCGGATAGGCAGCTTAGAAATTCCGCCAC
GTCCGGCTCGGGCGCGTCGAATTGTTTGCTGCSGGACAGGCAGTGCWAATAACAAAAAGACAACC

AGACACATCCGGAATCCCCCGTGTGAGGCGGATTAAGAATCAGACCTCGACGTTGAATCGCTCCCG
GGTAAAGCAGTGCMAACTGCGTCRTCGGACGTTTCCATTCGTGCCGGGAGCCGGCCCATTTCGCAA
CGACGTTGCGCAGGGCCAACCCAATCAGTTTGAGCGGGGCCTGCCCGAACCTTTCCACGCTTTTTC
AGGGGAGAATTCATGGTGAGCAAGGGCGAGGAGGATAACATGGCCATCATCAAGGAGTTCATGCG
CTWCAAGGTGCRCATGGAGGGMTCCGTGAACGGCCACGARTTCGAGATCGAGGGCSAGGGCGARG
GCCGCCCCTACGAGGGCACCCAGACCGCCAAGCTGAAGGTGACCAAGGGTGGCCCCCTGCCCTTC
GCCTGGGACATCCTGTCCCCTCAGTTCATGTACGGCTCCAAGGCCTACGTGAARCACCCCGCCGAC
ATCCCCGACTACTTGAARCTGTCCTTCCCCGAGGGCTTCAAGTGGGAGCGCGTGATGAACTTCGAG
GACGGCGGCGTGGTGACCGTGACCCAGGACTCCTCCTTGCAGGACGGCGAGTTCATCTACAAGGTG
AAGCTGCGCGGCACCAACTTCYCCTCCGACGGCCCCGTAATGCAGWMGAAGACCATGGGCTGGGA
GGCCTCCTCCGAGCGGATGTACTCCGACGACGGCGCCCTGAAGGGCKAGATCAAGCAAAGGCTGA
AGCTGAAGGACGGCGGCCACTACGACGCTGAGGTCAAGACCACCTACAAGGCCAAGAAAYCCGTG
CAGCTGCCCGRCGCCTACGACGTCAACATCARGTTGGACATCACCTCCCACAACGAGGACTAC

>pBBR1MCS-2::CRP1, specific primer

ATGTTGATTCCTCTCCCCCAACGTTCCTCCCGCCCGGTCCGCTCCTCCAGCTCCTGGGCTCCCCATCC
CGCCGCGCATTGCTCCACCTGTTCGATGCGGCACCTCTGCATGCCCCAAGGCCTCAATACCGAGGC
CGTCGAGCGCCTCGAGTCGGTGATCTGCGCGGCGCGCCCCGTGCGCCGCGGCGAAGCGCTGTTCCG
TGAAGGCGACGAGTTCGACAACCTCTACGCGGTGCGTTCCGGTTCGATCAAGACCATCGCCACGCG
CCAGGACGGCCGCGAGCAGGTAGCGGGCCTTCACCTGGCCGGCGAGGCGCTCGGCTTCGACGGCA
TCTGCGACAGCCACCATCCGCGCACCGCCGTCGCGCTCGAGGACAGCACCGTCTGCGTGATTCCCT
ACGGCTCGCTGCGCTCGCTGTGCTCCGAGGCCAGCACGCTGCAGGCACGCGTGCTGAAGCTGATGA
GCGAGCAGATCGTGCGCGAGACCACGCAGGCCATCCTGCTCGGGTCGCTGAACGCCGACGAGCGC
GTCGCCTCGTTCCTGCTCGACGTCTCGGCTCGCTACATGGTGCGCGGTTATTCGGCCACCGAGTTCA
ATCTGCGCATGACGCGCGAGGACATCGGCAGCTATCTGGGCATCACGCTCGAAACGGTCAGCCGC
ACGCTGTCGAAGTTCCAGCGGCAGGGCCTGCTCGTCATGCAGGGTCGCGTGGTTCGCGTGCTCGAT
TTCGACGGACTGCGCGCGATCTGA

>pBBR1MCS-2::CRP3, specific primer

ATGCTGACCGCCACGAAGCCCGCTCCGATCGCCCCCGACGTGCCACCGCCCGCGGCCGCGCAGCTC
GACGCGCTGAAGCAGCCCGGCGCGCGCTGTTCGAATTGCGCGACGCGCAACGTCTGCATGCCCGCG
GGACTCACGCACGCTGAATTCCGCCGGCTGGACACGCTGATCTGCATGACGCGCCACGTCAAGCGC
GGCGACGCGCTGTTCCGCGCCCAGGCCCCGTTCACGAGCCTCTATGCGGTGCGCACCGGCTCGTTC
AAGACGATCGTGATGCATCGCGACGGCCACGAGCAGGTGACCGGCTTCCAGATCACGGGCGAGAC
GCTCGGGCTCGACGGCCTCGGCGACGGCGAGCATCACAGCGACGCGATCGCGCTCGAGGACAGCA
CCGTCTGCATCATCCCGTTCGCGCAGCTCGAAGTGGCGTGCCGCGAGATGCGGCCGCTGCAGCAGC
ACCTGCATCAGTTGCTGAGCGGCGAGATCGTGCGCGAATCGCGCGCCATGATGCTGCTCGGCACCA
TGACGGCCGAGCAGCGCGTGGCCTCGTTCCTGTTGAACCTCTCGGCGCGCTTCAAGGCGCGCGGCT
ATTCGTCGGCCGAATTCAACCTGCGGATGACGCGCGAGGAAATCGGCTGCTATCTCGGCATGACGC
TCGAGACCGTGAGCCGCATGCTGTCGAAATTCCAGCGCAGCGGCATGATCGATTCACGAGGCCGGC
AGATCCGCATCACCGACGCGCAGCGGCTCGTGCAGGTCTGA

Table A3: Accession numbers of the transcriptome raw data

Accession number	Sample
SRR23143461	*B. plantarii* PG1 WT LB replicate 1
SRR23143460	*B. plantarii* PG1 WT LB replicate 2
SRR23143449	*B. plantarii* PG1 WT LB replicate 3
SRR23143438	*B. plantarii* PG1 WT M9 replicate 1
SRR23143437	*B. plantarii* PG1 WT M9 replicate 2
SRR23143436	*B. plantarii* PG1 WT M9 replicate 3
SRR23143435	*B. plantarii* PG1 pBBR2 LB replicate 1
SRR23143434	*B. plantarii* PG1 pBBR2 LB replicate 2
SRR23143433	*B. plantarii* PG1 pBBR2 LB replicate 3
SRR23143432	*B. plantarii* PG1 pBBR2 M9 replicate 1
SRR23143459	*B. plantarii* PG1 pBBR2 M9 replicate 2
SRR23143458	*B. plantarii* PG1 pBBR2 M9 replicate 3
SRR23143457	*B. plantarii* PG1 pBBR2::CRP1 LB replicate 1
SRR23143456	*B. plantarii* PG1 pBBR2::CRP1 LB replicate 2
SRR23143455	*B. plantarii* PG1 pBBR2::CRP1 LB replicate 3
SRR23143454	*B. plantarii* PG1 pBBR2::CRP3 LB replicate 1
SRR23143453	*B. plantarii* PG1 pBBR2::CRP3 LB replicate 2
SRR23143452	*B. plantarii* PG1 pBBR2::CRP3 LB replicate 3
SRR23143451	*B. plantarii* PG1 Δ*thiM* LB replicate 1
SRR23143450	*B. plantarii* PG1 Δ*thiM* LB replicate 2
SRR23143448	*B. plantarii* PG1 Δ*thiM* LB replicate 3
SRR23143447	*B. plantarii* PG1 Δ*thiM* M9 replicate 1
SRR23143446	*B. plantarii* PG1 Δ*thiM* M9 replicate 2
SRR23143445	*B. plantarii* PG1 Δ*thiM* M9 replicate 3

Glycolysis	Locus Tag	late exponential growth phase (48h)				late stationary growth phase (72h)		
		WT_M9_vs_WT_LB	ΔthiM_M9_vs_ΔthiM_LB	ΔthiM_LB_vs_WT_LB	ΔthiM_M9_vs_WT_M9	WT_M9_vs_WT_LB	WT_M9+T_vs_WT_LB	WT_M9+T-vs_WT_M9
		log2foldchange	log2foldchange	log2foldchange	log2foldchange	log2foldchange	log2foldchange	log2foldchange
a-D-Glucose-1P	BGL_1c07370	-0.17	-0.22	-0.34	-0.39	-1.45	-0.66	0.79
a-D-Glucose-6P	BGL_1c23360	-0.13	0.23	-0.23	0.12	-0.58	-0.06	0.52
ß-D-Fructose-6P	BGL_1c08770	-0.12	0.22	0.07	0.41	-2.93	-2.45	0.48
ß-D-Fructose-1,6P2	BGL_1c31200	-1.25	-1.19	-0.12	-0.07	-1.00	-0.13	0.86
Glyceraldehyde-3P	BGL_1c05210	-2.68	-1.98	-0.27	0.40	-2.54	-1.57	0.96
Glycerate-3P	BGL_1c31220	-0.89	-0.50	-0.24	0.13	-1.89	-1.20	0.69
	BGL_1c05590	0.08	-0.50	0.07	-0.46	-1.86	-0.69	1.17
Glycerate-2P	BGL_1c33550	-0.43	0.08	-0.01	0.49	-0.33	-0.01	0.32
Phosphoenolpyruvate	BGL_1c26070	-1.39	-1.63	0.24	0.02	-3.78	-3.28	0.50
	BGL_1c31210	-0.24	0.17	-0.31	0.09	-1.79	-0.82	0.97
Pyruvate	BGL_1c24440	-2.30	-1.28	-0.29	0.68	-1.65	-0.93	0.72
Lactate	BGL_2c26370	-0.49	-0.08	-0.17	0.19	0.58	1.40	0.82
Pyruvate	BGL_1c10940	-4.10	-3.84	-0.01	0.02	-8.10	-6.48	1.62
	BGL_2c26360	0.74	0.62	-0.06	-0.11	-0.77	-0.29	0.48
	BGL_2c08130	1.17	1.48	0.09	0.34	-1.21	-0.14	1.06
Hydroxyethyl-ThPP	BGL_1c10940	-4.10	-3.84	-0.01	0.02	-8.10	-6.48	1.62
	BGL_1c26360	-1.14	-1.21	0.25	0.19	-1.44	-0.50	0.94
	BGL_2c08130	1.17	1.48	0.09	0.34	-1.21	-0.14	1.06
S-Acetyl-dihydrolipoamide-E	BGL_1c22640	-0.43	-0.10	-0.06	0.13	-0.64	0.99	1.64
	BGL_1c26350	-0.65	-0.98	-0.09	-0.39	-1.98	-1.22	0.76
Acetyl-CoA	BGL_1c13110	0.75	0.51	0.09	-0.13	-0.96	-0.35	0.60
	BGL_1c27120	0.28	0.32	0.11	0.15	-0.76	-0.76	0.00
	BGL_2c08010	-5.83	-6.17	0.47	0.20	-0.80	-0.16	0.65
Acetate	BGL_1c00910	-0.38	0.12	0.13	0.56	4.56	3.91	-0.65
	BGL_1c29390	0.38	0.21	0.20	0.07	0.93	1.33	0.40
	BGL_2c16200	1.52	1.70	-0.04	0.12	-0.07	0.01	0.08
	BGL_2c05400	0.76	0.94	-0.10	0.06	-1.30	-0.07	1.23
	BGL_2c25130	-5.02	-6.42	0.04	-1.32	-5.19	-4.91	0.28
	BGL_2c25890	-1.56	-1.27	0.00	0.19	0.62	2.08	1.46
Acetaldehyde	BGL_1c31020	0.18	0.15	0.06	0.04	0.39	0.54	0.15
	BGL_2c09150	2.77	1.94	-0.01	-0.66	-0.86	-1.07	-0.21
	BGL_2c12510	-0.54	-1.03	-0.12	-0.58	-0.64	0.26	0.91
	BGL_2c21120	-2.89	-1.62	0.19	1.57	5.78	5.72	-0.05
Ethanol	BGL_2c07220	-4.76	-5.54	0.51	-0.08	1.69	2.43	0.74

Figure A5: Transcriptome analysis regarding to the glycolysis.

Citrate Cycle	Locus Tag	late exponential growth phase (48h)				late stationary growth phase (72h)		
		WT_M9_vs_WT_LB	ΔthiM_M9_vs_ΔthiM_LB	ΔthiM_LB_vs_WT_LB	ΔthiM_M9_vs_WT_M9	WT_M9_vs_WT_LB	WT_M9+T_vs_WT_LB	WT_M9+T-vs_WT_M9
		log2foldchange	log2foldchange	log2foldchange	log2foldchange	log2foldchange	log2foldchange	log2foldchange
Oxaloacetate	BGL_1c22690	3.01	2.05	0.44	-0.38	2.91	3.58	0.67
	BGL_1c30430	0.54	0.26	0.18	-0.06	0.63	0.83	0.20
	BGL_2c19150	0.65	1.17	-0.31	0.06	-1.76	-1.32	0.44
Citrate	BGL_2c09330	-1.48	-1.90	-0.09	-0.47	-3.73	-1.57	2.16
	BGL_2c18260	-1.34	-1.47	0.10	-0.02	-1.41	-0.68	0.73
cis-Aconitate	BGL_2c24440	0.85	0.84	0.03	0.02	-0.29	0.23	0.52
	BGL_2c09330	-1.48	-1.90	-0.09	-0.47	-3.73	-1.57	2.16
	BGL_2c18260	-1.34	-1.47	0.10	-0.02	-1.41	-0.68	0.73
	BGL_2c24440	0.85	0.84	0.03	0.02	-0.29	0.23	0.52
Isocitrate	BGL_1c30330	-0.43	0.02	-0.17	0.25	-1.75	-1.46	0.29
	BGL_1c30340	-0.42	-0.19	-0.15	0.08	0.04	1.04	1.00
Oxalsuccinate	BGL_1c30330	-0.43	0.02	-0.17	0.25	-1.75	-1.46	0.29
	BGL_1c30340	-0.42	-0.19	-0.15	0.08	0.04	1.04	1.00
2-oxo-glutarate	BGL_1c16180	-0.44	0.04	-0.03	0.43	-2.30	-1.80	0.50
3-Carboxy-1-hydroxypropyl-ThPP	BGL_2c27770	1.77	1.11	0.16	-0.29	-0.32	0.73	1.05
S-Succinyl-dihydrolipoamide-E	BGL_1c16200	-0.86	-0.96	-0.20	-0.30	-3.49	-2.85	0.63
Lipoamide-E	BGL_1c26340	-0.74	-1.19	0.00	-0.40	-2.06	-1.36	0.70
Dihydrolipoamide-E	BGL_2c02430	-3.85	-4.54	0.66	0.03	-5.27	-4.70	0.57
	BGL_1c16190	-0.88	-0.98	-0.14	-0.25	-2.50	-2.11	0.39
Succinyl-CoA	BGL_1c31420	0.57	0.50	-0.25	-0.33	-0.93	-0.34	0.59
	BGL_1c31430	0.42	0.37	-0.27	-0.34	-0.09	0.46	0.54
	BGL_2c16780	-5.28	-4.42	-0.25	0.50	-1.28	0.00	1.28
Succinate	BGL_2c18170	-1.10	-1.16	-0.14	-0.19	-0.56	-0.27	0.29
	BGL_2c18180	-1.46	-1.44	-0.25	-0.26	-1.65	-1.20	0.45
	BGL_2c18190	-2.47	-1.99	-0.22	0.18	-0.88	-0.36	0.52
	BGL_2c18200	-1.92	-1.68	-0.14	0.06	-0.46	0.14	0.60
Fumarate	BGL_1c09570	0.83	0.76	0.07	0.01	0.67	0.63	-0.04
	BGL_1c27150	-2.23	-2.61	-0.16	-0.52	-2.28	-1.85	0.43
	BGL_2c11260	0.07	0.09	-0.01	0.01	-0.78	-0.27	0.51
Malate	BGL_2c11270	0.97	0.18	0.65	0.04	0.61	1.39	0.78
Oxaloacetate	BGL_2c18220	0.14	-0.20	0.07	-0.27	-1.79	-0.90	0.89
^ Phosphoenolpyruvate	BGL_1c29450	-0.05	0.58	-0.11	0.48	-0.22	0.49	0.70

Figure A6: Transcriptome analysis regarding to the citrate cycle.

Oxidative Phosphorylation	Locus Tag	late exponential growth phase (48h)				late stationary growth phase (72h)		
		WT_M9_vs_WT_LB	ΔthiM_M9_vs_ΔthiM_LB	ΔthiM_LB_vs_WT_LB	ΔthiM_M9_vs_WT_M9	WT_M9_vs_WT_LB	WT_M9+T_vs_WT_LB	WT_M9+T-vs_WT_M9
		log2foldchange	log2foldchange	log2foldchange	log2foldchange	log2foldchange	log2foldchange	log2foldchange
Complex I NADH to NAD+ und H+	BGL_1c27610	-1.51	-2.39	0.18	-0.60	-2.68	-2.14	0.53
	BGL_1c27620	-1.70	-2.58	0.25	-0.51	-2.16	-1.72	0.44
	BGL_1c27630	-1.53	-2.13	0.34	-0.15	-2.82	-2.39	0.43
	BGL_1c27640	-1.66	-2.25	0.56	0.05	-2.79	-2.85	-0.06
	BGL_1c27650	-1.54	-2.53	0.37	-0.53	-2.56	-2.46	0.10
	BGL_1c27660	-1.87	-2.95	0.36	-0.63	-1.84	-2.05	-0.21
	BGL_1c27670	-2.12	-2.99	0.39	-0.42	-3.05	-3.08	-0.03
	BGL_1c27680	-2.84	-3.26	0.12	-0.25	-2.70	-2.68	0.03
	BGL_1c27690	-2.83	-3.67	0.10	-0.72	-2.68	-2.98	-0.30
	BGL_1c27700	-3.62	-4.11	0.08	-0.38	-2.26	-2.83	-0.56
	BGL_1c27710	-3.14	-4.17	0.07	-0.94	-1.68	-2.30	-0.63
	BGL_1c27720	-2.46	-3.26	0.12	-0.65	-1.71	-1.28	0.43
	BGL_1c27730	-2.37	-2.49	0.16	0.05	-0.80	-0.05	0.75
	BGL_1c27740	-1.77	-1.69	0.04	0.11	1.02	1.50	0.49
	BGL_1c20790	3.17	5.83	-0.38	1.74	4.27	5.12	0.85
	BGL_1c22880	-0.61	-0.61	-0.17	-0.17	-0.35	0.69	1.04
	BGL_21510	1.65	1.46	-0.11	-0.29	0.39	1.31	0.91
Complex II Succinate to Fumarate	BGL_2c18170	-1.10	-1.16	-0.14	-0.19	-0.56	-0.27	0.29
	BGL_2c18180	-1.46	-1.44	-0.25	-0.26	-1.65	-1.20	0.45
	BGL_2c18190	-2.47	-1.99	-0.22	0.18	-0.88	-0.36	0.52
	BGL_2c18200	-1.92	-1.68	-0.14	0.06	-0.46	0.14	0.60
Complex III Cyctochrome bc 1 complex	BGL_1c03410	-0.17	-0.73	0.65	0.10	-0.12	0.35	0.47
	BGL_1c03420	0.18	-0.47	0.58	-0.01	-0.60	-0.25	0.35
	BGL_1c03430	0.16	0.12	0.08	0.04	-1.18	-0.72	0.46
Complex IV Cytochrome c oxidase								
PPPi - PPi	BGL_1c12450	0.33	0.47	0.04	0.17	-1.58	-1.41	0.17
	BGL_2c08900	0.05	0.10	-0.08	-0.03	-1.24	-0.35	0.89
PPI - Pi ADP	BGL_1c29380	-0.35	-0.52	-0.04	-0.20	-3.13	-1.91	1.22
Cytochrome bd complex								
CydA	BGL_2c28310	4.08	6.13	-0.36	0.97	2.26	2.72	0.46
CydB	BGL_2c28320	3.45	6.04	-0.19	1.86	3.76	3.78	0.02
CydA	BGL_1c33180	-2.54	-1.76	0.07	0.79	2.11	2.43	0.32
CydB	BGL_1c33190	-2.93	-2.16	0.30	1.10	0.90	1.52	0.62
CydA	BGL_2c12170	0.64	1.15	-0.27	0.20	-0.65	-0.63	0.02
CydB	BGL_2c12180	0.81	1.06	0.04	0.29	-0.57	-0.52	0.05

Figure A7: Transcriptome analysis regarding to the oxidative phosphorylation.

Leucine degradation	Locus Tag	late exponential growth phase (48h)				late stationary growth phase (72h)		
	LocusTag	WT_M9_vs_WT_LB log2foldchange	ΔthiM_M9_vs_ΔthiM_LB log2foldchange	ΔthiM_LB_vs_WT_LB log2foldchange	ΔthiM_M9_vs_WT_M9 log2foldchange	WT_M9_vs_WT_LB log2foldchange	WT_M9+T_vs_WT_LB log2foldchange	WT_M9+T-vs_WT_M9 log2foldchange
L-Leucine	BGL_1c15820	-0.59	-2.02	0.79	-0.53	-8.05	-6.71	1.34
	BGL_2c02500	0.93	1.22	0.07	0.31	-3.61	-3.05	0.56
	BGL_2c03810	-0.14	-0.10	-1.49	-1.44	-0.81	-0.17	0.64
	BGL_2c07560	-2.49	-3.09	-0.23	-0.79	-4.44	-3.33	1.11
4-Methyl-2-oxopentanoate	BGL_2c02400	-4.85	-5.97	0.99	-0.09	-5.45	-5.02	0.43
	BGL_2c02410	-4.93	-6.17	0.93	-0.22	-6.50	-5.75	0.76
3-Methyl-1-hydroxybutyl-ThPP	BGL_2c02400	-4.85	-5.97	0.99	-0.09	-5.45	-5.02	0.43
	BGL_2c02410	-4.93	-6.17	0.93	-0.22	-6.50	-5.75	0.76
S-(3-Methyl-butanoyl)-dihydrolipoamide-E	BGL_2c02420	-4.44	-5.68	0.62	-0.46	-6.27	-5.64	0.63
3-Methylbutanoyl-CoA	BGL_1c14830	0.67	1.52	-0.05	0.57	-0.84	0.39	1.23
	BGL_1c20270	-2.53	-3.12	0.34	-0.12	-5.92	-5.20	0.73
	BGL_1c21020	0.27	-0.47	0.06	-0.59	-0.91	-0.61	0.31
	BGL_1c27530	-1.92	-1.93	0.26	0.25	-2.73	-1.66	1.07
	BGL_2c22380	0.37	0.50	0.05	0.16	-3.03	-1.96	1.07
	BGL_2c14630	-4.88	-4.75	-0.02	0.10	-3.93	-2.54	1.39
3-Methylbut-2-enoyl-CoA	BGL_2c14640	-4.40	-4.35	0.12	0.16	-3.63	-2.89	0.74
	BGL_2c14660	-3.73	-3.59	-0.04	0.08	-3.37	-2.86	0.51
3-Methyl-glutaconyl-CoA	BGL_2c14650	-3.74	-3.91	0.17	0.03	-2.70	-2.35	0.35
(S)-3-Hydroxy-3-methylglutaryl-CoA	BGL_1c34390	-0.70	-0.28	-0.26	0.15	-0.23	0.24	0.47
	BGL_2c09920	0.78	1.58	-0.61	0.06	1.15	1.59	0.45
Acetoacetate	BGL_1c15630	-1.84	-0.56	-0.20	0.93	-1.09	-0.31	0.78
	BGL_1c15640	-1.91	-0.68	-0.25	0.88	-0.04	0.66	0.71
Acetoacetyl-CoA	BGL_1c21770	-1.69	-1.37	-0.04	0.24	-0.71	0.28	0.99
	BGL_1c22180	-1.23	-0.48	-0.35	0.38	-1.17	-1.32	-0.15
	BGL_1c23220	-1.78	-1.67	-0.01	0.09	-2.88	-2.22	0.66
	BGL_1c34200	-0.74	-0.62	0.18	0.29	-0.56	-0.21	0.35
Acetyl-CoA	BGL_2c15200	0.66	2.44	0.13	1.97	2.88	4.86	1.98
(S)-3-Hydroxy-3-methylglutaryl-CoA	BGL_2c02420	-4.44	-5.68	0.62	-0.46	-6.27	-5.64	0.63
Dihydrolipoamide-E	BGL_1c16200	-0.86	-0.96	-0.20	-0.30	-3.49	-2.85	0.63
	BGL_2c02430	-3.85	-4.54	0.66	0.03	-5.27	-4.70	0.57
	BGL_1c26340	-0.74	-1.19	0.00	-0.40	-2.06	-1.36	0.70
Lipoamide-E	BGL_2c02400	-4.85	-5.97	0.99	-0.09	-5.45	-5.02	0.43
3-Methyl-1-hydroxybutyl-ThPP	BGL_2c02410	-4.93	-6.17	0.93	-0.22	-6.50	-5.75	0.76

Figure A8: Transcriptome analysis regarding to the leucine degradation.

Fatty acid biosynthesis	Locus Tag	late exponential growth phase (48h)				late stationary growth phase (72h)		
		WT_M9_vs_WT_LB log2foldchange	ΔthiM_M9_vs_ΔthiM_LB log2foldchange	ΔthiM_LB_vs_WT_LB log2foldchange	ΔthiM_M9_vs_WT_M9 log2foldchange	WT_M9_vs_WT_LB log2foldchange	WT_M9+T_vs_WT_LB log2foldchange	WT_M9+T-vs_WT_M9 log2foldchange
Acetyl-CoA	BGL_1c04910	0.11	-0.86	0.19	-0.73	-2.48	-2.07	0.41
	BGL_1c04910	0.11	-0.86	0.19	-0.73	-2.48	-2.07	0.41
	BGL_1c25370	-0.38	-0.21	0.23	0.40	-0.36	1.04	1.41
	BGL_2c17990	-0.70	-0.87	0.06	-0.10	-0.29	0.26	0.55
Malonyl-CoA	BGL_1c09890	-0.85	-1.28	0.04	-0.37	-2.23	-1.41	0.82
	BGL_1c12130	-0.68	-0.89	0.30	0.12	0.46	1.09	0.63
Malonyl-[acp]	BGL_1c12950	0.67	-0.67	0.47	-0.73	0.39	1.47	1.08
	BGL_1c12990	0.51	-0.64	0.31	-0.65	-1.71	-1.11	0.60
	BGL_1c09920	-0.28	-1.04	0.28	-0.46	-2.53	-1.61	0.92
	BGL_1c12980	0.07	-0.74	0.37	-0.33	-2.02	-1.24	0.78
	BGL_1c14030	-0.02	-0.04	-0.19	-0.22	-3.84	-3.50	0.34
	BGL_1c20310	-3.15	-3.96	0.31	-0.15	-6.65	-5.84	0.82
	BGL_1c20320	-3.45	-3.44	0.32	0.28	-7.38	-5.99	1.39
3-Oxo(6/8/10/12/14/16)-noyl-[acp]	BGL_1c09900	-0.67	-1.40	-0.08	-0.81	-2.26	-1.65	0.61
	BGL_1c12970	0.15	-0.65	0.37	-0.32	-1.17	-0.31	0.86
	BGL_1c19530	-1.60	-1.00	0.17	0.67	0.26	1.25	0.99
	BGL_1c20260	-2.34	-2.73	0.24	-0.03	-6.14	-5.27	0.88
	BGL_1c22080	-1.52	-0.27	-1.76	-0.45	6.70	2.56	-4.15
	BGL_1c24190	-0.11	-0.04	-0.03	-0.01	-1.28	-0.64	0.65
	BGL_1c28130	-0.38	0.12	-0.27	0.20	-0.19	0.55	0.75
	BGL_1c29400	-0.10	-0.59	0.40	-0.03	-0.67	-0.44	0.24
	BGL_2c03550	0.54	0.59	0.28	0.34	0.80	1.54	0.74
(R)-3-Hydroxy-(6/8/10/12/14/16)-noyl-[acp]	BGL_2c14390	1.00	1.31	0.09	0.37	0.63	0.43	-0.20
	BGL_2c18310	-0.26	-0.34	-0.49	-0.57	-2.91	-2.15	0.76
	BGL_1c20240	-2.85	-3.44	0.20	-0.13	-6.54	-5.03	1.51
	BGL_1c24500	-1.06	-1.19	-0.05	-0.17	-2.35	-1.78	0.57
trans-(6/8/10/12/14)-2-enoyl-[acp]	BGL_2c26670	-2.19	-2.60	0.11	-0.28	-2.19	-1.03	1.16
(6/8/10/12/14)-noyl-[acp]								
Acetyl-Co	BGL_1c01400	1.23	0.67	0.03	-0.48	-0.69	0.98	1.67
	BGL_1c01420	0.67	0.21	0.30	0.01	1.33	3.15	1.81
	BGL_1c09880	-0.65	-1.22	-0.05	-0.60	-3.27	-2.16	1.11
Acetoacetyl-[acp]	BGL_1c09900	-0.67	-1.40	-0.08	-0.81	-2.26	-1.65	0.61
	BGL_1c12970	0.15	-0.65	0.37	-0.32	-1.17	-0.31	0.86
	BGL_1c19530	-1.60	-1.00	0.17	0.67	0.26	1.25	0.99
	BGL_1c20260	-2.34	-2.73	0.24	-0.03	-6.14	-5.27	0.88
	BGL_1c22080	-1.52	-0.27	-1.76	-0.45	6.70	2.56	-4.15
	BGL_1c24190	-0.11	-0.04	-0.03	-0.01	-1.28	-0.64	0.65
	BGL_1c28130	-0.38	0.12	-0.27	0.20	-0.19	0.55	0.75
	BGL_1c29400	-0.10	-0.59	0.40	-0.03	-0.67	-0.44	0.24
	BGL_2c03550	0.54	0.59	0.28	0.34	0.80	1.54	0.74
(R)-3-Hydroxy-(6/8/10/12/14/16)-noyl-[acp]	BGL_2c14390	1.00	1.31	0.09	0.37	0.63	0.43	-0.20
	BGL_2c18310	-0.26	-0.34	-0.49	-0.57	-2.91	-2.15	0.76
	BGL_1c20240	-2.85	-3.44	0.20	-0.13	-6.54	-5.03	1.51
	BGL_1c24500	-1.06	-1.19	-0.05	-0.17	-2.35	-1.78	0.57
trans-(6/8/10/12/14)-2-enoyl-[acp]	BGL_2c26670	-2.19	-2.60	0.11	-0.28	-2.19	-1.03	1.16
(6/8/10/12/14)-noyl-[acp]								
beta-Oxidation, acyl-CoA synthesis								
Hexadecanoic acid	BGL_1c04380	-1.54	-1.46	0.08	0.15	-1.30	-0.84	0.45
	BGL_1c16420	-2.15	-2.30	0.74	0.59	-0.02	0.00	0.03
	BGL_1c20390	-3.05	-3.63	-0.01	-0.50	-7.62	-6.29	1.33
	BGL_1c30650	0.79	0.38	0.02	-0.36	0.20	-0.85	-1.05
Hexadecanoyl-CoA	BGL_2c00910	1.38	1.69	-0.18	0.08	-1.56	-0.79	0.77

Figure A9: Transcriptome analysis regarding to the fatty acid metabolism.

Arginine Biosynthesis	Locus Tag	late exponential growth phase (48h)				late stationary growth phase (72h)		
		WT_M9_vs_WT_LB log2foldchange	ΔthiM_M9_vs_ΔthiM_LB log2foldchange	ΔthiM_LB_vs_WT_LB log2foldchange	ΔthiM_M9_vs_WT_M9 log2foldchange	WT_M9_vs_WT_LB log2foldchange	WT_M9+T_vs_WT_LB log2foldchange	WT_M9+T-vs_WT_M9 log2foldchange
2-Oxoglutarate	BGL_1c05450	-1.58	-2.27	0.93	0.25	-3.24	-3.27	-0.03
Glutamate	BGL_1c04590	-1.30	-0.91	-0.12	0.26	-1.65	-0.66	0.99
	BGL_1c26680	0.32	0.03	-0.04	-0.30	-0.78	-0.48	0.31
	BGL_2c27580	-0.74	-1.33	0.07	-0.47	-0.93	0.33	1.26
N-Acetyl-glutamate	BGL_1c35670	-0.06	0.17	-0.15	0.05	0.49	1.42	0.92
N-Acetyl-glutamyl-P	BGL_1c02110	0.77	1.10	0.00	0.32	0.91	1.47	0.55
	BGL_2c09840	0.70	1.06	-0.29	-0.06	-0.66	1.21	1.87
N-Acetyl-glutamate semialdehyde	BGL_1c30000	-0.45	-0.36	-0.02	0.07	-2.68	-1.98	0.70
	BGL_2c09700	0.01	0.58	-0.20	-0.04	-0.65	0.63	1.28
N-Acetyl-ornithine	BGL_2c24590	0.48	0.05	0.00	-0.37	-0.03	0.75	0.78
	BGL_2c25800	0.20	0.58	-0.14	0.13	0.35	0.40	0.05
	BGL_1c23870	0.86	0.98	-0.02	0.10	0.45	0.32	-0.13
Ornithine	BGL_1c30600	-0.02	0.55	-0.59	-0.04	-0.40	-0.09	0.32
Citruline	BGL_1c26430	-2.87	-3.12	0.01	-0.19	-4.08	-3.65	0.43
	BGL_1c34660	-1.55	-1.40	-0.05	0.09	-1.36	-1.14	0.23
L-Arginosuccinate	BGL_1c29470	-0.88	-0.66	-0.25	-0.05	-2.63	-1.72	0.91
Arginine								
Ornithine	BGL_1c04590	-1.30	-0.91	-0.12	0.26	-1.65	-0.66	0.99
	BGL_2c27580	-0.74	-1.33	0.07	-0.47	-0.93	0.33	1.26
N-Acetyl-ornithine								
Glutamate	BGL_1c05450	-1.58	-2.27	0.93	0.25	-3.24	-3.27	-0.03
NH3	BGL_1c26610	-3.46	-3.25	-0.42	-0.25	-1.91	-2.03	-0.13
	BGL_1c26730	0.01	0.67	-0.36	0.19	-1.46	-1.00	0.46
	BGL_2c20390	-0.47	-0.74	0.20	0.03	-1.26	-0.86	0.40
Glutamine	BGL_1c07090	-0.52	-0.36	-0.06	0.04	-2.06	-1.48	0.58
	BGL_1c06540	0.32	-0.05	0.29	-0.02	-2.43	-1.92	0.51
NH3	BGL_2c24180	0.96	0.43	0.27	-0.20	-2.10	-1.55	0.55

Figure A10: Transcriptome analysis regarding to the arginine biosynthesis.

Appendix

Nitrogen metabolism	Locus Tag	late exponential growth phase (48h)				late stationary growth phase (72h)		
		WT_M9_vs_WT_LB log2foldchange	ΔthiM_M9_vs_ΔthiM_LB log2foldchange	ΔthiM_LB_vs_WT_LB log2foldchange	ΔthiM_M9_vs_WT_M9 log2foldchange	WT_M9_vs_WT_LB log2foldchange	WT_M9+T_vs_WT_LB log2foldchange	WT_M9+T-vs_WT_M9 log2foldchange
Nitrate (extracellular)	BGL_2c16820	-0.80	0.50	0.36	1.80	3.26	3.64	0.38
	BGL_2c23320	-2.36	-2.12	-0.49	-0.24	-0.60	0.08	0.68
Nitrate	BGL_2c23280	-7.24	-5.12	-0.87	0.99	-0.77	0.67	1.45
	BGL_2c23290	-4.54	-3.38	-1.04	0.04	-0.69	-0.14	0.55
	BGL_2c23310	-3.91	-3.38	-0.65	-0.10	-0.48	0.35	0.84
	BGL_2c2320	-2.36	-2.12	-0.49	-0.24	-0.60	0.08	0.68
	BGL_2c23290	-4.54	-3.38	-1.04	0.04	-0.69	-0.14	0.55
	BGL_2c23310	-3.91	-3.38	-0.65	-0.10	-0.48	0.35	0.84
Nitrite	BGL_2c16800	-2.26	-1.78	0.86	1.37	2.69	3.25	0.56
	BGL_2c16810	-2.93	-1.30	0.47	2.22	2.40	2.83	0.43
Ammonia	BGL_1c05450	-1.58	-2.27	0.93	0.25	-3.24	-3.27	-0.03
L-Glutamate	BGL_1c05450	-1.58	-2.27	0.93	0.25	-3.24	-3.27	-0.03
Nitroalkane -> Nitrite	BGL_1c01800	0.48	0.09	0.15	-0.16	-1.16	-0.53	0.64
	BGL_1c16490	-0.14	-0.56	0.39	0.00	-0.10	0.21	0.31
	BGL_1c21660	-4.91	-3.46	0.00	1.36	0.13	1.19	1.06
	BGL_1c34430	-2.27	-1.62	-0.19	0.30	-1.48	-1.32	0.16
Ammonia	BGL_1c26610	-3.46	-3.25	-0.42	-0.25	-1.91	-2.03	-0.13
	BGL_1c26730	0.01	0.67	-0.36	0.19	-1.46	-1.00	0.46
	BGL_2c20390	-0.47	-0.74	0.20	0.03	-1.26	-0.86	0.40
L-Glutamine	BGL_1c03070	-1.82	-0.53	-0.31	0.84	0.70	1.45	0.75
	BGL_1c03080	-0.02	0.63	-0.32	0.24	-0.40	0.09	0.48
L-Glutamate -> Glutamate metabolism								
Nitrile -> Ammonia	BGL_1c01330	0.22	0.60	0.03	0.32	-2.14	-1.44	0.70
	BGL_2c03350	0.84	0.69	0.01	-0.09	-1.52	-1.40	0.12
	BGL_2c09240	-0.31	-0.57	-0.09	-0.32	-1.61	-0.85	0.76
	BGL_2c10680	0.00	-0.35	0.18	-0.10	-1.21	-0.88	0.33
Formamide -> Ammonia	BGL_1c25530	-0.17	-0.48	-0.06	-0.32	-4.17	-2.92	1.25
Nitrite (extracellular)	BGL_2c16820	-0.80	0.50	0.36	1.80	3.26	3.64	0.38
	BGL_2c23320	-2.36	-2.12	-0.49	-0.24	-0.60	0.08	0.68
Nitrite								
Dissimilatory nitrate reduction								
Nitrate	BGL_2c23280	-7.24	-5.12	-0.87	0.99	-0.77	0.67	1.45
	BGL_2c23290	-4.54	-3.38	-1.04	0.04	-0.69	-0.14	0.55
	BGL_2c23310	-3.91	-3.38	-0.65	-0.10	-0.48	0.35	0.84
Nitrite	BGL_2c16800	-2.26	-1.78	0.86	1.37	2.69	3.25	0.56
	BGL_2c16810	-2.93	-1.30	0.47	2.22	2.40	2.83	0.43
Ammonia								
Denitrification								
Nitrate	BGL_2c23280	-7.24	-5.12	-0.87	0.99	-0.77	0.67	1.45
	BGL_2c23290	-4.54	-3.38	-1.04	0.04	-0.69	-0.14	0.55
	BGL_2c23310	-3.91	-3.38	-0.65	-0.10	-0.48	0.35	0.84
Nitrite								
Nitrification								
Nitarte	BGL_2c23280	-7.24	-5.12	-0.87	0.99	-0.77	0.67	1.45
	BGL_2c23290	-4.54	-3.38	-1.04	0.04	-0.69	-0.14	0.55
Nitrite								

Figure A11: Transcriptome analysis regarding to the nitrogen metabolism.

Histidine metabolism	Locus Tag	late exponential growth phase (48h)				late stationary growth phase (72h)		
		WT_M9_vs_WT_LB log2foldchange	ΔthiM_M9_vs_ΔthiM_LB log2foldchange	ΔthiM_LB_vs_WT_LB log2foldchange	ΔthiM_M9_vs_WT_M9 log2foldchange	WT_M9_vs_WT_LB log2foldchange	WT_M9+T_vs_WT_LB log2foldchange	WT_M9+T-vs_WT_M9 log2foldchange
PRPP	BGL_1c03240	0.11	0.31	0.13	0.33	-1.39	-1.41	-0.02
	BGL_1c22300	-0.16	-0.76	0.11	-0.45	-1.63	-0.98	0.65
Phosphoribosyl-ATP	BGL_1c03330	0.33	-0.11	0.06	-0.36	1.62	1.67	0.05
Phosphoribosyl-AMP	BGL_1c03320	0.04	-0.55	-0.12	-0.69	1.82	1.82	0.01
Phosphoribosyl-formimino-AICAR-P	BGL_1c03300	-0.44	-0.43	-0.15	-0.15	0.63	0.53	-0.10
Phosphoribulosyl-formimino-AICAR-P	BGL_1c03290	-1.16	-1.50	-0.05	-0.36	-0.75	-0.38	0.37
	BGL_1c03310	0.33	-0.04	-0.02	-0.39	0.61	0.66	0.05
Imidazole-glycerol-3P	BGL_1c03270	-0.23	-0.52	0.22	-0.04	-0.14	0.32	0.46
Imidazole-acetol-P	BGL_1c03260	-0.26	-0.35	-0.02	-0.11	-1.68	-1.58	0.11
	BGL_1c31590	1.39	0.45	0.20	-0.49	-1.26	-0.25	1.02
	BGL_1c33050	0.02	-0.12	-0.04	-0.17	-0.18	0.45	0.63
L-Histidinol-P	BGL_2c20570	1.95	1.47	0.00	-0.29	-0.60	0.44	1.04
L-Histidinol	BGL_1c03250	-0.38	-0.16	-0.04	0.17	-2.14	-2.01	0.13
L-Histidinal	BGL_1c03250	-0.38	-0.16	-0.04	0.17	-2.14	-2.01	0.13
L-Histidine	BGL_1c12910	0.74	-0.68	0.50	-0.76	-1.72	-0.58	1.14
	BGL_1c20660	-0.54	-0.56	-0.55	-0.50	-4.18	-3.34	0.84
	BGL_1c26840	-1.10	3.81	-4.27	0.35	-0.17	0.44	0.60
Urocanate	BGL_1c19980	-2.65	0.56	-2.73	0.30	-1.33	-0.77	0.56
	BGL_1c26820	-2.15	3.06	-4.73	0.25	-1.35	-0.45	0.90
4-Imidazolone-5-propanoate	BGL_1c26800	-1.79	2.77	-4.35	0.16	-1.44	-1.23	0.22
N-Formimino-L-glutamate	BGL_1c26790	-1.51	2.81	-4.35	0.05	-0.87	-0.62	0.24
N-Formyl-L-glutamate	BGL_1c26780	-1.51	2.61	-3.91	0.15	0.05	0.37	0.32
L-Glutamate								

Figure A12: Transcriptome analysis regarding to the histidine metabolism.

Thiamine metabolism	Locus Tag	late exponential growth phase (48h)				late stationary growth phase (72h)		
		WT_M9_vs_WT_LB	ΔthiM_M9_vs_ΔthiM_LB	ΔthiM_LB_vs_WT_LB	ΔthiM_M9_vs_WT_M9	WT_M9_vs_WT_LB	WT_M9+T_vs_WT_LB	WT_M9+T-vs_WT_M9
		log2foldchange	log2foldchange	log2foldchange	log2foldchange	log2foldchange	log2foldchange	log2foldchange
Purine metabolism								
1-(5'-Phospho-ribosyl)-5-aminoimidazole								
4-Amino-5-hydroxymethyl-5-methylpyrimidine phosphate	BGL_1c10790	3.67	3.63	0.32	0.30	0.04	-1.37	-1.41
4-Amino-5-hydroxymethyl-5-methylpyrimidine diphosphate	BGL_1c07140	0.58	0.95	0.11	0.46	0.62	0.89	0.27
	BGL_1c24820	0.34	-0.55	0.08	-0.75	-1.14	-0.30	0.84
Thiamine phosphate	BGL_2c23420	-1.63	-2.27	0.34	-0.20	-3.24	-2.93	0.31
Thiamine diphosphate	BGL_1c05130	0.44	0.61	0.03	0.19	0.51	1.11	0.59
Thiamine triphosphate	BGL_1c30540	-1.20	-0.47	-0.40	0.31	-0.36	0.63	0.99
Salvage pathway								
Thiamine phosphate	BGL_1c09450	-0.54	-0.49	-0.19	-0.14	0.08	0.07	-0.01
Thiamine	BGL_1c09450	-0.54	-0.49	-0.19	-0.14	0.08	0.07	-0.01
5-(2-Hydroxyethyl)-4-methylthiazole	BGL_2c23410	-1.97	-2.14	-0.08	-0.24	-2.92	-2.49	0.44
5-(2-Hydroxyethyl)-4-methylthiazole phosphate	BGL_1c18800	-4.30	0.00	0.00	0.00	-2.55	-1.77	0.78
	BGL_1c03130	2.36	1.99	0.63	0.27	1.29	0.26	-1.03
Thiamine phosphate	BGL_2c21760	0.65	0.42	0.12	-0.06	-1.48	-0.98	0.50

Figure A13: Transcriptome analysis regarding to the thiamine metabolism.

Oxidative stress	Locus Tag	late exponential growth phase (48h)				late stationary growth phase (72h)		
		WT_M9_vs_WT_LB	ΔthiM_M9_vs_ΔthiM_LB	ΔthiM_LB_vs_WT_LB	ΔthiM_M9_vs_WT_M9	WT_M9_vs_WT_LB	WT_M9+T_vs_WT_LB	WT_M9+T-vs_WT_M9
		log2foldchange	log2foldchange	log2foldchange	log2foldchange	log2foldchange	log2foldchange	log2foldchange
FMN dependent nitroreductase-like protein	BGL_2c11540	11.38	10.73	1.09	0.45	4.42	5.05	0.63
superoxide dismutase SodA	BGL_1c12730	9.90	9.31	0.26	0.12	-0.12	-0.74	-0.62
taurine catabolism dioxygenase TauD/TfdA	BGL_2c17000	6.58	5.55	0.97	0.02	-0.18	0.93	1.11
oxidoreductase	BGL_1c21960	3.50	5.64	-0.46	1.21	2.12	3.29	1.17
oxidoreductase alpha (molybdopterin) subunit	BGL_1c22010	2.57	4.83	-0.37	1.67	-0.41	0.68	1.09

Figure A14: Transcriptome analysis regarding to the oxidative stress response.

Iron metabolism	Locus Tag	late exponential growth phase (48h)				late stationary growth phase (72h)		
		WT_M9_vs_WT_LB	ΔthiM_M9_vs_ΔthiM_LB	ΔthiM_LB_vs_WT_LB	ΔthiM_M9_vs_WT_M9	WT_M9_vs_WT_LB	WT_M9+T_vs_WT_LB	WT_M9+T-vs_WT_M9
		log2foldchange	log2foldchange	log2foldchange	log2foldchange	log2foldchange	log2foldchange	log2foldchange
Heme transport and receptor	BGL_1c01980	10.33	10.11	0.47	0.32	1.71	2.41	0.71
	BGL_1c01990	10.47	9.55	1.04	0.18	3.29	4.46	1.17
	BGL_1c02000	9.87	9.68	0.56	0.42	4.50	5.44	0.95
Pycholin biosynthesis	BGL_1c20600	5.47	4.44	1.14	0.17	0.06	0.18	0.12
	BGL_1c20610	4.88	4.09	0.62	0.01	-0.60	-0.33	0.27
	BGL_1c20620	3.24	4.15	-0.04	0.32	0.07	0.39	0.32
	BGL_1c20630	4.57	3.75	0.78	0.06	1.40	1.88	0.48
Iron storage and transport	BGL_1c27180	5.39	5.34	0.67	0.63	0.32	0.32	0.00
	BGL_1c27190	5.90	5.00	0.56	-0.18	0.69	0.94	0.26
	BGL_1c27200	3.95	3.16	0.59	-0.12	0.28	0.70	0.42
	BGL_1c27210	3.31	2.85	0.52	0.11	0.90	1.36	0.46
Transmembrane transport (FTR)	BGL_1c27250	3.89	4.05	0.21	0.35	-0.90	0.10	1.00
	BGL_1c27260	4.07	4.03	0.53	0.50	-1.08	-0.05	1.03
	BGL_1c27270	3.59	3.48	0.31	0.25	-2.01	-1.07	0.94
	BGL_1c27280	3.77	3.90	0.07	0.19	-0.28	0.49	0.77
RND efflux transporter	BGL_2c04500	3.57	1.99	-1.32	-2.97	-0.58	-0.50	0.09
	BGL_2c04510	3.95	1.95	-0.93	-3.04	-1.80	-0.18	1.61
	BGL_2c04520	2.54	1.70	-1.50	-2.36	-1.22	-0.87	0.36
	BGL_2c04530	3.42	2.56	-0.97	-1.90	2.29	3.64	1.36
	BGL_2c04540	7.82	6.14	0.07	-1.38	4.19	5.22	1.03
hypothetical protein DUF2000 family	BGL_2c10500	3.23	3.05	0.12	0.02	-0.86	-0.26	0.60
manganese/iron transporter NRAMP family protein	BGL_2c10510	7.48	7.60	0.23	0.39	-1.28	-1.14	0.15
hypothetical protein	BGL_2c11530	10.12	10.02	0.54	0.48	3.06	4.17	1.11
FMN dependent nitroreductase-like protein	BGL_2c11540	11.38	10.73	1.09	0.45	4.42	5.05	0.63
sigma-24 (FecI-like) protein	BGL_2c13100	4.37	4.86	0.30	0.83	-3.60	-2.60	1.00
Fe2+-dicitrate sensor membrane component	BGL_2c13110	3.63	3.41	0.47	0.29	-4.91	-3.66	1.24
putative PepSY-associated TM helix domain protein	BGL_2c14570	4.27	3.81	0.28	-0.09	2.17	3.37	1.19
hypothetical protein	BGL_2c14580	3.35	2.79	0.21	0.11	1.68	3.12	1.43
hypothetical protein	BGL_2c16000	2.78	2.48	0.33	0.09	1.20	2.13	0.94
putative TonB-dependent receptor	BGL_2c16010	2.76	2.74	0.45	0.45	-0.30	0.77	1.07
transcriptional regulator AraC-family	BGL_2c16020	4.63	4.21	1.12	0.71	0.34	1.48	1.14
hypothetical protein	BGL_2c16030	4.27	3.40	1.08	0.27	1.39	2.76	1.37
nonribosomal peptide synthase (NRPS)	BGL_2c16040	2.80	1.95	0.93	0.12	-1.43	0.15	1.58
thiazolinyl imide reductase	BGL_2c16070	4.33	3.05	0.62	-0.31	-0.45	1.04	1.49
thioesterase type II NRPS/PKS/S-FAS family	BGL_2c16080	3.41	2.51	0.23	-0.08	1.42	2.50	1.09
Fur	BGL_2c16680	6.04	5.58	0.61	0.18	1.47	2.64	1.18
	BGL_2c16690	5.95	5.45	0.32	-0.06	2.07	3.02	0.95
putative NADPH nitroreductase	BGL_2c16700	6.84	5.57	0.70	-0.30	0.37	1.48	1.11
non-ribosomal peptide synthase	BGL_2c16900	4.80	4.46	1.19	0.84	0.63	2.67	2.04
non-ribosomal peptide synthase	BGL_2c16910	5.37	4.63	1.60	0.77	1.32	3.29	1.97
hypothetical protein YqcI and YcgG family	BGL_2c16920	6.51	5.05	1.41	0.08	0.76	2.89	2.13
hypothetical protein	BGL_2c16930	5.98	4.94	1.26	0.23	1.64	3.30	1.66
TonB-dependent siderophore receptor	BGL_2c16940	6.26	5.42	1.18	0.31	2.73	4.19	1.46
ABC transporter (FecCD)	BGL_2c16950	3.56	3.29	0.53	0.28	3.06	4.21	1.14
	BGL_2c16960	5.02	4.33	0.56	-0.05	2.84	4.08	1.24
	BGL_2c16970	4.34	3.93	0.41	0.05	1.54	3.14	1.60
non-ribosomal peptide synthase	BGL_2c16980	5.46	4.68	1.33	0.52	2.33	3.85	1.52
non-ribosomal peptide synthase	BGL_2c16990	4.82	4.14	1.19	0.49	1.81	3.33	1.51
taurine catabolism dioxygenase TauD/TfdA	BGL_2c17000	6.58	5.55	0.97	0.02	-0.18	0.93	1.11
thioesterase type II NRPS/PKS/S-FAS family	BGL_2c17010	6.48	5.74	0.67	0.05	-1.02	0.08	1.10
Siderophore receptor	BGL_2c18860	3.25	3.27	0.05	0.07	-1.13	-0.45	0.68
Heme transport	BGL_2c28240	4.64	4.91	-0.13	0.08	2.29	3.73	1.44
	BGL_2c28250	5.39	5.39	-0.05	-0.06	2.73	3.87	1.14
Siderophore receptor	BGL_2c28600	5.74	5.14	0.35	0.07	0.21	1.41	1.20

Figure A15: Transcriptome analysis regarding to the iron metabolism.

CRISPR/CAS	Locus Tag	late exponential growth phase (48h)				late stationary growth phase (72h)		
		WT_M9_vs_WT_LB	ΔthiM_M9_vs_ΔthiM_LB	ΔthiM_LB_vs_WT_LB	ΔthiM_M9_vs_WT_M9	WT_M9_vs_WT_LB	WT_M9+T_vs_WT_LB	WT_M9+T_vs_WT_M9
		log2foldchange	log2foldchange	log2foldchange	log2foldchange	log2foldchange	log2foldchange	log2foldchange
cas1	BGL_1c18810	-1.46	-2.11	-0.93	-1.58	-1.33	-0.56	0.76
cas3	BGL_1c18820	-1.17	-1.99	-0.43	-1.28	-1.35	-0.69	0.65
csy1	BGL_1c18830	-3.48	-5.78	1.54	-0.43	-1.69	0.21	1.91
csy2	BGL_1c18840	-3.67	-6.60	2.04	-0.45	-1.98	-0.37	1.60
csy3	BGL_1c18850	-3.41	-6.56	2.17	-0.52	-1.73	-0.60	1.13
csy4	BGL_1c18860	-2.69	-6.09	1.73	-0.61	-1.32	-0.71	0.61

Figure A16: Transcriptome analysis regarding to the CRISPR/CAS system.

Acknowledgements

First of all, I would like to thank Prof. Dr. Wolfgang R. Streit for the opportunity to accomplish this dissertation in his working group and the constantly support and helpful discussions during the last years. I would like to thank Prof. Dipl.-Ing. Dr. Agnes Weiß for reviewing this work and the friendly exchange.
I would like to thank PD Dr. Andreas Pommerening-Röser and Prof. Dr. Tim Gilberger for being part of my examination committee. Furthermore, I would like to thank all cooperation partners and for the opportunity to collect experience in the interdisciplinary field.

Furthermore, I would like to thank Dr. Christel Vollstedt and Dr. Ifey Alio for listening to any challenges and for all helpful discussions. I would like to thank Katrin Petersen and Hongli Zhang for the provided strains and constructs in this work.

I would like to say a special thank you to Angela Jordan, the heart of the lab, for her support, her patience, and the great working atmosphere in the lab. I would like to thank all other TAs for their constant support of all Bachelor, Master and PhD students in their work.

Finally, I would like to say a special thank you to my great colleagues who gave me an absolutely unforgettable time that I will miss in the future and my dear friends who have always supported me.